Relevant phenomena and process parameters in granulation for manufacturing of pharmaceutical, nutraceutical and zootechnical products

Veronica De Simone

UNIVERSITY OF SALERNO

DEPARTMENT OF INDUSTRIAL ENGINEERING

Ph.D. Course in Industrial Engineering
Curriculum in Chemical Engineering - XXXI Cycle

RELEVANT PHENOMENA AND PROCESS PARAMETERS IN GRANULATION FOR MANUFACTURING OF PHARMACEUTICAL, NUTRACEUTICAL AND ZOOTECHNICAL PRODUCTS

Supervisor
Prof. Anna Angela Barba

Ph.D. student
Veronica De Simone

Scientific Referee
Prof. Gaetano Lamberti

Ph.D. Course Coordinator
Prof. Ernesto Reverchon

To You…I raise my eyes...
To You…concrete absence of an eternal passage but more present of who is present...
To You…forever my Little Big Woman.

Publications

International journals

- **De Simone V.**, Dalmoro A., Lamberti G., d'Amore M., Barba A.A., "Central composite design in HPMC granulation and correlations between product properties and process parameters", New Journal of Chemistry, 41 (2017) 6504-6513
  doi: 10.1039/C7NJ01280B

- **De Simone V.**, Dalmoro A., Lamberti G., Caccavo D., d'Amore M., Barba A.A., "HPMC granules by wet granulation process: Effect of vitamin load on physicochemical, mechanical and release properties", Carbohydrate Polymers, 181 (2018) 939-947
  doi: 10.1016/j.carbpol.2017.11.056

- **De Simone V.**, Caccavo D., Lamberti G., d'Amore M., Barba A.A., "Wet-granulation process: phenomenological analysis and process parameters optimization", Powder Technology, 340 (2018) 411-419
  doi: 10.1016/j.powtec.2018.09.053

- **De Simone V.**, Dalmoro A., Lamberti G., Caccavo D., d'Amore M., Barba A.A., "Effect of binder and load solubility properties on HPMC granules produced by wet granulation process", Journal of Drug Delivery Science and Technology, 49 (2019) 513-520
  doi.org/10.1016/j.jddst.2018.12.030

Book chapter

- **De Simone V.,** Caccavo D., Dalmoro A., Lamberti G., d'Amore M.; Barba A.A., "Inside the phenomenological aspects of wet granulation: role of process parameters", chap. V in "Granularity in Materials Science", InTech Ed., 2018, ISBN 978-1-78984-308-8
  doi: 10.5772/intechopen.79840

Proceedings

International

- Barba A.A., d'Amore M., Dalmoro A., **De Simone V.**, Lamberti G., "Production of granulates of hydroxypropyl methylcellulose loaded with vitamin B12 by wet granulation process", 8th International Granulation Workshop-Granulation Conference, 28-30/06/2017, Sheffield (UK), England
- **De Simone V.**, Dalmoro A., Caccavo D., Lamberti G., d'Amore M., Barba A.A., "Vitamins-loaded HPMC granules by wet granulation process: impact of liquid binder/vitamin solubility on HPMC granules properties", 23rd International Congress of Chemical and Process Engineering CHISA 2018, 25-29/08/2018, Prague (CZ), Czech Republic
- **De Simone V.**, Caccavo D., Lamberti G., d'Amore M., Barba A.A., "Phenomenological analysis, process parameters optimization and mathematical modeling of a low-shear wet granulation process", 23rd International Congress of Chemical and Process Engineering CHISA 2018, 25-29/08/2018, Prague (CZ), Czech Republic
- **De Simone V.**, Caccavo D., Lamberti G., d'Amore M., Barba A.A., Dalmoro A., Low-shear wet granulation process: a new strategy in design and manufacturing of granular materials, to be presented to 3rd European Conference on Pharmaceutics, 25-26/03/2019, Bologna, Italy

National

- **De Simone V.**, Dalmoro A., Lamberti G., Barba A.A., "Design of Experiment's approach in granulation processes", national conference GRICU 2016, 12-14/09/2016, Anacapri (NA), Italy

Contents

Figures index

Tables index

Abstract

Wet granulation is a size enlargement process used in many fields, such as pharmaceutical, nutraceutical, zootecnichal, etc., due its ability to improve technological properties of the final product, compared to the powder form, and/or to realize suitable delivery systems for drug/functional molecules for oral administrations/food preparations and/or to produce intermediate processing products. In spite of its widespread use, economic importance and almost 50 years of research, granulates manufacture is still based on empirical approach. Moreover, phenomena involved in powders aggregation are not well understood, and thus it is difficult to successfully obtain a product with tailored features without extensive experimental tests.

In the scientific literature the approach to the granulation study is based on experimental tests, to investigate the impact of formulation and process variables on granules properties, or on modeling activities, to mathematically describe the involved phenomena. The two approaches, experimental and theoretical, are rarely applied together. In this study a novel integrate strategy of investigation was applied to elucidate the role of the phenomenological aspects, and their connection with the main operating parameters in granulation process, on the granules final properties, in order to develop physical-mathematical descriptions of the size enlargement unit operation, which can indubitably constitute a starting point for scale up purposes.

The first step of the Ph.D. research activity was the design and realization of a bench scale experimental set up, with the innovative feature of using an ultrasonic atomizer for spraying the wetting phase in order to improve its dispersion degree on the surface of powder bed. Four are the main sections composing the realized apparatus: feeding section, production section, stabilization section and separation section. For the preparation of granules, hydroxypropyl methylcellulose (*HPMC*) was used as powder model material due to its versatile properties. It is an easy to handle, available at low cost, odourless, hypoallergenic, biocompatible, and not toxic polymer, used as excipient in the formulation of hydrogel-based matrices in form of tablets or granules, in order to provide controlled release of oral solid dosage systems. Distilled water was used as binder phase. In the built configuration, the powder was placed in a low-shear granulator and agglomerated by spraying the binder phase. The produced wet granules were stabilized by dynamic drying in presence of a hot air flow, because the evaporation of the residual moisture slows down the degradation of the granules. The dry granules were

separated by manual sieving with cutoff sizes from top to bottom as follows: 2 mm, 0.45 mm and a collection pan. Three granules fractions were obtained by the separation step: a fraction of “big scrap”, i.e. particles with size larger than 2 mm, one of “small scrap”, i.e. particles with size smaller than 0.45 mm, and one of “useful”, i.e. particles with size between 0.45-2 mm. The range size 0.45-2 mm was considered as the fraction of interest being a size typical range of granules in the food, pharmaceutical and zootechnical fields. Finally, only the fraction of useful was subjected to characterization methods carried out adopting both the *ASTM* (American Society for Testing and Materials) standards and *ad hoc* innovative protocols. In particular, a new procedure for analysing the mechanical properties of granules, and an *ad hoc* built Dynamic Image Analysis (*DIA*) device, based on the free falling particle scheme, for monitoring the evolution of the *PSD* during the wet granulation process, were developed.

The experimental campaigns were planned by Design of Experiments (*DoEs*) approaches. A system with three process parameters (factors), i.e. impeller rotation speed (*rpm*), binder to powder ratio, and binder phase flow rate, each at three intensities (levels) was considered. Their impact on granules properties were assayed to find the best process operating conditions able to produce granules with tailored features, i.e. high product yield (% w/w of dry granules with size between 0.45 mm and 2 mm), low residual moisture content, and good flowability and compressibility properties. Under phenomenological point of view, it was observed that not all the combinations of parameter levels ensure good granulation. There are operating conditions, like low rpm with high binder phase flow rate and low binder to powder ratio, or, high rpm with lower binder phase flow rate and binder to powder ratio, which combined together can produce a high amount of granules with size lower than requested one (0.45-2 mm), i.e. failure of the aggregation phenomena. Others, like low rpm with high binder phase flow rate and high added binder phase amount, instead, can achieve clusters of powder and binder, i.e. over wetting phenomena, which is a condition to avoid. The best conditions of granulation were obtained with high rpm, high binder to powder ratio and low binder phase flow rate.

To fully understanding the behaviour of *HPMC* granules as active ingredient delivery systems, the intensities of process parameters, which are found to give the better product yield, were used in the production of loaded granules. In particular, the effect of three formulation variables, i.e. molecule payload, molecule solubility and binder type, on physical and mechanical properties of granules were investigated and, moreover, analysis of release mechanisms were speculated. A hydrophilic compound, vitamin B12, and a lipophilic one, vitamin D2, were employed as model molecules. First of all, the best loading method in *HPMC* granules for the hydrophilic molecule, vitamin B12 (payload 1 % w/w), was investigated. Vitamin B12 was

incorporated in the *HPMC* granules by two different loading methods: according to the method 1, the vitamin B12 was dissolved in the liquid binder phase (here the binder phase was a solution of distilled water and vitamin B12); according to the method 2, the vitamin B12 was pre-mixed with *HPMC* powders (here the powder was a mixture of *HPMC* and vitamin B12). It was observed that the loading method type does not influence the granules flowability properties and the product yield, however, a better dispersion of vitamin B12 inside the *HPMC* polymer matrix was achieved by using the method 1, perhaps for the uniform spraying of B12 together with the binder phase. Thus, by exploiting the most successful method 1, two different payloads of vitamin B12 and vitamin D2 (1 % and 2.3 % w/w) were assayed. Due to lipophilic properties of the D2, a binder phase made by a solution of ethanol and water with a 75/25 v/v ratio was used to produce vitamin D2 loaded *HPMC* granules. Results showed that the use of ethanol in the binder phase reduces the product yield and leads to the formation of granules with less defined shape, smaller mean size, less hard structure and worse flowability. Moreover, the presence of ethanol induces a slightly faster polymer erosion respect to granules obtained by using only water. The increase of payload both for the hydrophilic and lipophilic molecule leads to the formation of granules with a harder and more compact structure. The vitamins solubility influences their release mechanism: diffusion for the hydrophilic molecule (at 3 hours the vitamin B12 was fully released, regardless of the payload and of the *HPMC* erosion rate) and erosion for the lipophilic one (at 3 hours the amount of vitamin D2 released was similar to the amount of eroded *HPMC*).

Due to the relevance of size distributions in practical uses of granulates (the process yield is based on this parameter), hardware and software of a *DIA*-device for *PSD* analysis were designed, developed, tested and then used to perform studies on the growing of the powder agglomerates during the process. *PSD* measurements were used to obtain a basic understand of the phenomenological aspects for optimize the key process parameters, i.e.: process time, impeller rotation speed and binder phase flow rate. The process parameters optimization was carried out by Response Surface Methodology (*RSM*) and using the granulation yield (% w/w of wet granules within the size range 2-10 mm) as the main variable of interest. It was observed that the agglomeration, breakage and nucleation phenomena occur simultaneously in the granulator, with the predominance of the agglomeration during the binder addition phase, later balanced by the breakage phenomenon. Thanks to this initial phenomenological analysis, process time was optimized. Response surface studies indicated that the interaction between the impeller rotation speed and the binder flow rate influences the granulation yield (and in general the granules *PSDs*), especially at high rpm.

Agglomeration, breakage and nucleation phenomena experimentally observed by *PSDs* analysis were mathematically described by using the Population Balance Equations (*PBEs*) approach. *PBEs* were discretized in 60 classes, ranging from 60 to 20000 μm with a geometrical progression of $2^{1/6}$, therefore, the resulting model was a system of 60 Ordinary Differential Equations (*ODEs*), one for each class, which was implemented and solved numerically by MATLAB® 2014b software. Suitable mathematical functions to describe phenomena and parameters were selected from literature or purposely developed in this work. In particular, three models with increasing complexity were considered: a pure agglomeration model that disregards all the other phenomena; an agglomeration and breakage model; a complete model with agglomeration, breakage and nucleation. The different modeling structures were then validated by comparison with experimental data. As overall result, it was observed that a pure agglomeration model overestimates the granules formation and, despite the presence of the breakage factor improves the model capabilities, the best matching with experimental evidences was obtained using the complete model, which takes into account also the nucleation phenomena. Achieved results prove that the developed modeling structures respond to physical observed phenomena.

Chapter I
Introduction

I.1 Why granular?

Granulation, also known as agglomeration, pelletization, or balling, is a "size-enlargement process" of small particles (powders in crystalline or amorphous status) into larger coherent and stable masses, called granules, in which the original particles are still identifiable. The aim of the granulation process is to improve the properties of the final product compared to the powder form and/or to realize suitable delivery system for drug/functional molecules for oral administrations/food preparations and/or to produce intermediate processing products. Under technological point of view, due to more regular shape and larger size, the granules give better flow properties for safer and cheaper transport and storage, lower the caking and lump formation (especially for hygroscopic materials), improve heat transfer features, allow to obtain a more uniform distribution of the incorporated active molecule, lower the powder dispersion in the environment, linked to a reduced inhalation, handling and explosion risks hazard (Perry and Green, 1999, Iveson et al., 2001a).

In spite of its widespread use, economic importance and almost 50 years of research, granulation in practice was more of an art than a science, i.e., there were a qualitative understanding of both the granule growth mechanisms and the effects of different variables on agglomeration phenomena (Iveson et al., 2001a). Over the past decade, design, scale-up, and operation of granulation processes have been considered as quantitative engineering and significant advances have been made to quantify the granulation processes (Hapgood et al., 2003).

Basically, the granulation methods are divided into dry and wet ones (Shanmugam, 2015). Dry granulation is based on the mechanical compression (slugs) or compaction (roller compaction) of a dry powder, while the wet granulation exploits a granulation liquid called "binder phase" to agglomerate the powder particles. During wet granulation, the binder

phase is added to the powder in a tumbling granulator, high or low shear mixer granulator, fluidized bed granulator, or similar devices, allowing the particles agglomeration. The bonds between particles depend on a combination of capillary pressure, surface tension and viscous forces. This second process involves a final step of granules stabilization by removal of the wetting phase to make the relevant bonds permanent (Shanmugam, 2015, Iveson et al., 2001a, Iveson and Litster, 1998b).

Among these two techniques, wet granulation is the most widely used, as can be seen from data on scientific relevance of granulation process, reported in the paragraph I.2. Nowadays, wet granulation is recognized as an example of "powder particle design". The granule final features are controlled by a perfect combination of formulation variables (feed-materials properties, i.e.: binder phase viscosity, liquid-solid surface tension, Particle Size Distribution (*PSD*) and binder phase adhesive properties) and operating variables (i.e.: binder phase volume, binder phase flow rate, method of binder phase addition, impeller rotation speed and process time) (Mahdi et al., 2018, Luo et al., 2017). In addition, final granules properties depend on phenomena taking place in granulators, i.e. physical transformations of the powder particles, with kinetic mechanisms and aggregation rate controlled by formulation and process variables (Hapgood et al., 2003, Perry and Green, 1999). Therefore, to produce granular structures with tailored features (in terms of size and size distribution, flowability, mechanical and release properties, etc.), both a careful characterization of the feed-material properties and a deep understanding of operating parameters and phenomena involved during granule formation are needed (Hapgood et al., 2003, Suresh et al., 2017, Litster, 2003b). This can also lead to optimized processes in terms of production costs and other types of resources involved. However, the majority of literature is concerned experimentally with the role of material properties and process conditions on the properties of the product granules, while, quantitative aspects of the phenomena are still not well understood.

I.2 Scientific relevance of the granulation process

The granulation is a topic strongly treated in literature for almost 50 years. Some of the earliest pioneering work were performed by Newitt (1958) and Capes (1965) using sand in drum granulators. Since then, a large volume of work has been published that studying several materials, ranging from minerals to pharmaceuticals, and using several equipment, ranging from fluidised beds to high shear mixers. Over the years, a number of books and comprehensive review papers have been written to summarise the state of knowledge in this discipline (Iveson et al., 2001).

A query of the Web of Science (the well-known Thomson Reuter's database indexing the scientific journals), carried out in mid-September 2018

searching for papers with the "topic" containing the words "wet granulation" (using the option "All Databases), gave a list of 1647 papers published since 2007 to the date of the request, i.e. roughly in last ten years. These papers produced more than 10 thousand of citations during the time span of the investigation. The evolution with time of the published papers (patterned bars, visible on the left axes) and of the citations (grey bars, visible on the right axes) is show in Figure I.1 (a.) (data for 2018 were not reported since they are not yet complete).

a. b.

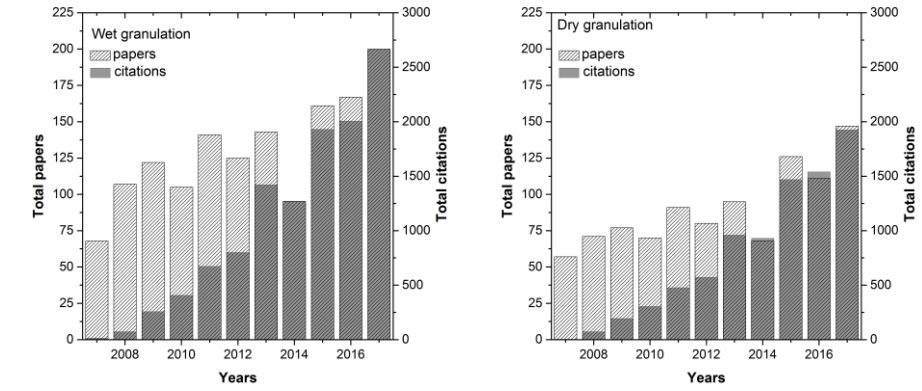

Figure I.1 *a. Published papers (patterned bars, axis y to the left) and citations (grey bars, axis y to the right) on the topic containing the words "wet granulation". b. Published papers (patterned bars, axis y to the left) and citations (grey bars, axis y to the right) on the topic containing the words "dry granulation". The data were obtained using the option "all data bases"*

a. b.

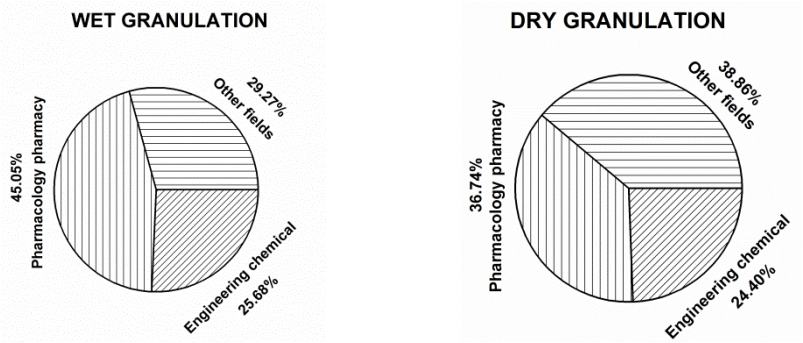

Figure I.2 *Wet and dry granulation are prevalently applied in pharmacology pharmacy and engineering chemical fields. The other fields are: chemistry medical, chemistry multidisciplinary, materials science multidisciplinary, engineering environmental, food science technological, metallurgy metallurgical engineering, chemistry physical, and chemistry applied*

As can see, the publishing rate has a constant trend until to 2014, and it is increased in time until today, signifying a mature subject of investigation. On the other hand, the number of citations have an increasing trend in time if the data of 2014 are not considered, showing an increasing interest for this topic from all over the world. The prevalent research area for this subject is "pharmacology and pharmacy" seen that the granules can constitute a good delivery system for drug/functional molecules for oral administrations/food preparations or intermediate products for the preparation of tablets. However, several journals in the area "engineering chemical" have treated this topic. In particular, of 1647 papers 742 (i.e. 45.05 %) fall within the area "pharmacology and pharmacy" and 423 (i.e. 25.68 %) in the area "engineering chemical", suggesting the strong interest of the wet granulation process from an engineering point of view (see Figure I.2 (a.)).

The same search (since 2007), done using "dry granulation" as topic, gave 993 published papers with about 8 thousand citations during the time span of the investigation (always from 2007 to 2017). The time evolution of the published papers (patterned bars, visible on the left axes) and of the citations (grey bars, visible on the right axes) is illustrated in Figure I.1 (b.). Also the dry granulation is predominantly used in the area "pharmacology and pharmacy". Of 1037 papers 381 (i.e. 36.74 %) regard the area "pharmacology and pharmacy" and 253 (i.e. 24.40 %) the area "engineering chemical" (see Figure I.2 (b.)).

All these data showed the continuous appeal of granulation for the scientific community and clearly underlined that among the two methods of granulation the wet one is the most studied and applied despite the fact that it involves multiple unit processes (such as wet massing, drying and sieving). Therefore, the wet granulation is the technique used for the granules production in this Ph.D. thesis.

I.3 Industrial relevance of the granulation process

Granulation finds application in a wide range of industries including mineral processing, agricultural products, detergents, pharmaceuticals, foodstuffs, nutraceuticals, cosmetics, zootechnical and specialty chemicals. For marketing reason and technological aspects, granules are used for processing both intermediate materials and final products of many industrial transformations. In the chemical industry alone it has been estimated that 60 % of products are manufactured as particulates solid and a further 20 % use powders as ingredients. The annual value of these products is estimated at US$1 trillion in the US alone (Iveson et al., 2001a). In pharmaceutical field, solid dosage forms remain an important part of the overall drug market, despite the success and the development of new pharmaceutical forms. The oral solid dosage forms market was of $571 million in 2011 and projected to reach $870 million at the end of 2018 (Wright, 2016). In particular, among

novel drugs approved by *FDA* (Food and Drug Administration), 46 % in 2014 and 32 % in 2016 were solid dosage products (Langhauser, 2017), most of them made of granules. The most important pharmaceutical industries, such as Patheon, Aesica, Rottendorf Pharma GmbH, Catalent Pharma, continually do investments in oral solid manufacturing solutions, including the development of granulation processing methods (Van Arnum, 2015). Granulated products are also highly used in the fertilizers field: about 90 % of fertilizers are applied as solids, less as powder, more in granular form. The global demand for fertilizer nutrients was estimated to be 184.02 million tons in 2015, and it is forecast to reach 201.66 million tons by the end of 2020 (FAO, 2017). The animal feed additives global market was estimated at 256.8 kilo tons in 2015, and in particular, industries aim to develop new technologies (Research, 2017), very often based on granulation principles, to provide stabilization and effective protection of the active components in the finished products.

I.4 Main aims of this thesis

Aim of this research project is to investigate the role of the phenomenological aspects, and their connection with the main operating parameters in granulation process, on granules final properties, in order to develop physical-mathematical descriptions of this enlargement unit operation, which will constitute the starting point for the scale up studies. To this scope granular structures with tailored features (in terms of size and size distribution, flowability, mechanical and release properties, etc.), through the design and realization of a bench scale experimental set up, were produced and characterized by standard and *ad hoc* innovative protocols.

The comprehensive approach of experimental and modeling studies constitutes the main novelty of this Ph.D. research activity.

I.5 Outline of the thesis

An introduction on the scientific and industrial importance of granulation process is followed, in particular, by the review of the literature on wet granulation process, concerning relevant physical phenomena, apparatuses, role of formulation and process parameters on the final granules properties, and mathematical approaches to describe the involved phenomena (Chapter two).

Development of dedicated protocols for granulated materials stabilization, separation and characterization and of experimental set up for granules manufacturing with tailored features (in terms of size and size distribution, flowability, mechanical and release properties, etc.) were described (Chapter three).

Several applications concerning bench scale production of granules unloaded and loaded with hydrophilic and lipophilic active molecules, by using the design of experiment statistical protocols are shown (Chapter four).

Studies of phenomenological aspects involved in the formation of the granules, correlated to the main process parameters, and operating conditions optimization are presented by experimental demonstrations (Chapter five).

Physical-mathematical models describing the observed phenomena are developed and approaches towards the scale up of wet granulation process are discussed (Chapter six).

The conclusive part endorses the main findings of this Ph.D. research project (Chapter seven).

The symbols and abbreviations list is reported.

Abstracts relative to the main publications inherent the Ph.D. researches are showed in the Appendix section.

Table I.1 *Thesis map*

Chapter two	Wet granulation: state of the art
Chapter three	Methodologies and experimental apparatus set up
Chapter four	Granulation process applications
Chapter five	Phenomenological analysis and process parameters optimization in wet granulation
Chapter six	Mathematical modeling of the low-shear wet granulation
Chapter seven	Conclusive remarks about the main findings of this Ph.D. research project
Symbols	Symbols list
Abbreviations	Abbreviations list
Appendix	Abstracts relative the main publications inherent the Ph.D. researches

Chapter II
Wet granulation: state of the art

II.1 Wet granulation process

Wet granulation is a size enlargement process of powder particles used in many fields, such as pharmaceutical, nutraceutical, and zootecnichal, to improve technological properties of powders such as flowability, compressibility, dosage and so on (Agrawal et al., 2003, Asgharnejad et al., 2000, Jona et al., 2007, Katdare and Kramer, 2004, Lintz and Keller, 2006, Pathare and Byrne, 2011, Phinney, 2000, Phinney, 2001). During wet granulation, a liquid phase called "binder" is added to the powder in a tumbling granulator, high or low shear mixer granulator, fluidized bed granulator, or similar devices, allowing the particles agglomeration (Iveson and Litster, 1998b). It is usually performed in four steps: 1) homogenization of dry powders; 2) wetting by binder addition; 3) wet massing with binder feeding system switched off; 4) drying of the wet granules (Nalesso et al., 2015). Newitt (1958) has described five states of liquid saturation for the granules during the wet granulation process (see Figure II.1), which depend on the amount of binder used to mixer the powder. Before the addition of binder to the dry powder the agglomerates only exist due to attractive forces like the Van der Waals forces. The pendular stage is the first saturation stage: here particles are held together by liquid bridges. With the addition of further binder, the funicular state is formed. It is an intermediary stage between the capillary and the pendular stage, where the voids are not fully saturated with liquid because the amount of added liquid is not sufficient. When these voids inside the agglomerate are saturated with liquid and the surface liquid is drawn back into the pores under capillary action, the capillary stage occurs. If the particles are held within or at the surface of a liquid drop, or if unfilled voids remain trapped inside the droplet, the droplet state and pseudo-droplet state occur respectively. The droplet stage corresponds to what is generally called over-wetting in granulation: the wetted mass loses most of its strength and turns into a paste until to give a

suspension with further liquid addition. It is possible to switch from the pendulum state to that of drops if the liquid binder is injected continuously, or if it occurs the consolidation phase which tends to reduce the granule pores. However, the capillary stage is the optimum state and supposed to give the highest granule strength. In fact, with an amount of liquid less than that required by the capillary state, little adherent granules will be formed. While, with a greater amount of liquid than that required by the capillary state, granules not properly adherent will be obtained (Iveson et al., 2001a).

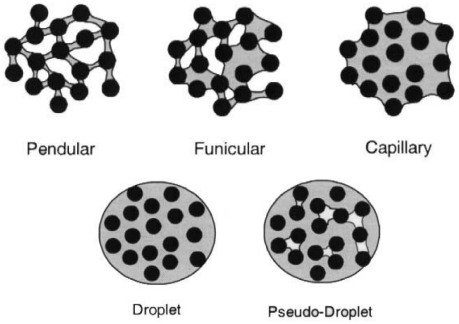

Figure II.1 *Saturation stages of granules (Newitt, 1958, Iveson et al., 2001a)*

The behaviour of the powder particles during the wet granulation process has been deeply investigated and rationally described by consecutive cyclic mechanisms such as wetting and nucleation, consolidation and growth, and attrition and breakage (Ennis and Litster, 1997, Iveson et al., 2001a), as reported in Figure II.2. Wetting and nucleation are the initial stages in all wet granulation processes, here the dry powder bed is brought into contact with liquid, and a number of particles adhere to give a distribution of nuclei granules that are small aggregates (Abberger, 2007, Chitu et al., 2011, Iveson et al., 2001a, Iveson et al., 2001b). Agglomeration (consolidation and growth) is the stages where the granules collide one on each other: collisions lead to an increase of compaction and size of granules (Abberger, 2007, Chitu et al., 2011, Iveson et al., 2001a, Iveson et al., 2001b). Attrition and breakage are the stages where the wet or dry granules, too large or weak and brittle, deform or break due to shear and impact forces: small particles are produced, generating new nuclei or granules that re-enter the cycle (Abberger, 2007, Chitu et al., 2011, Iveson et al., 2001a, Iveson et al., 2001b). These phenomena are also mathematically described by mechanistic models but the direct application of these models, despite their level of completeness, is still hindered by the impossibility to obtain an ab initio estimation of most of their parameters (Abberger, 2007, Hounslow et al., 1988, Sanders et al., 2009). They coexist in all the wet granulation processes, even if their importance is related to the process type. For example, in the

fluid-bed granulation the wetting phase prevails while in the high-shear granulation the consolidation step is predominant.

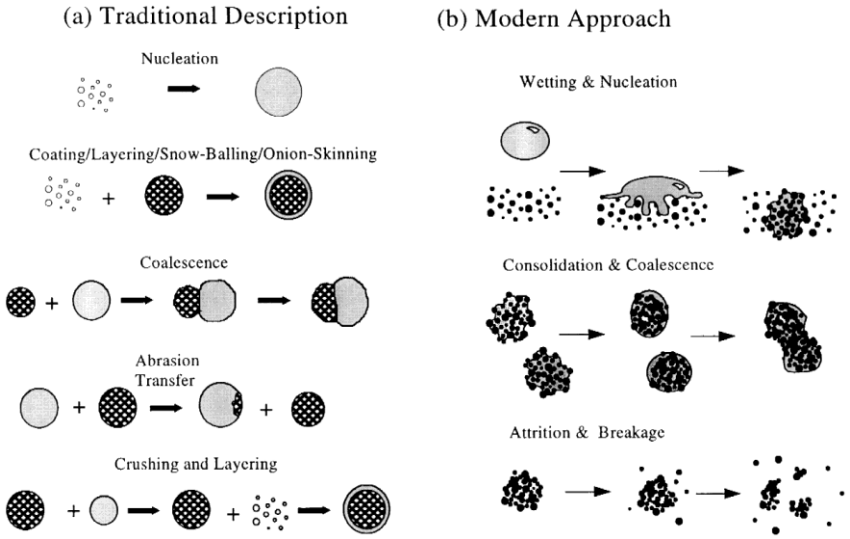

Figure II.2 *Formation mechanisms of the granules: (a) traditional description (Sastry and Fuerstenau, 1973); (b) modern approach (Ennis and Litster, 1997)*

These mechanisms control final granule properties, as the density and the size distribution, and depend on the chosen formulation as well as imposed operating conditions (Rajniak et al., 2007, Chitu et al., 2011, Iveson et al., 2001a, Litster, 2003b, Litster et al., 2001, Perry and Green, 1999). In particular, physicochemical properties of primary particles and binder phase determine surface wetting, spreading, adsorption and solid bridge strength.

II.2 Physical phenomena in wet granulation

II.2.1 Wetting and nucleation

Wetting and nucleation are the initial stages and more important in wet granulation process. Dry powder bed and liquid binder first come into contact through the wetting stage in a zone called “wetting zone”: the binder is sprayed onto the powder mass, attempting to distribute it evenly (Iveson et al., 2001a). After being wetted by the liquid binder, particles start to agglomerate forming initial nuclei of two or more particles, that are small granules: the nucleation stage refers to the formation of initial aggregates that are the result of interaction between the binder spray droplets and the powder in the granulator (Cameron et al., 2005, Iveson et al., 2001a). These initial stages are very important for the outcome of the wet granulation

process: low yields can be obtained if the powder has a poor wetting with the chosen binder, or if incorrect operating conditions are set.

Over the years, studies of wetting thermodynamics have highlighted that two are main parameters to be controlled: the angle of contact (θ) between solid particles and binder phase, and the spreading coefficients (λ) of the binder phase on the powder surface. These aspects are important to understand if the wetting stage is energetically favorable or not (Iveson et al., 2001a). The solid–liquid contact angle is the angle between the liquid drop on the solid surface and the same surface. It depends on the interaction between liquid and solid and affects the characteristics of the granulated product. Based on the solid–liquid contact angle value, a material can be easily wettable ($0° < \theta < 90°$), perfectly wettable ($\theta = 0°$) or borders on those value), and hardly wettable ($90° < \theta < 180°$). The solid – liquid contact angle can be calculated as a function of surface free energies (γ_{sv}, γ_{sl}, γ_{lv}: subscripts "*l*", "*s*" and "*v*" denote liquid, solid and vapour phase respectively) in according to Young–Dupre equation (see eq. (II.1)), valid for $\theta > 0°$.

$$\gamma_{sv} - \gamma_{sl} = \gamma_{lv} * \cos\theta \tag{II.1}$$

According to Krycer et al. (1983) and Zajic and Buckton (1990) the final granule properties are also correlated with the spreading coefficient (λ). The spreading coefficient is a measure of the tendency of a liquid and solid combination to spread over each other and is given by the difference between the works of adhesion and cohesion. It indicates whether spreading is thermodynamically favorable. There are three possibilities in spreading between a solid and a liquid: the liquid may spread over the solid (λ_{ls}) and create a surface film; the solid may spread or adhere to the liquid (λ_{sl}) but no film formation occurs; both the liquid and solid have high works of cohesion, and the solid–liquid interfacial area will be minimized. In particular, the spreading coefficient λ_{ls} is calculated as difference between work of adhesion for an interface (W_a) and work of cohesion for a liquid (W_{cl}), using the eq. (II.2), while, the spreading coefficient λ_{sl} is calculated as difference between work of adhesion for an interface (W_a) and work of cohesion for a solid (W_{cs}), using the eq. (II.3).

$$\lambda_{ls} = W_a - W_{cl} = (\gamma_{lv} \cdot (\cos\theta + 1)) - (2 \cdot \gamma_{lv}) \tag{II.2}$$

$$\lambda_{sl} = W_a - W_{cs} = (\gamma_{lv} \cdot (\cos\theta + 1)) - (2 \cdot \gamma_{sv}) \tag{II.3}$$

If λ_{ls} is positive stronger and denser granules are formed and the particles are maintained together by means of liquid bridges because the binder will spread and form a film over the powder surface. Instead if λ_{sl} is positive weaker and more porous granules are obtained and the bonds between the particles are few and they will create only where the liquid and powder

initially touch, considering that in this case the liquid will not spread or form a film.

As the wetting process proceeds, the drop penetrates into the pores of the powder surface and forms a nucleus that migrates outwards as the nucleus grows. The nucleation stage is composed by five steps, as shown in the Figure II.3 (Litster et al., 2001, Hapgood et al., 2002): (1) drops formation at the spray nozzle, from which they fall and impact the surface of the powder bed; (2) impact of the drops on powder bed and their possible breakage; (3) coalescence of the drops on the surface of the powder if the drops are slow to penetrate the surface or if the flux of drops on the surface is high, leading to a broad nuclei size distribution; (4) penetration of the drops into the pores of the powder bed by capillary action to form a nucleus granule; (5) mixing of the liquid binder and powder by mechanical dispersion.

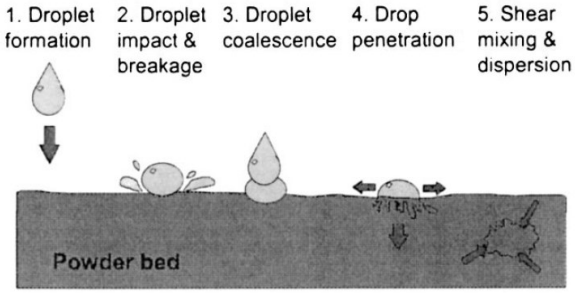

Figure II.3 *The five steps of nucleation: (1) drops formation; (2) impact of the drops on powder bed and possible breakage; (3) coalescence of the drops on the surface of the powder; (4) drops penetration into the pores of the powder bed; (5) mixing of the liquid binder and powder by mechanical dispersion (Litster et al., 2001, Hapgood et al., 2002)*

The ideal nucleation conditions occur when for each drop, which is sprayed from the nozzle and penetrates into the powder bed, one nucleus granule is produced (drop controlled nucleation) (Iveson et al., 2001a, Hapgood et al., 2002).

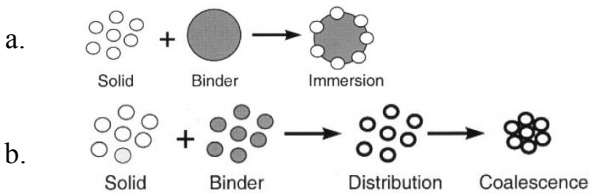

Figure II.4 *Nucleation mechanism by (Schæfer and Mathiesen, 1996): a. immersion mechanism; b. distribution mechanism*

The nucleation mechanism depends on the drop size relative to the primary powder particles. According to Schæfer and Mathiesen (1996) two

different nucleation mechanisms can occur, as illustrated in Figure II.4, which firstly were proposed for melt agglomeration and later extended to wet granulation by Scott et al. (2000). If the droplets are larger compared to the size of the powder particles, the binder phase has a high viscosity and the impeller speed of granulator are low, nucleation will occur by immersion of the smaller particles into the larger drop and nuclei with saturated pores will be produced (see Figure II.4 (a.)). If the droplets are smaller compared to the size of the powder particles, the binder phase has a low viscosity and the impeller speed of granulator are high, nucleation will occur by distribution of the drops on the surface of the particles, which will then start to coalesce, and nuclei with air trapped inside will be developed. Therefore, a better distribution of the binder within the agglomerates can be obtained by the distribution mechanism (see Figure II.4 (b.)).

With regard to the wetting and nucleation phenomena, Litster et al. (2001) postulated that three nucleation regimes exist: drop controlled regime, mechanical dispersion regime and intermediate regime. Based on this idea, Hapgood (2000), Hapgood et al. (2002) and Hapgood et al. (2003) proposed a nucleation regime map (*MRN*), reported in Figure II.5.

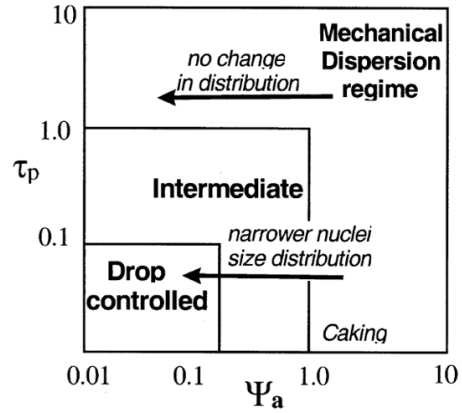

Figure II.5 *Nucleation Regime Map (MRN) (Hapgood et al., 2003)*

The Nucleation Regime Map is based on two key parameters: the drop penetration time (t_{dp}), in comparison to circulation time of the process (t_c), and the dimensionless spray flux (ψ_a). In particular, in *MRN* the dimensionless spray flux is shown on the horizontal axis (axis *y*) and a magnitude (τ_p) attributable to ratio between drop penetration time and circulation time is reported on the vertical axis (axis *x*).

The drop penetration time is the time taken for a drop of liquid to penetrate fully in the porous powder bed after its initial impact on surface and it is controlled by the formulation properties, as show in the eq. (II.4). In particular, it depends on both wetting thermodynamics, represented by the adhesion tension ($\gamma_{lv} \cdot cos\theta$), and the wetting kinetics, strongly affected by

the liquid viscosity (μ) and effective pore size (R_{eff}) of the powder bed. Moreover, it a function of the total volume of the droplets that are sprayed in the granulation section (V_d) and of the surface porosity (ε_{eff}), which may differ from the bed porosity (Parikh, 2016).

$$t_{dp} = 1.35 \cdot \frac{{V_d}^{\frac{2}{3}}}{{\varepsilon_{eff}}^2} \cdot \frac{\mu}{R_{eff} \cdot \gamma_{lv} \cdot \cos\theta} \quad \text{(II.4)}$$

The dimensionless spray flux is a measure of binder coverage on the powder surface and is defined by actual spray rate, or spray flux, in comparison to solids flux, or mixing rates. Litster et al. (2001) have quantified spray conditions as a function of process parameters, as shown in the eq. (II.5). In particular, in the spray zone, the drops sprayed by the nozzle at a given volumetric flow rate ($\dot{V}$) with an average drop size (d_d) cover a certain projected area of powder per unit time.

This area of droplets is distributed over some spray area on the powder bed surface. Moreover, if is used a flat spray perpendicular to the direction of powder flow, the powder flux through the spray zone ($\dot{A}$) is simply by eq. (II.6), where *v* is the speed of the powder after spray and (W) is the powder size after it has been wetted by the binder.

$$\psi_a = \frac{3 \cdot \dot{V}}{2 \cdot d_d \cdot \dot{A}} \quad \text{(II.5)}$$

$$\dot{A} = v * W \quad \text{(II.6)}$$

A high (ψ_a) value indicates that the binder was added too fast compared to the speed of the powder flow. In this case, the sprayed droplets will tend to overlap on the surface of the powder bed, causing coalescence and a wider nuclei size distribution is obtained. Instead, a low (ψ_a) value indicates that the ratio of powder flux to solution and the nuclei are swept out of the spray zone before being re-wet by another drop. Low values ($\psi_a << 1$) result in a well-dispersed binder where one a droplet tends to form one granule. However, low (ψ_a) is a necessary but not sufficient a condition for drop controlled nucleation because the drop must also wet the powder and have a small penetration time (Parikh, 2016, Iveson et al., 2001a, Litster et al., 2001).

In drop controlled regime of the *MRN*, the nuclei size distribution is essentially controlled by the drop size distribution: each individual drop wets completely and quickly into the powder bed to form a single nuclei granule (Guigon et al., 2007). In mechanical dispersion regime the nuclei size distribution is independent of the drop size distribution: binder distribution occurs only by breakage of lumps or granules due to mechanical forces

within the powder bed (Guigon et al., 2007). In intermediate regime the nuclei size distribution is sensitive to formulation properties and operating parameters. This regime is intermediate between drop controlled and mechanical dispersion: some agglomeration does occur in or near the spray zone without complete caking or pooling. This is a difficult regime to control (Guigon et al., 2007).

II.2.2 Consolidation and growth

The last decade has seen a rapid advancement in the understanding of growth and consolidation of the granules, mechanisms that occur simultaneously to the process of wetting and nucleation in agitated wet granulation processes. These phenomena may begin with the injection of the liquid binder on the powder bed and terminate or when all the solution has been injected or when the granulation process is completed.

Granule growth occurs when material in the granulator collides and sticks together by coalescence or layering (see Figure II.6).

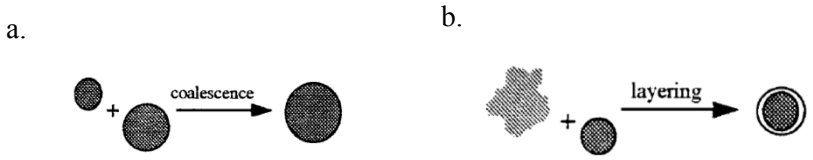

Figure II.6 *Granule growth: a. growth by coalescence; b. growth by layering (Ennis et al., 2007)*

The granule growth is traditionally referred to as coalescence when two large granules come together to form an entity with a largest size: the entity obtained has a volume equal to the sum of the volumes of the individual starting entities and its surface area is less to the sum of the surface areas of the individual entities. In particular, the coalescence occurs following the collision and consolidation of nuclei/granules deformable, provided that these then remain cohesive despite the cutting forces exercised by the impeller. Instead, it is termed layering when the sticking of fine material onto the surface of large pre-existing granules occurs: the layers increase the size of solid particles compared to the initial. Both the mixing of powder and binder and binder quantity contribute to the growth of the granule and to its consolidation. The mixing increases the probability of impact between the solid particulate and an increase in energy of mixing involves a greater consolidation of the granule. However, if the binder liquid is not introduced in sufficient quantity the growth is not promoted and the granule size is determined solely by the nucleation conditions. The distinction between these two mechanisms is arbitrary because it depends on the cut-off size used to demarcate fine from granular material (Iveson et al., 2001a).

As granules collide with other granules and are subjected to the action of mechanical moving parts of the equipment (blades or impellers), they gradually consolidate. The consolidation has a pronounced effect on granule properties. It reduces the granules size and porosity, increases their yield stress and also increases the pore saturation, which in turn increases granule plasticity and the availability of liquid at the granule surface. Therefore, the granules become harder, less deformable and more elastic with the consolidation.

Iveson and Litster (1998b) have proposed a granule growth regime map to seek describe the different growth behaviours exhibited by the granule on a their formulation properties basis (see Figure II.7).

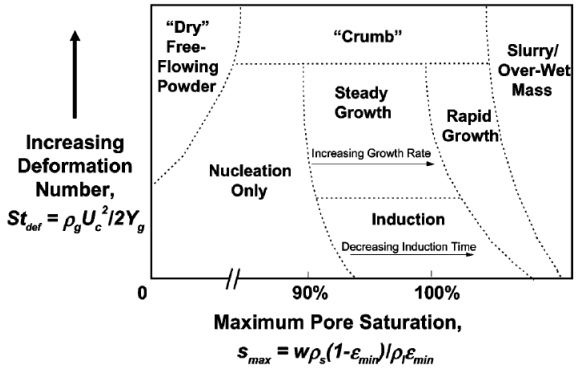

Figure II.7 *Growth Regime Map (GRM) (Iveson et al., 2001b)*

The granules growth behaviour depends on two parameters: the maximum pore saturation and the granule deformation during impact. In particular, in growth regime map the maximum pore saturation is shown on the horizontal axis (axis *y*) and the Stokes deformation number, parameter attributable to granule deformation during impact is reported on the vertical axis (axis *x*).

The maximum pore saturation (s_{max}) is a measure of the amount of liquid present in the pores inside the granules and it is determined by eq. (II.7), in which (w) is the liquid to solid mass ratio, (ρ_s) is the solid particles density, (ρ_l) is the liquid density and (ε_{min}) is the minimum porosity the formulation reaches for the operating conditions set.

$$s_{max} = \frac{w \cdot \rho_s \cdot (1 - \varepsilon_{min})}{\rho_l \cdot \varepsilon_{min}} \qquad \text{(II.7)}$$

The amount of deformation during impact was characterised by the Stokes deformation number (St_{def}). The Stokes deformation number is a measure of the ratio of impact kinetic energy to the plastic energy absorbed per unit strain and it is calculated by eq. (II.8). It takes into account both the

process agitation intensity (see U_c in eq. (II.8) that is a representative collision velocity in the granulator) and the granule properties (see ρ_g and Y_g in eq. (II.8) that are the granule density and the granules dynamic yield stress, respectively).

$$St_{del} = \frac{\rho_g \cdot U_c^2}{2 \cdot Y_g} \qquad \text{(II.8)}$$

Iveson and Litster (1998b) postulated that two were the main granules growth behaviour: steady growth and induction growth. When the granules are weak and deform easily occurs the steady growth, i.e. the average granule size increases steadily with time, forming large areas of contact during collision. Induction growth, also called the nuclei region (Kapur, 1978) or compaction stage (Hoornaert et al., 1998), is when there is a long period of little or no growth, followed by a period of rapid growth. Generally, the induction period can be reduced increasing the binder content. Other types of behaviour include: nucleation only (Butensky and Hyman, 1971) when after the initial nuclei formation, the binder is not enough to obtain the next phase of growth; crumb behaviour occurs when the formulation is too weak to form stable granules, in fact, products in the form of "crumbs" are obtained; and over-wetting when the binder content is in excess to that required and oversaturated slush or slurry are produced (Iveson et al., 2001b).

II.2.3 Attrition and breakage

Capes (1965) and Sastry et al. (1977) have carried out some of the early studies of attrition and breakage phenomena in the wet granulation process, stating that crushing and layering are the mechanisms by which granules grow in tumbling drum granulators (Reynolds et al., 2005). Nowadays, these mechanisms are generally considered as attrition and breakage by Ennis and Litster (1997) (see Figure II.8 (a. and b.), respectively).

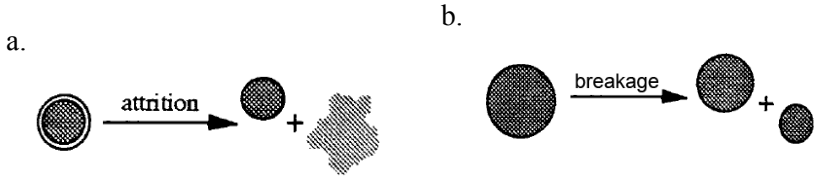

Figure II.8 *Mechanisms of granules size reduction: a. attrition; b. breakage (Ennis et al., 2007)*

Breakage and attrition occur when the wet or dry granules, too large or weak and brittle, deform or break due to shear and impact forces: small particles are produced, generating new nuclei or granules that re-enter the cycle (Abberger, 2007, Chitu et al., 2011, Iveson et al., 2001a, Iveson et al.,

2001b). In particular, the dry granules by attrition between themselves and with the granulator walls undergo superficial erosion, which leads to reduction of granules size and the reformation of powder fines situation to be avoided because the aim of most granulation processes is to remove fines (Iveson et al., 2001a). On the other hand, breakage of wet granules is a function of the hardness of the granules and of the shear force to which they are subjected. If the impact force is greater than the resistance of the granule, this will break into smaller granules. Breakage influences and controls the final granule size distribution and, in some circumstances, can be used to limit the maximum granule size or to help distribute a viscous binder (Iveson et al., 2001a). Breakage for wet granulation processes have not been widely studied in the past. There is very little quantitative theory or modelling available to predict conditions for breakage, or the effect of formulation properties on wet granule breakage (Tan et al., 2004, Fu et al., 2005, Reynolds et al., 2005). Discrete element simulations have also been extensively used to predict the granule breakage behaviour (Moreno-Atanasio and Ghadiri, 2006, Ning and Ghadiri, 2006). Tardos et al. (1997) and Keningley et al. (1997) have presented the only two serious attempts to predict conditions for breakage of wet agglomerate. Tardos et al. (1997) used the Stokes deformation number as a criterion for granule breakage, according to which granules will deform and break in shear fields if there is sufficient externally applied kinetic energy (Iveson et al., 2001a, Tardos et al., 1997). Keningley et al. (1997) developed a relationship for breakage crumb, paste or survival of granules in high shear mixer granulation by equating the kinetic energy of impact to energy absorbed by plastic deformation of granules (Iveson et al., 2001a, Keningley et al., 1997).

II.3 Apparatuses and technologies in wet granulation

On the basis of the shear strength it generates on the powder bed during the wet granulation process, the most common apparatuses used for granules production are classified into the following three major categories: 1) tumbling granulator; 2) both batch and continuous low and high-shear mixer granulator; 3) medium-shear granulator, for example, fluid-bed granulator (Parikh, 2016). In tumbling granulators (including discs, drums, pans and similar equipment) the particles motion is assured by the tumbling action caused by the balance between gravity and centrifugal forces. In particular, the powder feed is fed to the disc, typically at the edge of the rotating granular bed, and the binder is added through a series of nozzles distributed across the face of the bed. Discs and drums generally operate continuously and have large throughputs, thus they are extensively used in mineral processing and fertilizer granulation (Litster and Ennis, 2013). Low and high shear mixers are mechanically agitated containers that promote an efficient mixing, especially of cohesive materials. Such mixers exert intense local

shear force actions on the powder which break the small cohesive aggregates, promoting good dispersion of the liquid and effective consolidation of the product (Nalesso et al., 2015). The low-shear granulators generate lesser shear than medium or high shear granulator, because of agitator speed (lower than 100 rpm), sweep volume, or bed pressures on the powder bed. For example of low-shear granulators include ribbon and paddle blenders, planetary mixer granulators, orbiting screw granulators, sigma blade mixer and rotating-shape mixer/granulators (Parikh, 2016). The high-shear granulators consist of a mixing bowl with shape cylindrical or conical, a three-bladed impeller, and an auxiliary chopper. The impeller is employed to mix the dry powder at a speed ranging from 100 to 500 rpm and to spread the granulating fluid. The chopper is used to break down the wet lumps into granules with a rotation speed ranges from 1000 to 3000 rpm. On the basis of the orientation and the position of the impeller, his granulator can be both vertical and horizontal (Parikh, 2016). In fluid bed granulators, the powder bed is first fluidized by a flow of air injected upward through a distributor plate at the base of the granulator, and then the liquid binder is sprayed through a nozzle onto the fluidized bed to agglomerate powder in granules. When binder spraying is stopped, the granules continue to dry in the fluidizing airstream, avoiding the use of a following drying step (Morin and Briens, 2014). This type of granulator is flexible, relatively easy to scale, difficult for cohesive powders, and good for coating applications (Parikh, 2016).

Traditional wet granulation method involves spraying of liquid binder onto a moving powder bed to granulate the powder particles in the granulator. New alternative methods were developed in over years, such as steam granulation, moisture-activated dry granulation, thermal adhesion granulation, melt granulation, freeze granulation, foam granulation, and reverse wet granulation (Shanmugam, 2015, Agrawal and Naveen, 2011, Solanki et al., 2010, Saikh, 2013). The steam granulation exploits water steam as binder, providing a more rapid diffusion into the powder and a more favourable thermal balance during the drying step. Equipment such as high speed mixer with steam generator/regulator would be enough for this technique, even if this method requires high energy inputs for steam generation (Shanmugam, 2015, Hammer, 1984, Albertini et al., 2003). The moisture-activated dry granulation adds a very little water, usually less than 5 % (1-4 % preferably), to the mixture of drug, binder and other excipients in order to facilitate the agglomeration. This technique could not be used for the preparation of granules that require high drug load and for moisture sensitive drugs and hygroscopic drugs. A high-shear mixer coupled with a sprayer would be suitable equipment for the moisture-activated dry granulation process (Takasaki et al., 2013, Shanmugam, 2015). The thermal adhesion granulation uses both water and solvent as granulation liquid and the heat to facilitate the process. This technique is not suitable for all

binders, is sensitive to thermolabile drugs and requires considerably high energy inputs and special equipment for heat generation and regulation. A tumble blender or similar equipment coupled with heating system is suitable for this process (Lin et al., 2008, Shanmugam, 2015). Melt granulation, also defined as thermoplastic granulation is a good alternative to wet granulation for water-sensitive materials. Here is used a molten binder as granulation fluid to establish liquid bridges between particles in a heated powder bed. The major drawback of this process is the need of high temperature during the process, which can cause degradation and/or oxidative instability of the ingredients, especially of the thermolabile drugs. High-shear mixer and fluidized bed granulator are the equipment that could be used for melt granulation. (Guigon et al., 2007, Shanmugam, 2015, US et al., 2013, Parikh, 2016, Chen et al., 2014). Freeze granulation technology involves the spraying a powder suspension into liquid nitrogen: the sprayed drops are instantly frozen into granules, and in the subsequent freeze drying process, the granules are dried by sublimation of ice without any segregation effects. The spray freezer coupled with freeze dryer is the equipment more used (Stuer et al., 2012, Shanmugam, 2015). The foam granulation technique involves the addition of liquid/aqueous binder as foam instead of spraying or pouring liquid onto the powder particles. Standard equipment such as high/low shear mixer or fluidized bed granulator coupled with foam generator/regulator could be used for this technology (Tan and Hapgood, 2011a, Tan and Hapgood, 2012, Tan and Hapgood, 2011b, Shanmugam, 2015, Cantor et al., 2009). The reverse wet granulation technique is generally performed in a high speed mixer and involves the immersion of the dry powder formulation into the binder liquid followed by controlled breakage to form granules (Shanmugam, 2015).

II.4 Parameters in wet granulation process

Several parameters can play a fundamental role on the basic mechanisms of wet granulation and therefore on the product final properties (Guigon et al., 2007). In particular, granule features depend on formulation ingredient (binder and powder properties and their interaction and proportion), and operating variables. These latter depend on the used apparatus and have an impact on mixing, agglomerating, and drying operations. For example, process variables in fluid bed granulators agglomeration is highly dependent on: process inlet air temperature; atomization air pressure; fluidization air velocity and volume; liquid spray rate; nozzle position and number of spray heads; product and exhaust air temperature (Bareschino et al., 2017). Inlet process air temperature depends on both the binder type and the heat sensitivity of powder bed: higher temperatures will cause binder faster evaporation with the relevant production of smaller and friable granules (Srivastava and Mishra, 2010). Process variables in high/low-shear mixers

are essentially related to the impeller and chopper relative speed, amount of added granulating solution, both global granulation and wet-massing time (Badawy et al., 2000). Thus, both material and operating variables together define the kinetic mechanisms and rate constants of wetting, growth, consolidation, and attrition (Parikh, 2016). Therefore, optimization of these variables can improve the performance of the system in order to obtain the maximum benefit from it, for example in terms of yield, size or granules flowability properties, without increasing the process costs.

This section is concerned with the effects of formulation and operating variables in high/low-shear mixers.

II.4.1 Feed material properties

II.4.1.1 Powder properties

Powder particles size influences the amount of binder to be used, the dynamic yield stress, porosity, size and growth rate of granules. There is an inverse relationship between the minimum amount of binder and powder size: a larger liquid amount is required to establish liquid bridges between the powders of lower size, thus with a high surface area (Schaefer et al., 1990, Bellocq et al., 2018). However, a larger solubility of the solid excipient in the granulating solvent is able to decrease the solvent amount needed for granule formation, and granules with uniform particle size distribution and a reduced friability will be formed (Sakr et al., 2012). According to Van den Dries and Vromans (2002), the dynamic yield stress of a granule is directly proportional to the particle surface area and is inversely proportional to the particle size and to the intragranular porosity. This means that the high surface area allows the availability of more contact points between colliding particles bringing as final result to stronger granules, which however have a less porous structure (Iveson and Litster, 1998b, Iveson et al., 1996, Iveson and Litster, 1998a). Perhaps the larger surface area allows also a higher growth tendency of the smaller particle fraction probably due to a more efficient nucleation and coalescence (Badawy and Hussain, 2004). According to Mackaplow et al. (2000) primary particle size had a strong effect on granule growth rate, granule porosity, and wet granule size distribution: larger primary particles produce weaker, more deformable wet granules, favoring growth by coalescence and/or crushing and layering.

II.4.1.2 Binder phase properties

Binder viscosity and surface tension are the properties which more influence the granulation process because the collision energy necessary to agglomerate particles depends on them (Sakr et al., 2012, Bertín et al., 2018). Binder viscosity is important in understanding both granulation mechanisms involved and strength of the resulting granules(Chitu et al.,

2011). In particular, the mechanisms of agglomerate formation and growth depend on the interaction between powder particle size and binder viscosity: powder with a large particle size need a high viscosity binder in order to achieve an agglomerate strength that is sufficient to prevent the breakage of agglomerates (Johansen and Schæfer, 2001). According to Johansen and Schæfer (2001) the growth mechanisms as nucleation and coalescence predominate in the agglomeration of small powder particles with low viscosity binder. When the binder viscosity becomes very high, immersion of particles in the binder droplets will be the agglomerate formation mechanism dominating, and growth will proceed by continued layering of particles on the surface of the agglomerates. According to van den Dries and Vromans (2002), the tensile strength of a granule under dynamic conditions is directly proportional to the viscosity of the binder liquid. Moreover, several authors have shown that an increase in viscosity has a benefit effect on granulation up to a certain critical value (Mills et al., 2000, Johansen and Schæfer, 2001). A higher binder solution viscosity could lead to larger granule size and less needed binder amount to start the granule growth in both high-shear (Hoornaert et al., 1998, Schæfer et al., 2004) and fluid-bed (Ennis and Litster, 1997) granulation processes. This is due to the fact that a high liquid viscosity requires more energy to break up the liquid droplets (less binder spread ability), hence larger droplets are formed, which consequently give larger granules. However, at too high viscosity, droplets will be unable to spread throughout the bed causing the reduction in collisions and relevant growth (Seo et al., 2002).

Surface tension and capillary forces always act to pull particles together, and their magnitudes depend on the liquid bridge formed between the particles (Fan et al., 2009). Ritala et al. (1986) found that the power consumption of the granulator increases with increasing binder surface tension. According to Ennis et al. (1991) granulation mechanisms depend essentially on the competition between the capillary and viscous forces. According to Iveson and Litster (1998b) the reducing binder surface tension causes the decrease in the capillary suction pressure and friction resistance, leading therefore to an improved wettability and spreading efficiency. However, also the solvent used for the formulation of the binder solution (only water, alcoholic or hydroalcoholic solutions are usually used) could significantly change granule properties for its impact on binder wettability and spread ability (Sakr et al., 2012).

II.4.2 Operating variables

II.4.2.1 Liquid to solid ratio and binder addition rate

It is well known that the wet granulation is induced by a liquid phase, necessary for binding the powder particles and making the wet mass more deformable (Bouwman et al., 2005). Therefore, it is natural to think that an

increase of liquid during the granulation could help and improve the results of the process. This is not completely true! It is important define the ratio between the liquid and solid phases to achieve granules with tailored features (Verstraeten et al., 2017). If the liquid/solid ratio increases (due to a high amount of used liquid) nucleation is favored, but at the same time it is possible that over-wetting phenomena may occur, with consequent formation of a mixture and not granules, a situation which must be avoided. Moreover, as the quantity of the added liquid increases, the granule saturation, i.e. the ratio between the liquid volume and the interstitial granule volume, changes. However, the addition of too much liquid implies a larger granules size because of a high saturation, in the same way a low saturation does not allow the granules to growth. Some of the literature work also shows that the amount of liquid to be added is inversely proportional to the size of the powder particles to be granulated: the needed amount of liquid must be increased as the size of the powder particles decreases (Guigon et al., 2007, Sarkar and Chaudhuri, 2018, Walker et al., 2006). Others have recognized that increasing the binder addition rate increases the granule size and the granule bulk density due to increased penetration and wetting by the binder solution (Oulahna et al., 2003). In contrast, Benali et al. (2009) shown that the increase in the binder addition rate does not affect the granule mean size.

II.4.2.2 Binder phase delivery method

Binder addition method can have an impact on the growth and properties of granules (in terms of shape, density, drug content, particle size, porosity, flowability, segregation and friability) and is therefore of vital importance to the understanding of wet granulation process (Morkhade, 2017, Osborne et al., 2011). The addition of the binder phase can take place in three different ways, i.e. by pouring, by spraying, or by making it melt, and it is closely linked to the nucleation regime, which has in turn a substantial effect on the product final features (Knight et al., 1998, Morkhade, 2017). Both when pouring and when spraying the *PSD* is initially bimodal and it tends to be unimodal for high granulation times (Oka et al., 2017, Knight et al., 1998). In melting technique, however, the obtained granules will be less coarse compared with the pour-on technique and only for high granulation times a bimodal distribution will develop (Guigon et al., 2007, Osborne et al., 2011). A uniform liquid spray with small droplets size will have the greatest coverage throughout the powder bed and will prevent localized over wetting of the granules, which can result in oversized particles (Parikh, 2016). Holm (1987) found that liquid addition without atomisation gave rise to inhomogeneous liquid distribution (especially at low impeller and chopper speeds) and that the atomisation of the binder led to better liquid distribution.

II.4.2.3 Impeller rotation speed

The speed with which the powder is mixed in the granulation section effects the final granules properties: a good mixing allows a better distribution of the binder phase on the powder bed (Salman et al., 2006a). For a high-shear mixer, the amount of energy input into the system can be increase through the impeller and the chopper, which blades rotate at low and high speed, respectively. According to Schæfer et al. (1993) the impeller speed produces no significant difference on the intra-granular porosity, in contrast, the use of chopper produces granules with a size slightly smaller but no create significant effect on the intra-granular porosity or the granule size distribution. According to Knight et al. (2000) the granule growth is limited by breakage phenomena if the powder is mixed at high impeller speeds, while, the chopper narrows the granule size distribution if used after the nucleation phase. According to Benali et al. (2009) the impeller rotational speed has a great importance on granule growth. An optimal interval of impeller speed operation exists ranging from 150 to 200 rpm: uncontrollable agglomerate size and localized over-wetting are obtained to low shear granulation (40 and 100 rpm), instead, for impeller speed higher than 200 rpm the mechanism of the granule breakage occurs. According to Oulahna et al. (2003) the higher the impeller speed, the lower is the porosity and friability of the granules, and the narrower is the size distribution.

In addition to mixing the impeller and chopper are also responsible for the energy input in the process. Therefore, the influence of the impeller speed and of the chopper speed on the final granule properties depends on how the granules respond to the energy input of the process. Several researchers (Knight, 1993, Knight et al., 2000) shown that the granule size and growth rate increase if the increase in impact energy causes in more deformation of the granules. In contrast, at high-energy inputs, where granule deformation leads to granule breakage, a decrease in granule size is observed when the impeller speed is increased (Schaefer et al., 1990, Knight et al., 2000, Ramaker et al., 1998).

II.4.2.4 Process time

At first glance, it would be expected that higher process time causes an increase in granule size and a narrower granule particle size (Knight et al., 1998, Knight et al., 2000, Schæfer and Mathiesen, 1996). However, some studies have evidenced that not always an increase in the process time results in an increase in granule size because a granulation carried out for long times can lead to a reduction in the size of the solid particulate due to breaking phenomena (Salman et al., 2006a). According to Hoornaert et al. (1998) the granules formation is characterized by an initial period of no granule growth in which the granules become more densified (consolidation) due to the repeated impacts of the mixer arms on the granules, while the saturation is

still too low to cause granule growth. This period could last until the saturation is sufficient to promote granule coalescence and sometimes is followed by a rapid granule growth phase. Due to the densification the interstitial granule volume is reduced because the constituent particles within the granule becoming more closely packed. That is also the reason that usually a pronounced decrease in porosity is observed during the initial process time, whereas almost no change is observed at prolonged process times (Knight et al., 1998, Schæfer and Mathiesen, 1996, Scott et al., 2000).

Generally, the process time is defined by a "addition binder time" and a "wet massing time". Addition binder time is a term used to describe the period of binder addition and it is given by the ratio between binder addition amount and binder addition rate. Wet massing time is the term used to describe mixing that takes place in the granulator after granulating liquid addition is complete. Some researchers have shown that these times have impact on the granules, in terms of growth, morphology, porosity and granule particle size. Badawy et al. (2012) have investigated that increasing wet massing times can increase coalescence and growth of the granules with a significant effect on granule densification, but at the same time can lead to enhanced breakage. Moreover, the increase in binder addition time has minimal impact on granule porosity. According to Oka et al. (2015) the wet massing time exhibits an inverse correlation to granule porosity.

II.5 Mathematical approach to describe the phenomena involved in wet granulation

Mathematical models, in particular, one based on the physics of process, are essential tools to design, optimization and control of product and process. The success of mathematical models relies on their predictive capabilities.

As been seen above, wet granulation is a process described by three principal mechanisms occurring simultaneously in a granulator (Iveson et al., 2001a): wetting and nucleation; consolidation and growth; attrition and breakage. These mechanisms control the final granule properties and are influenced by a combination of formulation design (feed-materials properties) and process design (operating conditions). Therefore, an integrated model that accounts for these major sub-processes, as well as the effects of the formulation and process variables, can enable an analysis of the system dynamics and the formulation of a suitable control strategy, thereby avoiding inefficient operation (Poon et al., 2008). There are several approaches to modeling the wet granulation process. At one extreme we have mechanistic modeling, called "white box" approach. At the other end of we have the empirical modeling, called "black box". In between we have the so-called "grey box" models, which represent that is really developed.

The empirical models are obtained from the regression of large set of experimental data at fixed time intervals, which derive from the design of

experiments statistic technique (see Chapter IV, paragraph IV.1.4.3), (Aleksić et al., 2014, Mangwandi et al., 2013a). The model is built by selecting a model structure and then fitting the model parameters to get the best fit of the model to the experimental data. Various information criterion like that of Akaike (1970) can be used to understand if the increase in the number of parameters (regression coefficients) really improves the prediction of a model. Empirical models have the advantages of being very simple (often polynomial equations), easy to obtain (regression of data), quite reliable within the investigated range. The drawback of this approach is that it is a black box approach: the application range of such a model is limited to the range of data and thus it provides very little (or none) information on the underlying mechanisms. Therefore, this approach can be very useful if is needed a model quick to be used for a control application without no significant insight of the process physic (Cameron et al., 2005).

The mechanistic models are more complex and required more time respect to empirical models because they seek to incorporate the physics and chemistry into the models. The mechanistic model, as above reported, is the so-called "white box" approach that applies both the thermodynamic conservation principles for mass, energy and momentum, and the population balances to track particle size distributions as various particulate phenomena take place, and develops appropriate constitutive relations that define the particle growth and breakage mechanisms, i.e. intensive properties, mass and heat transfer mechanisms. Inevitably, even the best mechanistic models require some data fitting, as well as must be must be available adequate data to carry out the validation studies. This leads to the concept of "grey box" models (Cameron et al., 2005).

Table II.1 gives a comprehensive overview of models used mainly for wet granulation but also for dry powder mixing, with their respective characteristics, advantages and disadvantages.

Apart from the empirical models, the Discrete Element Method (*DEM*) models and the Population Balances Equations (*PBEs*) are the modeling approaches more used.

DEM models are the most detailed type of mathematical model for particulate systems (Sen et al., 2014). Thanks to mass and momentum balances on each particle of the powder bulk, *DEM* models aim to describe the evolution of the analysed system. There are four main classes of discrete element models: cellular automata, Monte Carlo methods, hard-particle methods, and soft-particle methods (Ketterhagen et al., 2009). The advantage is that the description is very detailed (as each particle is tracked individually) but it is so computational power demanding that rarely it is applied to systems of more than hundreds of thousand particles. They are often used to obtain parameters useful for higher scale models (Lee et al., 2017).

Table II.1 *An overview of different granulation models ranging from pure empirical to more or less mechanistic ones (Björn et al., 2005)*

	Method	**Characteristics**	+/-
Empirical	Multivariate process modelling	Statistical models	+Good results within experimental space -Totally empirical
	Relative swept volume	Relative swept volume held constant during scale-up	+Simple to use -Weak physical relevance
	Tip speed	Tip speed held constant during scale-up	+Simple to use -Weak physical relevance
	Dimensionless impeller work	Different dimensionless numbers held constant during scale-up	+Simple to use -Weak physical relevance
	Normalized impeller work	Energy/mass=const	+Theoretical relevance -Calibration required
	Powder consumption and/or temperature	Power consumption as end point	+New, promising -Macroscopic
	Integrated powder over time	Mixer work as endpoint	+New, promising -Macroscopic
	Solid mechanics models	Friction models	+Mechanistically derived -Dry powders only
	Population balances	Coalescence probability Coalescence factors functions of process variables	+Mechanistically derived -Some empirical fitting required
Mechanistic	*DEM* models	Flow patters	+Mechanistically derived -Few particles in models

The *PBEs* based models are widely used for granulation (Ennis and Litster, 1997, Adetayo and Ennis, 2000, Adetayo et al., 1995, Iveson, 2002, Darelius et al., 2005, Sanders et al., 2003) and in other particle formation and growth processes, such as aggregation (Smit et al., 1995), crystallization (Ranodolph, 2012), pelletization (Sastry and Fuerstenau, 1970) and aerosol production (Landgrebe & Pratsinis, 1989) (Landgrebe and Pratsinis, 1989). In them the powder bulk is described as a population with a distribution of

certain characteristics (internal coordinates i.e. size, binder content) that can vary in space (external coordinates) and time (Ramkrishna, 2000). Therefore, the *PBEs* based models describe the evolution of the number of particles of a given characteristic in time and space (Abberger, 2007) and require a less computational power respect to the *DEM* models, despite the complexity of the involved equations (integro-differential). Less computational demanding methods, like the method of moment (which focus only on the moments of distributions), are preferred when the *PBE* has to be combined with Computational Fluid Dynamic (*CFD)* models to describe the multiphase flow (i.e. the movements inside the granulator) (Marchisio and Fox, 2013).

II.6 Chapter II remarks

In this chapter, a literature overview was reported on topics related to:

- phenomena involved in wet granulation;
- devices and techniques used for wet granulation with the relative discussion of the process parameters that have a primary role in granule formation;
- modeling approaches able to describe/predict the granules formation/their characteristics.

In the light of these analyzes, it was possible to better address the research developed in the activities described in the following chapters.

Chapter III
Methodologies and experimental apparatus set up

III.1 Generalities

In this chapter, the discussion of the methodologies and experimental apparatus used for all the granulation campaigns, carried out in order to observe the phenomenological aspects involved in the wet granulation process, is reported. Therefore, in the following chapters the experimental procedures and set-ups used will only be recalled and briefly described.

III.2 Granulation experimental set up layout

In this Ph.D. thesis, a bench scale granulation apparatus was designed and realized in order to obtain product granular and study the wet granulation process. In Figure III.1 shows a schematization of the designed and realized experimental apparatus. Four are the main sections composing the realized experimental set-up: a feeding section, a production section, a stabilization section and a separation section.

The feeding section consists in two independent lines: the first includes a tank, filled with binder phase, and a peristaltic pump, indicated as elements T-1 and P-1 in Figure III.1 respectively; the second line regards the powder to feed to granulator. The binder phase is conveyed in a silicon tube, through the single head peristaltic pump (SP 311 Peristaltic Pump, VELP Scientifica). The silicon tube has an internal diameter of (1.6 mm), a thickness of (1.6 mm), a length of (35 cm), it is able to withstand an operating temperature range from -50 to 200° C (it is suitable for pharmaceutical and food applications) and it ends by a stretch of plastic, not flexible, tubing. The peristaltic pump is made by a polyamide, acetal and stainless pump head and a permanent magnet gear-motor. Among the several pumping systems (gear pumps, piston pumps, syringe pumps, gravity

systems, pressurized canisters), peristaltic pump was chosen because it offers many advantages: it can pump different fluid kinds, in large amount and with a flow rate that can be modulated accurately and kept constant; the pump components does not interact with the treated fluid and thus the cleaning and the changing of tube are easy and quick; lastly it is suitable for large-scale processes (Dalmoro et al., 2014). The used peristaltic pump is able to modulate ten fluid flow rates, ranging from 4 ml/min to 62 ml/min if the pumped fluid is distilled water.

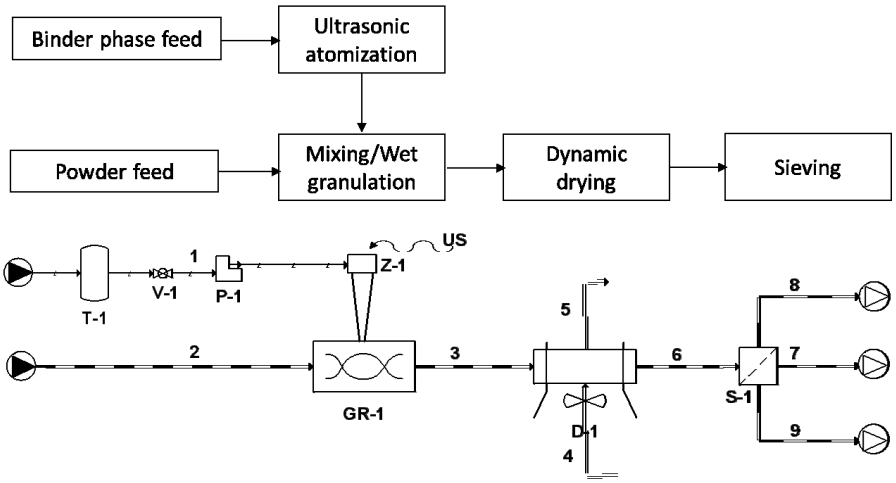

Equipment	
D-1	Fluid-bed dryer
GR-1	Low-shear granulator
P-1	Pump for binder phase
S-1	Sieve
T-1	Binder phase tank
V-1	Valve
Z-1	Ultrasonic atomizer
Key to abbreviation	
US	Ultrasound source

Line	
1	Binder phase
2	Powder
3	Wet granules
4	Hot air
5	Cold air
6	Dry granules
7	Dry granules (size between 0.45-2 mm)
8	Dry granules (size greater than 2 mm)
9	Dry granules (size lower than 0.45 mm)

Figure III.1 *Process schematization of granules production through the wet granulation technique; the main sections are reported: the liquid binder phase (1) is pushed through peristaltic pump to the ultrasonic atomizer (Z-1), which sprays it on the powders (2) placed in the low-shear granulator (GR-1), where the wet granules (3) are formed. Then, the wet granules are subjected to the dynamic drying process (D-1), using hot air (5). After this step, the obtained dry granules (6) are separated by sieves (S-1) in three fractions (7-8-9). Finally, only the fraction of interest (7) is recovered and characterized*

In the production section the granules are formed. It includes a granulator (GR-1 in Figure III.1) and an atomizer assisted by ultrasonic energy (Z-1 in Figure III.1). The granulator is a vertical low-shear mixer with two impellers and a bowl. In this latter the powder is placed to be granulated. It has five mixing speeds, i.e. 72-78-93-102 and 112 rpm. The atomization device (VCX 130 PB Ultrasonic Processors 130 W, 20 kHz, mean droplet size of 90 μm – @ 20 kHz, Sonics &Materials Inc., CT, USA), is connected to an ultrasonic generator (broadband ultrasonic generator mod. 06-05108-25k Sono-Tek corporation) that converts energy into vibratory mechanical motion. The atomizing nozzle is connected to the feed line of binder phase (line 1 of Figure III.1) through the end part of silicone tube. It allows to improve the degree of binder phase dispersion on the surface of powder bed and to operate under controlled conditions of size distribution of liquid droplets (mean droplet size: 90 μm – @ 20 kHz).

The stabilization section is made by a dynamic drying device (D-1 of Figure III.1) which uses a hot air flow to evaporate the residual moisture from the granules, slowing down their degradation and the development of mould and bacteria. In particular, at first, the granules stabilization process was carried out in a home-made dynamic dryer that had the disadvantage to dry low amount of granules (about 10 g) in large times (about 1 hour at 65 °C). Therefore, the stabilization section was improved and a fluid bed dryer was selected and purchased (Fluid Bed Dryer TG 200, Verder Scientific, Italy). By this device, temperature (40-130 °C, depending on air throughput rate), drying time (5-20 min, depending on product type, amount, and moisture content) and air flow can be set digitally and adjusted continuously. The air flow depends on the fan power levels (minimum level is 10, maximum level is 99). This device allows stabilizing about 25 g of granules for each granulation batch, obtaining low moisture in short times (about 10 minutes at 65 °C). In particular, the hot air stream is supplied to the bed with the maximum level of the fan power for the first three minutes, after, it is reduced (level 35) and kept constant until to 10 minutes, to avoid excessive drag and friction between the granules.

In the separation section (S-1 in Figure III.1) is assessed a first one particle size distribution of the dry granular material. It consists in a manual sieving with two standard sieves (cut-off sizes of 0.45 and 2 mm) and a collection pan. Approximately 10 g of dry granules are put on the sieve with cut-off size of 2 mm and shaken for 5 min. Three granules fractions were obtained by this separation method: a “big scrap (B_p)” (line 8 in Figure III.1), i.e. % w/w of dry granules with size greater than 2 mm; a “useful fraction or product yield (y_p)” (line 7 in Figure III.1), i.e. % w/w of dry granules within the size range 0.45-2 mm; a “small scrap (S_p)” (line 9 in Figure III.1), i.e. % w/w of dry granules with size lower than 0.45 mm. The range size 0.45-2 mm was considered as the fraction of interest being a size typical range of commercial granulated food, pharmaceutical and

zootechnical products. A similar range size was taken into account in other several literature works (Albertini et al., 2004, Chevalier et al., 2010, Hussein et al., 2008).

III.3 Granules manufacture

III.3.1 Preparation of unloaded granules

The unloaded granules were prepared by using the wet granulation process and applying dedicated protocols of stabilization and separation, as described in the paragraph III.2. Briefly, the powder was placed in a laboratory scale low-shear granulator and agglomerated by spraying the binder phase, under controlled conditions of flow rate, exploiting an ultrasonic atomization device. Based on the preliminary studies, granulation time for all experiments was of about 20 minutes. The powder amount (each batch: 50 g), the frequency (20 kHz) and the ultrasonic energy amplitude (45 %) of the atomization device were kept constant. The spray time was defined by the ration between binder phase volume and binder phase flow rate. The impeller rotation speed, the binder to powder ratio and the binder phase flow rate were varied to assess their impact on the resulting granulated product.
The produced wet granules were underwent stabilization by dynamic drying, collected and then separated by sieving. Finally, only the useful fraction (size 0.45-2 mm) was subjected to characterization protocols carried out adopting both the *ASTM* (American Society for Testing and Materials) standards and ad hoc developed methods.

III.3.2 Preparation of loaded granules

The loaded granules were achieved by using the same production procedure of unloaded granules (see paragraph III.3.1). However, the feeding section was modified. The active molecule was incorporated in the granules by two different loading methods: method 1 and method 2.

According to the method 1, the active molecule was fully dissolved in the binder phase using a magnetic stirrer (Arex Heating Magnetic Stirres, VELP Scientifica) (M-1 in Figure III.2). In this case, the binder phase was a solution containing active molecule (line 1 in Figure III.2), which was sprayed on the powder bed.

According to the method 2, the active molecule was conveyed together with the powder in the granulator (line 2’ and 2 in Figure III.3, respectively). Molecule and powder was pre-mixed at an impeller rotation rate of 78 rpm for 10 min. In this case, the powder bed was made of a powder-active molecule mixture.
The payload percentages were defined in agreement with eq. (III.1).

$$payload = \frac{mass\ of\ active\ molecule\ (g)}{mass\ of\ active\ molecule\ (g)\ +\ mass\ of\ HPMC\ powder\ (g)} \cdot 100 \qquad \text{(III.1)}$$

For each batch the mass of powder was 50 g. The mass of active molecule was the initial amount of molecule included in the formulation, which depend on the investigated payload.

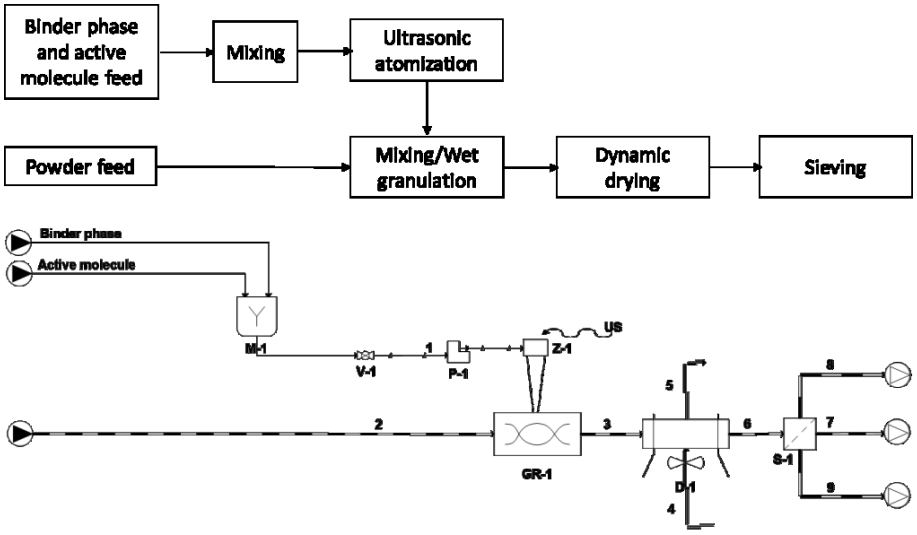

Equipment	
D-1	Fluid-bed dryer
GR-1	Low-shear granulator
M-1	Magnetic stirrer
P-1	Pump for binder phase
S-1	Sieve
V-1	Valve
Z-1	Ultrasonic atomizer
Key to abbreviation	
US	Ultrasound source

Line	
1	Binder phase with active molecule
2	Powder
3	Wet granules
4	Hot air
5	Cold air
6	Dry granules
7	Dry granules (size between 0.45-2 mm)
8	Dry granules (size greater than 2 mm)
9	Dry granules (size lower than 0.45 mm)

Figure III.2 *Process schematization of loaded granules production according to the method 1 (dissolution of active molecule in binder phase)*

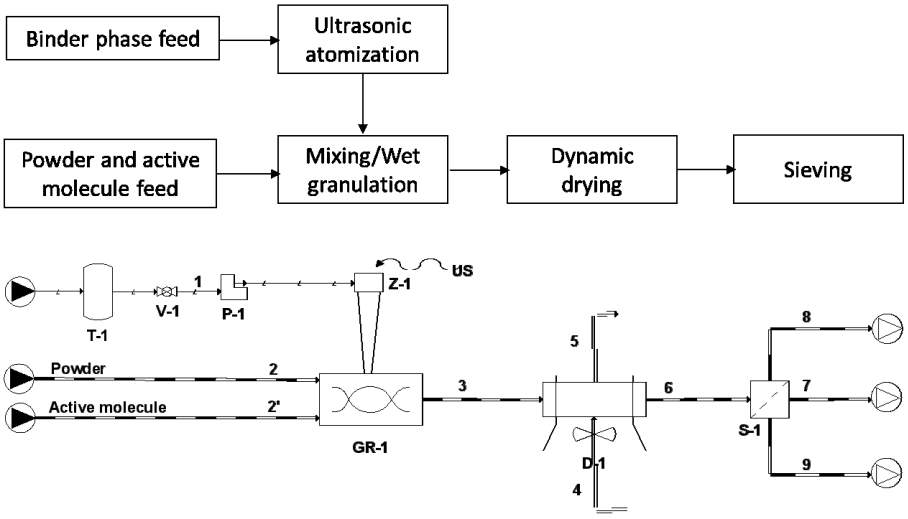

Equipment	
D-1	Fluid-bed dryer
GR-1	Low-shear granulator
P-1	Pump for binder phase
S-1	Sieve
T-1	Binder phase tank
V-1	Valve
Z-1	Ultrasonic atomizer
Key to abbreviation	
US	Ultrasound source

Line	
1	Binder phase
2	Powder
2'	Active molecule
3	Wet granules
4	Hot air
5	Cold air
6	Dry granules
7	Dry granules (size between 0.45-2 mm)
8	Dry granules (size greater than 2 mm)
9	Dry granules (size lower than 0.45 mm)

Figure III.3 *Process schematization of loaded granules production according to the method 2 (pre-mixing of active molecule with the powder at 78 rpm for 10 min)*

III.4 Techniques of Design of Experiments

The techniques of Design of Experiment (*DoEs*) are engineering typically approaches which combine equipment, people and other resources to achieve better and cheaper products (Tamhane, 2009). In recent years, *DoEs* techniques have been increasingly recognised as key tools to build an important link between the experimental and the modelling world; to identify the influence of a factor or their interactions on the response of interest; to plan the experimental campaign, minimising the number of experiments, i.e. the resources (personnel time, machine time, energy,

materials, work, etc.), and maximizing the information on the system behaviour and operating variables (Tamhane, 2009, Franceschini and Macchietto, 2008). Due to its versatility, the *DoEs* approaches can be applied across a broad range of fields in manufacturing or research, such as marketing, accounting, chemistry, management, engineering, biology, agriculture, medicine, education, psychology, procurement, and reliability (Condra, 2001). According to *DoE* principles, the experiment (run) is a system composed of independent input variables (or factors) and dependent output variables (or responses of interest). The levels are the different intensities of a treatment factor, which can be set by experimenter. Blocking (grouping of experiments carried out with similar external factors), randomization (realization in random order the experiments) and replication (repetition of the experiment on the same set of input data) are the strategies that improve the precision of experiment (Tamhane, 2009). Therefore, defined the aim, the problem should will be analysed with the help of the following questions:

- what is known?
- What is unknown?
- What do we need to investigate?
- Which experimental variables can be investigated?
- Which responses can be measured?

This will allow to plan the experiments in a rational way (Lundstedt et al., 1998). In recent years, many researchers (Aslan, 2008, Ghafari et al., 2009, Tsapatsaris and Kotzekidou, 2004, Rajmohan and Palanikumar, 2013, Acharya et al., 2014, Sun et al., 2010, Vicente et al., 1998, Mangwandi et al., 2013b, Mahours et al., 2017) have used a design of experiments (*DoEs*) method to plan the experimental campaign, minimizing the experiments number to be performed. Several are the techniques available for the *DoE*, but the better approach depends on the problem nature, the factors number to be studied, the levels number for each factor, the resources and budget available for the experiment, and the aims to be achieved. The commonly used experimental design techniques are the Full Factorial Design (*FFD*) (Pani and Nath, 2014, Acharya et al., 2014) and the Central Composite Design (*CCD*) (Tsapatsaris and Kotzekidou, 2004, Rajmohan and Palanikumar, 2013). Each technique allows the construction of an experimental work plan in matrix form, that shows the runs number (matrix rows) and the operating conditions (matrix columns) for each run experimental.

Often the *Do*E is followed by the Response Surface Methodology (*RSM*), a statistical and mathematical technique, useful for the improvement and optimization of processes, in which a response (or a set of responses) of interest is related to several variables (process parameters) (Baş and Boyacı, 2007, Bezerra et al., 2008). The *RSM* was introduced by Sir George Box in the 1940s and 1950s (Bruns et al., 2006) and it is based on the fit of a

polynomial equation to the experimental data, obtained in relation to experimental design (Bezerra et al., 2008). The *RSM* allows to simultaneously optimizing the levels of the independent variables to obtain the best performance of the system, performing a small number of experiments (Baş and Boyacı, 2007, Bezerra et al., 2008).

III.4.1 Full Factorial Design

The Full Factorial Design (*FFD*) allows the investigator to study the effect of each factor on the response variable, as well as the effects of all interactions between factors on the response variable. In a *FFD* are needed L^kexperiments numbers to investigate the effects of *k* variables on response. For example, with two factors, each taking two levels, the factorial experiment is planned by four combinations in total, with two factors, each at three levels, the *FFD* will give 3^2 experiments, etc. (Lundstedt et al., 1998). In Table III.1 and Table III.2 are reported the *FFD* matrices for two variables, each at two and three level respectively.

The *FFD* is the only means to completely and systematically study all interactions between factors, but it becomes expensive as the number of experiments increases. If the number of combinations in a *FFD* is too high to be logistically feasible, a fractional factorial design or a *CCD* may be done, in which some of the possible combinations are omitted. Therefore, for the vast majority of full factorial design, each factor has only two levels.

Table III.1 *2^2 Full Factorial Design matrix for a combination of two factors (x_1 and x_2), each taking two levels. The levels are conventionally given by minus one (-1), for low level, and plus one (+1), for high level*

Two variables		
Runs	Variables	
	x_1	x_2
1	-1	-1
2	+1	-1
3	-1	+1
4	+1	+1

Table III.2 3^2 *Full Factorial Design matrix for a combination of three factors (x_1 and x_2), each taking three levels. The levels are conventionally given by minus one (-1), for low level, plus one (+1), for high level, and zero (0), for the medium level)*

Three variables		
Runs	Variables	
	x_1	x_2
1	-1	-1
2	-1	0
3	-1	-1
4	0	+1
5	0	0
6	0	+1
7	+1	-1
8	+1	0
9	+1	+1

III.4.2 Central Composite Design

Central Composite Design (*CCD*) is an experimental design technique used in alternative to the 3^k *FFD*, with $(k \geq 2)$, to reduce the experiment number, i.e. cost of running of experiments. A Central Composite Design consists of the following parts (Khuri and Cornell, 1996, Lundstedt et al., 1998):

- a 2^k Full Factorial Design, where the factors levels are coded as −1 and +1 (low and high level of variable);
- a set of 2^k axial points where, for each run, only one level of the factor is coded as -1 or +1, the other are coded as 0 (medium level of variable);
- a center point (n_0) where all levels of factors are coded as 0. The center point is often replicated in order to improve the precision of the experiment.

The total number of design points is thus $\left(N_t = 2^k + 2 \cdot k + n_0\right)$, with n_0 the integer closest of $[\alpha \cdot (2^{k/2} + 2)^2 - 2^k - 2 \cdot k)]$. The α value depends on the factors number: α is 0.7844 for two factors, α is 0.8385 for three factors, etc. (Khuri and Cornell, 1996).

In Table III.3, the *CCD* matrix for three factors (x_1, x_2 *and* x_3), each at three levels, is presented.

Table III.3 *Central Composite Design matrix for three factors (x_1, $x_2$and x_3) and three levels (conventionally encoded as -1, 0 and +1). The center point is replicated six once*

Three variables			
Runs	Variables		
	x_1	x_2	x_3
1	-1	-1	-1
2	+1	-1	-1
3	-1	+1	-1
4	+1	+1	-1
5	-1	-1	+1
6	+1	-1	+1
7	-1	+1	+1
8	+1	+1	+1
9	-1	0	0
10	+1	0	0
11	0	-1	0
12	0	+1	0
13	0	0	-1
14	0	0	+1
15	0	0	0
16	0	0	0
17	0	0	0
18	0	0	0
19	0	0	0
20	0	0	0

III.5 Granules characterization by standard protocols

Anyone who handles powders or granules on a regular basis will know that their physical properties influence the speed of a production line, packaging and storage capabilities, flowability and thus transport of the material. Therefore, residual moisture content, bulk density (ρ_b), tapped

density (ρ_t), Carr Index (*CI*), Hausner Ratio (*HR*), Angle of Repose (*AR*), morphological and thermal features, particle size distribution, mechanical and release properties, for each batch of produced granules, were investigated because they are the main parameter that control the behaviour of granules.

All characterizations were performed adopting the appropriate *ASTM* (American Society for Testing and Material) standard protocols. To ensure reproducibility of the experimental data, every measurement has been performed in triplicate.

III.5.1 Residual moisture content

Residual moisture content of granules was determined immediately after the drying step by using a moisture analyser (Ohaus mod MB4). The measurement was based on the thermogravimetric principles and it was performed following the standard *ASTM D 2216–98*: Standard Test Method for Laboratory Determination of Water (Moisture) Content of Soil and Rock by Mass. Briefly, approximately 0.5 g of dry sample were placed in an aluminium pan. During the test, the sample was weighted by an internal balance, the moisture losses for evaporation were recorded and automatically reported as percent residual moisture content.

III.5.2 Compressibility and flowability

The compressibility and flow characteristics of granules were investigated by determining bulk density, ρ_b, tapped density, ρ_t, Hausner Ratio, *HR*, Carr Index, *CI*, and Angle of Repose, *AR*, for each formulation. The knowledge of these properties gives some information about the handling features of granules, useful for many industrial sectors.

The bulk density of a solid depends on both the density of powder particles and the spatial arrangement of particles in the powder bed. The tapped density is an increase of the bulk density attained after mechanically tapping a container containing the powder sample. The measurement of bulk density and tapped density were determined by using the method proposed by the standard *ASTM D7481–09*: Standard Test Methods for Determining Loose and Tapped Bulk Densities of Powders using a Graduated Cylinder. In particular, an amount of granules (in range size 0.45-2 mm) was poured in a graduated cylinder of 10 ml. The mass of the untapped sample (m), the bulk volume (V_b), that includes the interparticulate void volume, the tapped volume (V_t), obtained by subjecting the bulk volume to 80 taps from a height of few millimeters, were determined and used to calculate the bulk density (see eq. III.2) and the tapped density (see eq. III.3). Although the international unit of the bulk and tapped densities is kilogram per cubic metre, these densities are expressed in grams per millilitre (g/ml) because the measurements are made using a graduated cylinder.

$$\rho_b = \frac{m}{V_b} \quad \text{(III.2)}$$

$$\rho_t = \frac{m}{V_t} \quad \text{(III.3)}$$

The Hausner Ratio, Carr Index, and Angle of Repose are the main physical variables used to characterize the flow properties of particulate solids. The *HR* (dimensionless) and *CI* (in percentage) were calculated by using the bulk and tapped densities values (see eqs. (III.4) and (III.5) respectively), according to the standard *ASTM D6393-99:* Standard Test Method for Bulk Solids Characterization by Carr Indices (Test F-Calculation of Carr Compressibility). The *HR* and the *CI* permit an assessment of interparticulate interactions by comparison of the bulk and tapped densities: if the bulk and tapped densities will be closer in value, the material will be free-flowing and the interactions are less significant; if there are a greater difference between the bulk and tapped densities, the material is poorly flowing and greater interactions will be observed.

$$HR = \frac{\rho_t}{\rho_b} \quad \text{(III.4)}$$

$$CI = \frac{\rho_t - \rho_b}{\rho_t} \cdot 100 \quad \text{(III.5)}$$

The static Angle of Repose was measured using the fixed funnel and free standing cone method, proposed by the standard *ASTM C1444-00*: Standard Test Method for Measuring the Angle of Repose of Free-Flowing Mold Powders. Briefly, an amount of granules was carefully poured into funnel and made to flow freely on a horizontal plan until to form on it a material heap at cone shape. The angle of repose was then calculated, in degrees, using the eq. (III.6), where *h* and r equalled height and radius of the cone respectively.

$$AR = \tan^{-1}\frac{h}{r} \quad \text{(III.6)}$$

In agreement with U.S. Pharmacopeia (see Table III.4), *CI* less than 10% and greater than 38 % indicate excellent and poor flowability properties, respectively. In addition, an excellent flowability can be found in a particulate with *HR* 1.00–1.11 and an *AR* of 25-30 °, instead, materials with *HR* and *AR* greater than 1.60 and 66 °, respectively, have poor flowability properties. Therefore, the smaller the *HR*, *CI* and *AR* the better the flow properties of granules. For example, $CI \leq 10$ %, *HR* between 1-1.11, and *AR* between 25-30 ° indicate an excellent flowability degree of the material.

Table III.4 *U.S. Pharmacopeia table: flowability degree respect to carr index, hausner ratio and angle of repose values*

Carr Index	Hausner Ratio	Angle of Repose	Flowability
≤10	1.00-1.11	25-30	Excellent
11-15	1.12-1.18	31-35	Good
16-20	1.19-1.25	36-40	Fair
21-25	1.26-1.34	41-45	Passable
26-37	1.35-1.45	46-55	Poor
32-37	1.46-1.59	56-65	Very poor
>38	>1.60	>66	Very very poor

III.5.3 Granulometry and morphology

Technological properties of powders or granules (bulk density, flowability, etc.) depend on the particle size (granulometry) and particle shape (morphology), which are the main characteristics of a solid particulate (Mikli et al., 2001).

Size (d_g) and Particle Size Distribution (*PSD*) of powders or granules was obtained by using the method proposed by the standard *ASTM E 2651–08*: Standard Guide for Powder Particle Size Analysis. Briefly, an amount of particles, roughly 250 mg, was first dispersed on a plan and then captured by a digital camera (Canon IXUS 850 IS). The obtained images were analysed by using the software Image-Pro Plus 6.0 (from Media Cybernetics) and Excel.

Shape of powders or granules samples was investigated both by the microscope (LEICA DM-LP), using 4 X magnification, and the field Emission-Scanning Electron Microscope (FESEM, mod. LEO 1525, Carl Zeiss SMT AG, Oberkochen, Germany). In this latter, samples were spread onto a carbon double adhesive tab previously stuck to an aluminium stub, sputter-coated with gold and then examined.

Subsequently, the dispersion and representation of the particle population in terms of size and shape was then improved developing a hardware and software of a device based on Dynamic Image Analysis (*DIA*), which has been extensively described in the paragraph III.6.2.

III.5.4 Thermal behaviour

Thermal properties of powders or granules were investigated by using the method of Differential Scanning Calorimetry (*DSC*, Mettler Toledo DSC-822 instrument, Mettler, Switzerland), in order to evaluate if the granulation process changes the solid state (amorphous or crystalline) of powders and

loaded active molecules. Thanks to its speed, simplicity, and availability, the *DSC* is the most used thermal analysis method. It is mostly used for quantitative analysis and only a few mg of sample are required to run the analysis (Kodre et al., 2014). Briefly, an amount of powders or granules, about 10 mg, was weighed and sealed in a perforated aluminium pan. *DSC* tests were carried out at a heating rate of 10 °C/min within a temperature range from 25 °C to 300 °C using a continuous purge of nitrogen (50 ml/min).

III.5.5 In vitro dissolution

In vitro dissolution tests were performed to determine both the loaded active molecules dissolution rate and the polymer erosion rate of achieved solid dosage forms (granules).

III.5.5.1 Release of active molecules

In vitro release tests of produced granules (lots of dried particles with size 0.45-2 mm) loaded with vitamins were carried out by using an apparatus that replicates the USP II – paddles device. In particular, the used setup has been composed by a magnetic stirrer (Arex Heating Magnetic Stirres) with hotplate and a glass vessel positioned up it. The granules were accurately weighted (1 g for each test, experiments made in triplicate) and then put in the vessel containing a given volume (1000 ml) of dissolution medium (distilled water) at pH 6.5 and under magnetic stirring (50 rpm). The temperature (25 °C) of the dissolution medium inside the vessel was controlled by the Vertex VTF digital thermoregulatory. It is important to note that this approach (dissolution in distilled water) is a simplified release study not close to the real physiological conditions; it was applied just to achieve fast information about both polymer erosion and active molecule release from granular matrix. Moreover, these conditions (temperature /distilled water) were used also to study the erosion phenomena of *HMPC* pure granules (see Figure IV.18, paragraph IV.3.4.3), thus it was possible to evaluate the vitamin loads effect.

The cumulative release of the active molecule was observed at different time intervals by withdrawing samples of the dissolution medium. The samples were first filtered through a membrane of polyvinylidene difluoride (CHROMAFIL® Xtra CA-45/25, pore size 0.45 μm) and then analysed spectrophotometrically (Perkin-Elmer Lambda 35, Monza, Italy) at wavelength of signal acquisition, which depend on the analysed active molecule. The percentage of active molecule released from granules (R) in the dissolution medium was calculated in agreement with eq. (III.7). In this latter the m_t is the active molecule mass released at predetermined time intervals, determined by the Lambert Beer law, whose constant was obtained by calibration curves *ad hoc* built for the treated molecules; m_i is the mass

of active molecule loaded in the granules (for example, in an 1 g of loaded granules, the molecule amount is 10 mg for a payload of the 1 %).

$$R = \frac{m_t}{m_i} \cdot 100 \qquad \text{(III.7)}$$

Moreover, in order to evaluate the stability of granules structure, dissolution tests were performed on aged granules, with method and operating conditions described above, after 1 month of storage at room conditions.

III.5.5.2 Erosion of polymer

The time erosion profile of the granules were obtained in the same operating conditions used for the active molecules release tests, i.e. 1 g of granules was dissolved in 1000 ml of distilled water at room conditions and 50 rpm. The granules were produced using the powders of hydroxypropyl methylcellulose (*HPMC*) as polymer. Therefore, it was necessary to use the phenol/acid sulfuric colorimetric method for determination of the erosion degree of polymer (Dubois et al., 1956). Briefly, during the test, 2 ml of the dissolution medium were withdrawn and placed in a glass vial. In this latter first 500 µl of 80 % w/w of phenol in water solution and then 5 ml of sulfuric acid were added. The sulfuric acid was added rapidly and directly inside the liquid. After 10 min, the test tubes were shaken and placed in a water bath at 25 °C for other 10 min. This method produces a yellow/orange solution: its colour intensity is proportional to the concentration of sugar (*HPMC*) and it is stable for several hours. The samples in the test tubes were assayed by UV spectroscopy (Perkin-Elmer Lambda 35, Monza, Italy) at wavelength of 492 nm. The percentage of *HPMC* eroded from granules (E) was calculated in according to eq. (III.8).

$$E = \frac{M_t}{M_i} \cdot 100 \qquad \text{(III.8)}$$

In this latter the M_t is the mass of eroded *HPMC* at predetermined time intervals, determined by the Lambert Beer law, whose constant was obtained by referring to a standard curve, previously constructed; M_i is the mass of *HPMC* introduced in the dissolution medium, i.e. 1 g.

III.5.6 Statistical analysis

All the characterization measurements were carried out in triplicate to obtain results with a greater statistical reliability. The response values were expressed as mean values ± standard deviation. Experimental data were compared using Student T-test. The (p) stands for probability and its value measures how likely it is that any observed difference between groups is due to chance. Being a probability (p) can take any value between 0 and 1. In

particular, ($p < 0.05$) suggest that the observed difference is unlikely to be due to chance, i.e., there is a difference statistically significant between the two compared samples, on the contrary, ($p > 0.05$) indicate no difference between the groups other than due to chance, i.e. the two samples are similar (Dahiru, 2008).

III.6 Granules characterization by *ad hoc* methods

III.6.1 Mechanical properties

The mechanical properties of granules (hardness and elastic module) were investigated performing compression tests by a texture analyser (Texture Analyser XT Plus instrument, EN·CO, Venice, Italy), technique often used to characterize the behaviour of hydrogels in wet conditions (Cascone et al., 2014). The principle of a texture measurement system is to physically deform with a probe a test sample in a controlled manner and measure its response. Preliminary studies have highlighted that useful of this technique on more granules together involved significant errors in the measurements: the heterogeneity of granules in shape and size made it difficult to establish a compression force homogeneous over the whole sample. For this reason, the compression tests were performed on one granule at a time. In particular, to have more homogeneous size granules, particles fraction 0.45–2 mm were furthermore sieved in three sub-fractions (0.45–0.71 mm; 0.71–1 mm; 1–2 mm) and, for each of them, about 10 samples were analysed. To perform the tests, a stainless steel probe with diameter of 5 mm and a 5 kg loading cell were used (Chitu et al., 2011). The compression speed was kept constant at 0.1 mm/s for all test time, and the instrument recorded the force (F) necessary to compress matrix and the granule size (d_g). In particular, data acquisition started when the probe touches the sample and it ended when the probe reached 90 % of the total sample size (which is previously evaluated by a proper instrument calibration). A recording rate of 100 point/s was set. Force-deformation curve was obtained for each granule. The maximum value of the force represents an index of the granules hardness. In particular, the granule strength (i.e. the granule hardness) was defined as the maximum force value on the granule surface: for granules with similar size, the lower the granule strength, the lower the hardness and vice versa. Single granule mechanical strength (σ) was calculated according to eq. (III.9), assuming circular the granule cross-section (Bika et al., 2005).

$$\sigma = 4 \cdot \frac{F}{\pi \cdot d_g} \qquad \text{(III.9)}$$

$$F = \frac{1}{3} \cdot \sqrt{d_g} \cdot \frac{E_l}{1 - \nu_l^2} \cdot \sqrt{\Delta^3} \qquad \text{(III.10)}$$

Granule deformation can be elastic or plastic. Elasticity describes the ability of a (solid) material to resist a distorting influence and to return to its original size and shape when that influence or force is removed. The plasticity describes the deformation of a (solid) material undergoing non-reversible changes of shape in response to applied forces. In engineering, the transition from elastic behaviour to plastic behaviour is called yield. Therefore, granule behaviour was investigated applying the methodology described by Mangwandi et al. (2007). According to it the compression tests data were analysed by using the Hertz equation (eq. (III.10)). This latter describes the relation between the force (F) and the total displacement of the moving platen (Δ) when a sphere is under compression between two platen. In this equation E_l is the young modulus and ν_l is the poisson ratio, which is typically 0.23 for porous material (Mangwandi et al., 2007, Lade and Nelson, 1987).

III.6.2 Dynamic Image Analysis device

Studies on granules size distribution can offer a good initial understanding of both process phenomena and effects of variables on granules size and shape (Rajniak et al., 2007, Ramachandran et al., 2008, Hu et al., 2008). Many techniques for measuring the particle size distribution (PSD), such as sieving (Washington, 2005), static image analysis (Laitinen et al., 2003), laser diffraction (Beuselinck et al., 1998), are able to analyse only a small number of particles (100-500 particles/photos for the static image analysis) and do not allow to have a continuous and statistically significant control of their size. Recently, thanks to the continuous increasing of the computational power, particular interest has been given to the Dynamic Image Analysis (*DIA*) technique for monitoring the evolution of the *PSD* during the solids processing. This technique has the advantage of analysing many particles (millions) in a relatively short time (depending on the computational power), ensuring a good statistical result and allowing obtain information on the size and also on the shape of the particles. Despite such a potentiality, in literature, very few works that use this technique to monitor a granulation process are reported. Watano and Miyanami (1995) and Watano et al. (2000) were the first to report the use of this technique (despite limited to 256 low resolution pictures) to monitor a granulation process.

In light of that, the hardware and software of a *DIA*-based device were developed in collaboration with researchers of the TPP group. The designed and built device was a tool able to analyze dynamically the *PSD* and the morphology of each particle during granulation process, in agreement with

the standard ISO (ISO 9276-6:2008 and 13322-2:2006). It exploited the natural dispersion achieved during the free falling of the particles to obtain pictures/frames/video analyzable with the aid of a PC.

Briefly, in the *DIA*-based device (a scheme is given in Figure III.4) the wet granules, loaded in the hopper, were discharged and distributed on an inclined plane thanks to the vibration of an eccentric rotating mass (ERM) motor (voltage: DC 3V; speed: 1200 rpm; size: 25x30 mm; weight: 47 g).

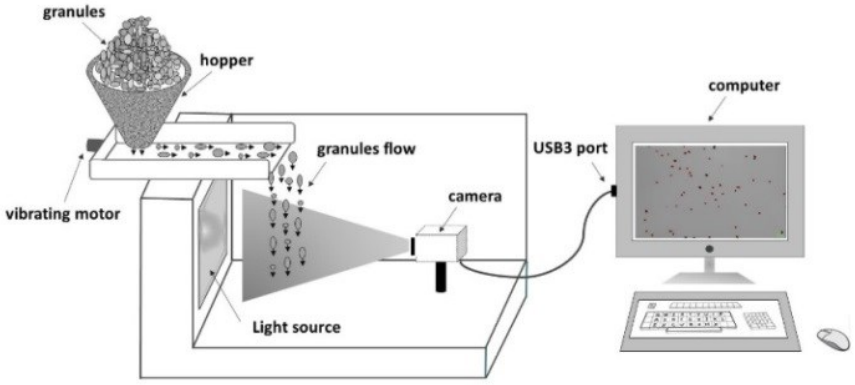

Figure III.4 *DIA device based on the free falling particles scheme, in agreement with the standard ISO 13322-2:2006*

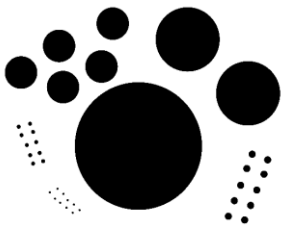

Figure III.5 *Proper calibration sheet made of 38 disks of known dimensions: one of 2 cm, two of 1 cm, five of 5 mm, ten of 500 μm and ten of 200 μm*

At the end of the inclined plane, the granules falling tidily and a camera (Chameleon3 1.3 MP Mono USB3 Vision with the lens Fujinon HF25HA-1B) recorded their passage. The camera had a CCD sensor (charge-coupled device) and a global shutter mechanism that captured all pixel of a frame in the same instant, avoiding distortion of the moving objects. The exposure time was set at 0.1 ms, ensuring a good compromise between brightness and sharpness. In the "free falling particles configuration" for the dynamic image analysis the use of a telecentric lens for the camera is not mandatory since the falling particles lay always in the same volume that, having a negligible thickness, is with a good approximation a plane. Therefore, it was used a non-telecentric lens (HF25HA-1B Fijifilm) and the instrument calibration it

was performed with a proper calibration sheet (see Figure III.5) placed in the same "plane" of the falling particles, to avoid any distortion related to the use of non-telecentric lenses.

The calibration sheet was made of 38 disks of known dimensions: one of 2 cm, two of 1 cm, five of 5 mm, ten of 1000 μm, ten of 500 μm and ten of 200 μm. The conversion factor was calculated on the 2 cm disk and the threshold level was optimized minimizing the sum of the squared error between the measurements of all the other disks and their true dimensions. The calibration procedure of camera (essential to relate pixel to μm and vice versa) ensured a proper conversion factor (μm/px) as well as a reliable threshold level for the binarization.

To ensure proper lighting (and according to the ISO 13322-2:2006 Annex C.6) a monochrome panel light source (power 12 W, 20x20 cm, weigh 300 g) was diametrically placed at the camera, so that the free falling plane was between the light source and the camera. This last communicated through a USB3 port with a PC that caught grayscale video at 30 frames per second, which were split in a series of frames that were binarized and analyzed in MATLAB® 2014b thanks to a customized script. The binarization converts a grayscale image in a binary image depending on a threshold level, optimized with the calibration procedure of camera. The binarized image of the falling particles were analyzed, using the "regionprops" MATLAB function, measuring the projected area, the major axis length, the minor axis length and the extrema of each particles. The particles falling on the boundaries of the region of interest, equivalent to the entire image, were excluded from the measurements. The particles falling into region of interest were highlighted with a red bounding box on the original grayscale frame and used to reconstruct the video. Only for latter, the projected area was used to calculate the area-equivalent diameter whereas the major axis length, the minor axis length the ellipse ratio, used to quantify the particles morphology. Through the binning procedure the particles were categorized, depending on their area-equivalent diameter, in size classes from about 60 μm to about 20000 μm, with a geometric progression of $2^{1/6}$. Therefore, by the use of the particles area-equivalent diameter and the number of particles in each class, corrected with the Miles-Lantuejoul method (ISO 13322-2:2006), was possible to obtain the distribution density (q) and undersize cumulative distribution (Q) by number (subscript 0) and by volume/mass (subscript 3), as well as the arithmetic mean size ($x_{1,0}$) and the volume-weighted mean size ($x_{1,3}$) of the distribution (ISO 9276-2:2014).

The advantage of using an image analysis technique relies on the fact that other information rather than just dimensions can be extracted. Through a proper binning procedure it is possible to combine the particle size information to the morphological information, in accordance with the standard ISO 9276-6:2008.

From the *DIA*, the Ellipse Ratio (*ER*) was calculated for each particle. An image useful to individuate the impact of the *ER* value on the shape of the particle is provided in Figure III.6.

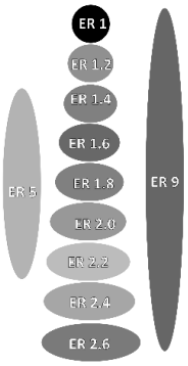

Figure III.6 *Impact of the Ellipse Ratio (ER) value on the shape of the particle*

The instrument were calibrated and validated against particles of known dimensions (between 500 µm and 800 µm). The results showed that 90 % of the particles had a diameter between 500 µm and 800 µm, and thus, the built device and its software are able to describe with reasonable accuracy a particle population.

In the current configuration, the device analyse millions of particles within few minutes (about 2 min), in the range 60 µm to 2 cm, and allow to obtain a greater statistic reliability of the results.

III.7 Chapter III remarks

A massive production of granules by the wet granulation process has been possible due to the developed apparatuses with dedicated protocols of stabilization, separation and characterization. The innovative points of the study done are:

- ultrasonic atomizer for the wetting of the powders;
- *ad hoc* procedure for the analysing the mechanical granules properties;
- technique of Dynamic Image Analysis (*DIA*) for monitoring the evolution of the Particle Size Distribution (*PSD*) during the solids processing.

The use of atomization ultrasonic device allows improving the degree of binder phase dispersion on the surface of powder bed and operating under controlled conditions of flow rate and size distribution of liquid droplets.

Due to the heterogeneity of granules in shape and size, the compression tests must be performed on one granule at a time to establish a compression force homogeneous over the whole sample. In particular, to have more homogeneous size granules, if the particles fraction to be analyse has a size range of 0.45–2 mm, three sub-fractions (0.45–0.71 mm; 0.71–1 mm; 1–2 mm) must be obtain by sieving and, for each of them to assay about 10 samples.

The built *DIA*- device has the advantage of analysing, in size and shape, many particles (millions) in a relatively short time (about 2 min). Despite the potentiality of the *DIA* technique, in literature (i.e. on Scopus and Web of Science databases under the headings “dynamic AND image AND analysis AND granulation”) there are no works that explicitly affirm to use this technique to monitor granulation processes. Sometimes, in the granulation field, it is used under the heading of “online image analysis” but, also in this case (i.e. searching for “(online OR on-line OR one AND line) AND image AND granulation”) very few works are present.

Chapter IV
Granulation process applications

IV.1 Production of HPMC granules by Design of Experiment approach

IV.1.1 Generalities

Over the past decade, design, scale-up and operation of granulation processes have been considered as "quantitative engineering" and significant advances have been made to quantify the granulation processes (Hapgood et al., 2003). Due to the great industrial interest in granules, for marketing reason and technological aspects, studies on correlations between granule properties and process parameters are highly desirable to predict the final product quality. However, an onerous collection of experimental data is required to build and to validate a correlation. Therefore, the experiments must be planned in a systematic way to avoid loss of time and resources.

As seen in "Methodologies-experimental set-up" section (paragraph III.4), the techniques of Design of Experiment (*DoEs*) are engineering statistical approaches used to organize efficient and systematic a campaigns of runs with the minimum experiment number and to identify the influence of a factor or interactions between factors on the response of interest, in order to achieve better and cheaper products. In the literature, there are many papers in which the correlations between process parameters and final product properties were investigated applying the *DoE* techniques in different fields (Bu et al., 2016, Tsapatsaris and Kotzekidou, 2004, Rajmohan and Palanikumar, 2013). Experimental designs dealing with the granulation process have been applied in several studies but on apparatuses and final products (tablet) different from those used in this Ph.D. thesis (Acharya et al., 2014, Badawy et al., 2000, Costa et al., 2011, Gaikwad et al., 2016, Rambali et al., 2001, Westerhuis et al., 1997).

The aim of the following study was produce granules of hydroxypropyl methylcellulose (*HPMC*) with a defined size (0.45-2 mm) and good

flowability together with a high product yield, to reduce manufacturing scrap. The runs were performed by using a bench scale granulation apparatus, presented and discussed in the paragraph III.2. The experimental campaign was planned by *DoE* technique. The influence of impeller rotation speed (rpm), binder to powder ratio and binder phase flow rate on granules properties (residual moisture content, flow indices, product yield) was investigated. The results of the experimental campaign have been used to develop predictive correlations with the aim of pointing out a reliable tool for *HPMC* granules production or for manufacturing of powders with similar behaviour of *HPMC*.

IV.1.2 Materials

As seen in "state of art" section the wet granulation is a process that requires the use of a binder phase to agglomerate the powder particles. Therefore, for the preparation of granules, hydroxypropyl methylcellulose *HPMC* 20 (supplied by Pentachem Srl, San Clemente, RN-Italy) was used as polymeric powder, and distilled water as binder phase. Some relevant properties of *HPMC* 20, provided by Pentachem Srl, are presented in Table IV.1.

Table IV.1 *Hydroxypropyl methylcellulose (HPMC 20) powder properties, provided by Pentachem Srl (San Clemente, RN-Italy)*

Properties	Values
Methoxyl group percentage	28-30 %
HydroxyPropyl group percentage	7.5-12 %
State	powder
Colour	white-beige
Density	0.350-0.500 kg/dm^3
Granulometry	Min. 95%<0.180 mm
Moisture	max 4.0 %
Solubility in water	totally soluble
Water retention	Min. at 60% after 8 minutes
Purity degree	95-97%
Storage	In a protected dry place
Aqueous solution characteristics	
Surface activity	Weak
Viscosity at 20°C (aqueous solution 2% w/w)	20.000-30000 mPa·s (Brookfield RV)

IV.1.2.1 Why hydroxypropyl methylcellulose?

Hydroxypropyl methylcellulose (*HPMC*) powder, also known as hypromellose, is a water swellable hydrophilic polymer, widely used especially in the manufacturing of pharmaceutical (Huichao et al., 2014, Chouinard and Jacques, 1999) and food products (Laguna et al., 2014, Kim et al., 2015). It is a cellulose derivative, obtained from the substitution of the cellulose hydroxyl groups with methoxylic and hydroxypropoxylic moieties onto the glucose units (Chakraborty et al., 2009, Sannino et al., 2009, Viridén et al., 2009). It is a polymer easy to handle, low cost, odourless (Huichao et al., 2014), hypoallergenic, biocompatible (Barba et al., 2013) and not toxic (Sung et al., 1996). It can be dissolved slowly in cold water (under 40 °C (Huichao et al., 2014)) to form a viscous solution, it is practically insoluble in hot water, where instead gelation occurs (Huichao et al., 2014). It is insoluble in pure chloroform, ethanol, or ether, but it dissolves in most polar solvents or binary systems of chloroform and alcohol or methylene chloride (Williams et al., 2001). Nowadays, *HPMC* is the most employed excipient in the formulation of hydrogel-based matrices in form of tablets or granules in order to provide the drug release in a controlled manner (Jamzad and Fassihi, 2006, Pani and Nath, 2014, Barba et al., 2009b, Herder et al., 2006, Li et al., 2005, Siepmann and Peppas, 2012).

IV.1.3 Methodologies

HPMC granule production (size 0.45-2 mm), using distilled water as binder phase, was obtained in according to the procedure describe in the "Methodologies-experimental set-up" section (see paragraph III.3.1). In particular, on the basis of preliminary experimental runs, granulation tests were performed keeping several parameters constant: initial dry powder mass (50 g), process time (20 min), and ultrasonic energy amplitude (45 %).

Table IV.2 *The intensities (levels) values for each factor*

Factors	Levels		
	-1	0	+1
Impeller rotation speed, [rpm]	72	93	112
Binder to powder ratio, [-]	1	1.5	2
Binder phase flow rate, [ml/min]	17	34	58

Three process operative parameters (factors) were changed: impeller rotation speed, binder to powder ratio determined as added binder phase mass [*kg*]/initial dry powder mass [*kg*], and binder phase flow rate. For each factor three intensities (levels) have been used (see Table IV.2). In particular, the values of the liquid to solid ratio were calculated keeping

constant the initial dry powder mass (50 g) and varying the binder phase volume (50 ml, 75 ml, and 100 ml). The experimental campaign was planned by using the *CCD* statistical protocol, one of the *DoE* technique already discusses in the paragraph III.4.2. In Table IV.3 the experimental work plan for three variables at three levels was reported.

Table IV.3 *Experimental work plan for three variables at three levels, according to the CCD statistical protocol*

Factors (independent variables)			
Runs	Impeller rotation speed [rpm]	Binder to powder ratio [-]	Binder phase flow rate [ml/min]
1	72	1	17
2	112	1	17
3	72	2	17
4	112	2	17
5	72	1	58
6	112	1	58
7	72	2	58
8	112	2	58
9	93	1.5	34
10	72	1.5	34
11	112	1.5	34
12	93	1	34
13	93	2	34
14	93	1.5	17
15	93	1.5	58

It is important to note that by using the *FFD* approach (see paragraph III.4.1) 3^3=27 experiments are needed whereas the *CCD* method allows us to reduce the number of experiments from 27 to 15, considering a single replication at center point (see paragraph III.4.2).

The residual moisture content, bulk density (ρ_b), tapped density (ρ_t), Hausner Ratio (*HR*), Carr Index (CI), Angle of Repose (*AR*), product yield (y_p), and manufacturing scraps (small scrap (S_p) and big scrap (B_p)) were selected as the dependent variables (results of interest), on which to

investigate the combined effect of the three factors. In particular, the dependent variables measurements were obtained characterizing the granules by the *ASTM* (American Society for Testing and Material) standard protocols, shown in the paragraph III.5. The product yield was defined as the % w/w of dry granules within the size range 0.45-2 mm that is a size range usually used in the commercial granulated food, pharmaceutical and zootechnical products, taken into account already in other several literature works (Albertini et al., 2004, Chevalier et al., 2010, Hussein et al., 2008). The small scrap was defined as the % w/w of dry granules with size lower than 0.45 mm, and the big scrap was defined as the % w/w of dry granules with size greater than 2 mm.

$$y_p = \frac{wgt_{0.45-2mm}\,(g)}{wgt_{0.45-2mm}(g) + wgt_{<0.45mm}(g) + wgt_{>2mm}(g)} \cdot 100 \qquad \text{(IV.1)}$$

$$S_p = \frac{wgt_{<0.45mm}\,(g)}{wgt_{0.45-2mm}(g) + wgt_{<0.45mm}(g) + wgt_{>2mm}(g)} \cdot 100 \qquad \text{(IV.2)}$$

$$B_p = \frac{wgt_{>2mm}\,(g)}{wgt_{0.45-2mm}(g) + wgt_{<0.45mm}(g) + wgt_{>2mm}(g)} \cdot 100 \qquad \text{(IV.3)}$$

Product yield, small scrap and big scrap were calculated in according to eqs. ((IV.1), (IV.2) and (IV.3)) respectively, where $wgt_{<0.45mm}$ was the fraction of dry granules obtained after sieving with size lower than 0.45 mm, $wgt_{0.45mm-2mm}$ was the fraction of dry granules obtained after sieving with size between 0.45-2 mm, and $wgt_{>2mm}$ was the fraction of dry granules obtained after sieving with size greater than 2 mm.

IV.1.4 Results and discussions

IV.1.4.1 Screening of process parameters

Experimental design by *DoE* technique was performed to have a basic knowledge of wet granulation process of a *HPMC* powder in presence of the only distilled water as binder phase, using a low shear granulator as agglomeration apparatus. In particular, at the beginning of my Ph.D. work, the aim was focused on the choice of process conditions that produced granules with good flowability properties together with a high product yield, to reduce manufacturing scrap.

In a wet granulation process there are several parameters that can play a fundamental role on the product final properties (Guigon et al., 2007). In light of this, firstly, a screening work on all process parameters was carried out in order to determine the variables having a significant influence on granules properties. On the basis of screening experiments, constant and

variable parameters were defined: impeller rotation speed, binder to powder ratio and binder phase flow rate are the parameters that have greater influence respect to initial dry powder mass, process time, and ultrasonic energy amplitude. In particular, the initial dry powder mass was set at 50 g considering the size of the granulation section, and the process time was fixed to 20 min because it was observed, during the preliminary tests, that longer times allow granule breaking phenomena. Always during the preliminary studies, three intensities value, were associated for each factor on the basis of granules qualitative aspects. It was observed that, for the examined system (made of *HPMC* and distilled water), a high binder to powder ratio, i.e. high added binder phase amount (greater than 100 ml), or a high binder flow rate (greater than 58 ml/min) cause the phenomena of over wetting; a low binder to powder ratio, i.e. low added binder phase amount (lower than 50 ml), does not form granules; a high impeller rotation speed (greater than 112 rpm) generates the breaking of the solid particulate.

IV.1.4.2 Process parameters effect on granules properties

Granules production was performed setting the operating conditions defined for each run in the work experimental plan (see Table IV.3). In order to obtain the results with a greater statistical reliability, a randomized execution mode of the runs was applied, and each run was replicated three times. The values of all measured responses were expressed as an average with standard deviation (*SD)*. In Table IV.4, for each run, the product yield (eq. (IV.1)), the small scrap (eq. (IV.2)) and the big scrap (eq. (IV.3)) were reported.

The experimental results showed that different yields and scraps were obtained by varying the combinations of levels and thus the operative parameters. The maximum product yield (75.2±5.5 %) and the slightest scrap, in terms of big scrap (20.5±5.1 %) and of small scrap (4.2±0.3 %), were produced under the operating conditions of run 4 (see Table IV.3), i.e. high impeller rotation speed (112 rpm), high added binder phase amount (100 ml) and low binder phase flow rate (17 ml/min). Considerable quantities of materials with sizes lower than 0.45 mm were obtained using the operating conditions of the run 11 (32.7±16.6 %), i.e. with high impeller rotation speed and medium values of binder to powder ratio and binder phase flow rate. Similar result was observed with the run 5 (32.5±3.7 %). A high amount of granules with size greater than 2 mm (58.8±2 %) were achieved using the operating conditions of run 7, thus spraying quickly a large amount of binder phase and keeping to a minimum value the impeller rotation speed. This latter result was in agreement with what was reported in some literature papers Oulahna et al. (2003), in which it was demonstrated that the increase of the binder phase volume can cause a rapid and uncontrolled increase of large granules growth, at a point close to over wetting.

Table IV.4 *Average values with standard deviation of the product yield (% w/w of dry granules within the size range 0.45-2 mm) and of the manufacturing scraps (small scrap: % w/w of dry granules with size lower than 0.45 mm; big scrap: % w/w of dry granules with size greater 0.45 mm)*

	Responses (dependent variables)		
Runs	$y_p \pm SD$ [%]	$B_p \pm SD$ [%]	$S_p \pm SD$ [%]
	x_1	x_2	x_3
1	46.7±5.9	28.2±2.8	25.1±3.5
2	56.1±6.3	26.1±5.5	17.9±0.9
3	61.0±1.6	35.3±1.1	3.7±0.7
4	75.2±5.5	20.5±5.1	4.2±0.3
5	26.4±3.4	41.1±6.1	32.5±3.7
6	32.9±4.5	47.9±1.4	19.3±4.3
7	33.9±3.5	58.8±2	0.07±0.02
8	48.5±4.2	48.0±3	3.5±1.3
9	48.6±2.1	32.9±4.1	0.2±0.02
10	29.8±10.7	48.4±4.2	21.8±+6.6
11	37.9±17.3	29.5±1.6	32.7±16.6
12	47.9±4.7	26.6±4.6	25.5±0.4
13	55.7±2.7	36.4±5.6	7.9±4.9
14	72.6±4.7	18.1±3.4	9.3±2.2
15	46.3±3.4	38.7±4	15±3.2

The effect of a single parameter on product yield and manufacturing scraps were investigated by using the results of work plan matrix (see Table IV.4) and keeping constant the intensities of the other key factors. Firstly, it was observed the effect of binder phase flow rate keeping constant the impeller rotation speed and binder to powder ratio (run 1 vs run 5, run 2 vs 6, run 3 vs 7, run 4 vs 8, run 12 vs run 14 vs run 15): an increase of binder flow rate produced a decrease of the product yield and an increase of the scraps. Instead, the effect of rpm was observed keeping constant the binder phase flow rate and binder to powder ratio (run 1 vs run 2, run 3 vs 4, run 5 vs 6, run 7 vs 8): an increase of rpm produced an increase of the product yield. These latter considerations are in agreement with the effects caused of

the binder to powder ratio at constant intensity of rpm and binder phase flow rate: an increase of added binder phase amount produced an increase of yield.

Table IV.5 *Average values with standard deviation of the moisture, bulk density, and tapped density of the granules with size 0.45-2 mm*

	Responses (dependent variables)		
Runs	Moisture±SD [%]	ρ_b±SD [g/ml]	ρ_t±SD [g/ml]
1	$5.7\pm9.8\times10^{-1}$	$1\times10^{-1}\pm1.7\times10^{-3}$	$1.5\times10^{-1}\pm8.2\times10^{-4}$
2	$4.6\pm3.5\times10^{-1}$	$7.5\times10^{-2}\pm2.2\times10^{-4}$	$1.8\times10^{-1}\pm2.9\times10^{-3}$
3	$4.2\pm3\times10^{-1}$	$2.4\times10^{-1}\pm4\times10^{-2}$	$2.6\times10^{-1}\pm4.1\times10^{-2}$
4	$3.3\pm2.5\times10^{-1}$	$2\times10^{-1}\pm4.7\times10^{-3}$	$2.1\times10^{-1}\pm5.34\times10^{-3}$
5	$4.6\pm3.9\times10^{-1}$	$1.4\times10^{-1}\pm6.6\times10^{-3}$	$1.8\times10^{-1}\pm1.33\times10^{-3}$
6	$6\pm5.6\times10^{-1}$	$1.7\times10^{-1}\pm2.1\times10^{-2}$	$1.9\times10^{-1}\pm2.35\times10^{-2}$
7	$5.4\pm3.7\times10^{-1}$	$1.9\times10^{-1}\pm7.3\times10^{-3}$	$1.2\times10^{-1}\pm1.89\times10^{-3}$
8	$5.1\pm4\times10^{-1}$	$2.9\times10^{-1}\pm4.2\times10^{-2}$	$3\times10^{-1}\pm4.04\times10^{-2}$
9	$4.1\pm3.4\times10^{-1}$	$1.3\times10^{-1}\pm5.4\times10^{-3}$	$1.6\times10^{-1}\pm3.97\times10^{-3}$
10	$4.3\pm2.3\times10^{-1}$	$1.3\times10^{-1}\pm6.8\times10^{-3}$	$1.5\times10^{-1}\pm5.67\times10^{-3}$
11	$4.4\pm3\times10^{-1}$	$1.2\times10^{-1}\pm8.8\times10^{-3}$	$1.5\times10^{-1}\pm6.98\times10^{-3}$
12	$4\pm4\times10^{-1}$	$1.1\times10^{-1}\pm2.9\times10^{-3}$	$1.5\times10^{-1}\pm2.17\times10^{-3}$
13	$4.8\pm6.5\times10^{-1}$	$1.7\times10^{-1}\pm1.2\times10^{-2}$	$2\times10^{-1}\pm1.13\times10^{-2}$
14	$3.2\pm4.1\times10^{-1}$	$1.8\times10^{-1}\pm6.1\times10^{-3}$	$2\times10^{-1}\pm3.05\times10^{-3}$
15	$4.1\pm3.8\times10^{-1}$	$1.5\times10^{-1}\pm4.8\times10^{-3}$	$2\times10^{-1}\pm1.02\times10^{-2}$

Table IV.6 *Average values with standard deviation of the Hausner Ratio, Carr Index and Angle of Repose of the granules with size 0.45-2 mm*

	Responses (dependent variables)		
Runs	HR±SD [-]	CI±SD [%]	AR±SD [degree]
1	$1.5\pm2.5\times10^{-2}$	32.2±1.2	61.5±11.1
2	$1.6\pm3.8\times10^{-2}$	36.2±1.2	59.5±9.2
3	$1.1\pm2\times10^{-2}$	9±1.7	31.5±1.4
4	$1.1\pm8.2\times10^{-3}$	8.3±0.7	34.6±1.6
5	$1.3\pm7.1\times10^{-2}$	23.7±4.1	55±17
6	$1.1\pm3\times10^{-2}$	10.7±2.4	43.9±3
7	$1.1\pm3.5\times10^{-2}$	11.8±2.8	32.6±1.2
8	$1\pm9.6\times10^{-3}$	3±0.9	28±0.7
9	$1.2\pm5.7\times10^{-2}$	18±3.8	50.6±2.5
10	$1.2\pm2.8\times10^{-2}$	18±1.9	48.6±8.7
11	$1.3\pm4.6\times10^{-2}$	21.3±2.9	35.8±6.9
12	$1.4\pm6\times10^{-2}$	30±2.9	53.1±7.7
13	$1.2\pm1.5\times10^{-2}$	13.8±1.1	37.5±1.9
14	$1.1\pm3.1\times10^{-2}$	9.1±2.5	45.9±1.4
15	$1.2\pm3.6\times10^{-2}$	16.4±2.6	46±2.4

A first property that you want to have in a solid particulate is the good flowability. Information on the ability of a powder to flow can be obtained by characterizing the granules in terms of the Hausner Ratio, Carr Index and Angle of Repose. The lower these parameters are the better the flowability. According to the U.S. Pharmacopeia, a solid material has an excellent flowability if HR=1–1.11, CI≤10 %, and AR=25°–30°, as described in the paragraph III.5.2. Moreover, the moisture is another important property to be monitored in the manufacture and processing of some materials, because high moisture in the product can promote its degradation over time. Therefore, dry granules fraction with size between 0.45-2 mm, produced for each run, was characterized in terms of residual moisture content and compressibility and flowability properties (Hausner Ratio, Carr Index and Angle of Repose) in order to experimentally correlate the desired features for

the granules with the process operating conditions. The responses were reported as average values with standard deviation in Table IV.5 and Table IV.6.

The results showed that, for example, granules with good flowability and low moisture content (*HR*=1.1±8.2x10^{-3}, *CI*=8.3±0.688 %, *AR*=34.6±1.6 °, moisture=3.3±2.5x10^{-1} %) were produced under the conditions of run 4. Similar moisture contents were also found for the granules achieved working under the conditions of run 14 (3.2±4.1x10^{-1} %). Instead, at the operating conditions of run 1, a material with a high moisture (5.7±9.8x10^{-1} %) and a very poor flowability (*HR*=1.5±2.5x10^{-2}, *CI*=32.2±1.2 %, *AR*=61.5±11.1 °) was produced.

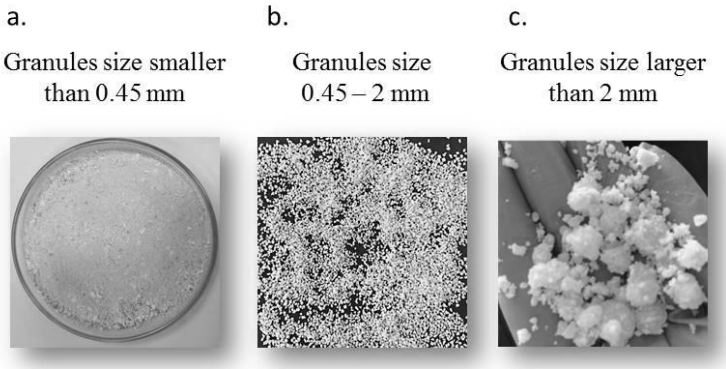

Figure IV.1 *Granules obtained with different combination of factors and levels: a. particles with size smaller than 0.45 mm, b. particles with size between 0.45 and 2 mm, that is the size range required, and c. particles with size larger than 2 mm*

Summarizing, the performed runs have underlined that not all the combinations of parameter levels ensure good granulation. There are operating conditions, like those of the run 11 or run 5, which combined together can produce a high amount of granules with size lower than requested one (0.45-2 mm), i.e. failure of the aggregation phenomena (see Figure IV.1 (a.)). Others (see run 7), instead, can achieve clusters of powder and binder, i.e. over wetting phenomena that is a condition to avoid (see Figure IV.1 (c.)). The best conditions of granulation, able to produce granules with a defined size (0.45–2 mm) and good flowability together with a high product yield, were obtained by working with a high impeller rotation speed, i.e., 112 rpm, a high binder to powder ratio, i.e. with a binder phase volume of 100 ml, and a low binder phase flow rate, i.e., 17 ml/min (see Figure IV.1 (b.)).

IV.1.4.3 Mathematical semi-empirical correlations

Mathematical semi-empirical correlations between granule properties and process parameters were developed by using the experimental data of the work matrix. In particular, experimental measurements of the product yield, Hausner Ratio, and Angle of Repose were fitted by several model equations. In these equations y_i was the dependent variable (i.e. y_p or *HR* or *AR*); x_i was the intensity of the key factors (i.e. impeller rotation speed, binder to powder ratio and binder phase flow rate); and a_{ij} represented the regression coefficients. Models linear (see eq. (IV.4)), semi-quadratic (see eq. (IV.5)) and quadratic (see eq. (IV.6)) were used.

$$y_i = a_{i0} + a_{i1} x_1 + a_{i2} x_2 + a_{i3} x_3 \quad \text{(IV.4)}$$

$$y_i = a_{i0} + a_{i1} x_1 + a_{i2} x_2 + a_{i3} x_3 + a_{i4} x_1 x_2 + a_{i5} x_1 x_3 + a_{i6} x_2 x_3 \quad \text{(IV.5)}$$

$$y_i = a_{i0} + a_{i1} x_1 + a_{i2} x_2 + a_{i3} x_3 + a_{i4} x_1 x_2 + a_{i5} x_1 x_3 + a_{i6} x_2 x_3 + a_{i7} {x_1}^2 + a_{i8} {x_2}^2 + a_{i9} {x_3}^2 \quad \text{(IV.6)}$$

The eq. ((IV.4), (IV.5) and (IV.6)) were fitted to experimental data and the regression coefficients are reported in Table IV.7, Table IV.8 and Table IV.9.

Table IV.7 *Regression coefficients of the tested correlations by using a linear model*

Regression coefficients of linear model			
	y_p	HR	AR
a_{i0}	0.919382	1.004212	28.34874
a_{i1}	-0.00076	-0.13374	0.270736
a_{i2}	0.009597	1.210582	10.61904
a_{i3}	-0.00278	-0.1355	-0.58098

Table IV.8 *Regression coefficients of the tested correlations by using a semi-quadratic model*

Regression coefficients of semi-quadratic model			
	y_p	HR	AR
a_{i0}	0.694293	109.2417	2.296001
a_{i1}	0.012854	-0.18509	0.399152
a_{i2}	0.002261	-0.84799	0.399519
a_{i3}	0.00697	0.014923	-0.05789
a_{i4}	-0.00011	0.002982	$-5.3x10^{-5}$
a_{i5}	-0.00015	-0.00468	-0.00281
a_{i6}	0.00005	0.003751	-0.00342

Table IV.9 *Regression coefficients of the tested correlations by using a quadratic model*

Regression coefficients of quadratic model			
	y_p	HR	AR
a_{i0}	2.43505	-0.02107	-179.975
a_{i1}	-0.00200	2.13873	6.48339
a_{i2}	-0.02689	-0.64221	-0.88212
a_{i3}	0.00953	-0.12999	-2.63559
a_{i4}	0.00000	0.00230	0.00514
a_{i5}	-0.00011	-0.005	-0.00049
a_{i6}	0.00014	0.003	-0.00234
a_{i7}	0.00003	-0.012	-0.03580
a_{i8}	0.00011	-0.001	0.00501
a_{i9}	-0.00017	0.003	0.03004

To assess how well a model describes (and potentially predicts) the experimental data, the coefficient of determination (R^2) was calculated (see Table IV.10). In statistical analysis, R^2, commonly known as ‘‘R-squared’’, is a guideline to measure the accuracy of the model equation to describe the experimental values (if $(R^2 = 0)$ the model does not describe well the data; if $(R^2 = 1)$ the data are explained and predicted very well from the model).

Table IV.10 *R-square values of the response variables (y_p, HR, and AR)*

	R-square (R^2)		
Responsive variables	y_p	HR	AR
Linear model	0.581	0.101	0.310
Semi-quadratic model	0.720	0.725	0.951
Quadratic model	0.988	0.892	0.962

Before choosing the type of correlation to be used as a predictive tool in a granulation study, a further comparison between the different proposed regression models was made performing the Akaike analysis (Snipes and Taylor, 2014, Akaike, 1974). The Akaike Information Criterion (*AIC*) is a measure of how the increase in the number of parameters (regression coefficients) really improves the prediction of a model. The selection of the best predictive model, according to Akaike, was determined by using the eq. (IV.7), where n is the number of data points; SSE_2 is the sum of square errors for the model with more parameters; SSE_1 is the sum of square errors for the model with fewer parameters; and $\Delta\pi$ is the difference between the number of parameters for the two compared models (Barba et al., 2009a).

$$\Delta AIC = n\, ln\,(SSE_2/SSE_1) + 2\,\Delta\,\pi \qquad \text{(IV.7)}$$

If the ΔAIC is negative the model with more parameters is more correctly used. In this case, the use of the chosen correlation was also statistically justified. In this study Akaike Information Criterion analysis results (Table IV.11) and R-square calculations (Table IV.10) have shown that the best suitable correlation was attained by using the second-order polynomial equation (quadratic model, eq. (IV.6)) for the product yield and *HR*, whereas *AR* experimental data were well described by the semi-quadratic one (eq. (IV.5)).

Table IV.11 ΔAIC values of the response variables (y_p, *HR*, and *AR*)

	ΔAIC		
Responsive variables	y_p	HR	AR
Compared linear/semi-quadratic model	-0.0562	-9.33	-27.66
Compared semi-quadratic/quadratic model	-41.60	-10.50	2.12

Experimental data and calculated values of product yield, Hausner Ratio and Angle of Repose were compared and illustrated in Figure IV.2, IV.3 and IV.4, respectively. It is noteworthy that experimental data are nicely fitted from the developed correlations.

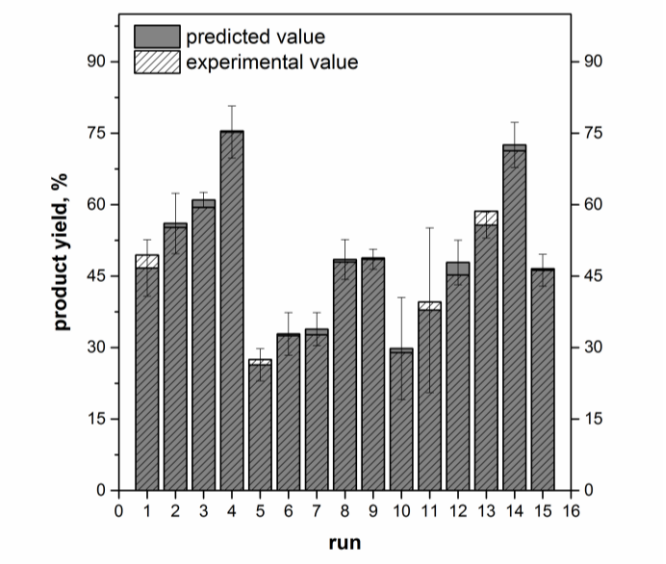

Figure IV.2 *Comparison between experimental and calculated product yield data (calculated using a semi-quadratic fitting model)*

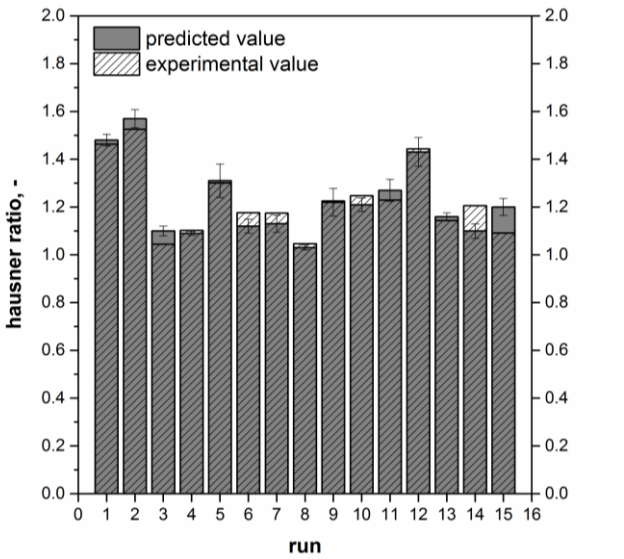

Figure IV.3 *Comparison between experimental and calculated Hausner Ratio data (calculated using a semi-quadratic fitting model)*

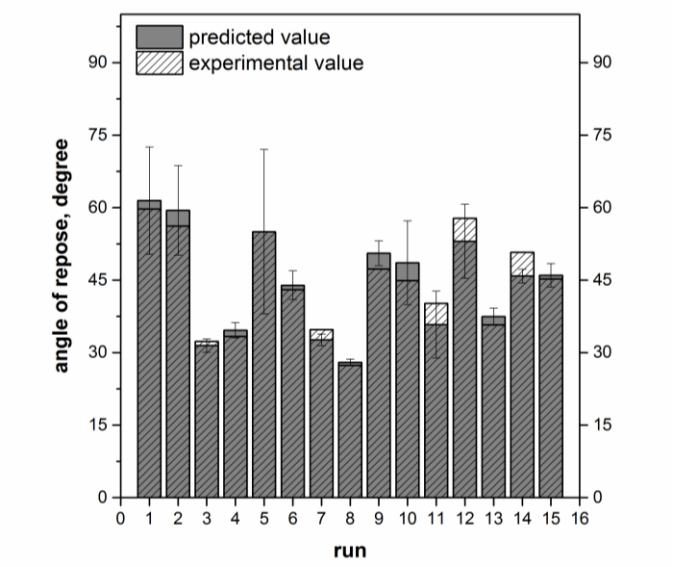

Figure IV.4 *Comparison between experimental and calculated Angle of Repose data (calculated using a semi-quadratic fitting model)*

Table IV.12 *Combination of levels not present in the plan work*

	Operative variables		
run	Impeller rotation speed [rpm]	Binder to powder ratio [-]	Binder phase flow rate [ml/min]
1	112	2	34
2	93	2	58
3	72	1	34

Table IV.13 *Correlations' validations: experimental data and predicted value for combination of levels not present in the plan work*

	Responsive variables					
run	y_p [%]		HR [-]		AR [degree]	
	Exp.	Pred.	Exp.	Pred.	Exp.	Pred.
1	66.1±1.8	51.8	$1.1\pm3\times10^{-2}$	1.2	34.3±3.6	29.7
2	42.6±5.4	55.0	$1.1\pm1\times10^{-2}$	1.1	36.9±1.7	35.8
3	27.6±5	28.1	$1.3\pm3\times10^{-2}$	1.5	55.1±5.9	56.6

With the aim of validating the proposed correlations several granulation tests were carried out by applying the combination levels of operative parameters not included in the work plan (see Table IV.12). These experimental tests have been intended as possible changes of conditions in granulation processes. As can be seen from data reported in Table IV.13, the developed correlations showed high predictive performance. In principle, these correlations are thus capable of predicting the value of variable responses at different operating conditions, being limited to the investigated system. However, they can be extended to *HMPC* similar particulate solids (i.e. materials with comparable features or non-perturbing active ingredients included in *HPMC* granules).

IV.2 Effect of vitamin payload on physicochemical, mechanical and release properties of *HPMC* granules

IV.2.1 Generalities

As already presented in the previous chapters, granules can constitute a good delivery system for drug/functional molecules for oral administrations/food preparations. Under technological point of view, granules present better global handling performances respect to powders: they are easy to dose, to dissolve and to administrate and they improve several properties of the powders, such as size, flowability and compressibility. These are the reasons for wide studies focused on their possible applications (Scala-Bertola et al., 2009, Hussein et al., 2008, Soni et al., 2013, Singh et al., 2015). Furthermore, many literature studies reported that the hydroxypropyl methylcellulose (*HPMC*), thanks its properties, described in the paragraph IV.1.2.1 is the most employed excipient in the formulation of hydrogel-based matrices in form of tablets or granules in order to obtain controlled release oral solid dosage systems (Barba et al., 2009b, Herder et al., 2006, Li et al., 2005, Siepmann and Peppas, 2012).

In light of that, in the following study, unloaded *HPMC* granules (used as control) and *HPMC* granules loaded with a model molecule, vitamin B12, were produced by the wet granulation process, with the aim to investigate their technological properties when active ingredients are added (influence of the payload on granules properties). Systems composed of *HPMC* and vitamin B12 are available on the market in form of tablets (for an example HealthAid Tablets with Cyanocobalamin 1000 μg, daily suggested dose) which contain microcrystalline cellulose, *HPMC* and di-calcium phosphate as bulking agent. Thus the efficacy of *HPMC* to get a sustained release of B12 is already demonstrated. Granules, however, can offer several advantages in order to realize customized dosage and oral administration to patients who have difficulty taking tablets. Therefore, the features of unloaded and loaded *HPMC* granules (size 0.45-2 mm) were studied in terms of physicochemical, mechanical and release properties to explore the effect of vitamin load and to understand if the *HPMC* is suitable, in granular form, to entrap and protect the vitamin B12.

IV.2.2 Materials

Hydroxypropyl methylcellulose (*HPMC* 20, purchased from Pentachem Srl, San Clemente RN – Italy) was used as polymeric powder, whose properties were described in the paragraph IV.1.2.1. Vitamin B12 (hydrophilic molecule, CAS 68-19-9, supplied by Sigma-Aldrich Srl, Milan – ITALY) was used in powder form as model molecule. Polymeric and B12

powders were used as received. Distilled water was used as binder liquid phase.

IV.2.2.1 Vitamin B12

Vitamin B12 (or Cyanocobalamin) is a hydrophilic molecule (solubility in water at 25 °C=12.5 g/l) that prevents the cardiovascular diseases and plays a key role in the formation of blood and in the normal functioning of the nervous system and brain (Knyazev et al., 2014). Literature studies showed that the absorption of vitamin B12 from food is not sufficient for subjects with high deficiency of it (Eussen et al., 2005). The deficiency is usually treated by intramuscular injections of vitamin B12, although, it was observed that the oral administration by food supplementations is more effective than intramuscular injections (Eussen et al., 2005). Moreover, oral administration has more patient compliance and it is less invasive.

IV.2.3 Methodologies

Unloaded *HPMC* granules (G_1 granules, used as control) and vitamin B12-loaded granules (G_1-B12) were manufactured by the wet granulation process, using operating conditions optimized in the previous study (see paragraph IV.1.4.2) in order to produce a high product yield and a solid particulate with good flow properties. In particular, the unloaded and loaded granules production was performed using the procedure reported in the paragraph III.3.1 and III.3.2, respectively, and applying dedicated protocols of stabilization and separation, as described in the paragraph III.2. Briefly, each batch (50 g of *HPMC* powders) was processed in a single pot using an impeller with the rotation speed of 112 rpm, a binder to powder ratio of 2, i.e. a binder phase volume of 100 ml, and a binder phase flow rate of 17 ml/min. Three different payloads of vitamin B12 (1 %, 2.3 % and 5 % w/w) were assayed and the payload was determined in agreement with the eq. (III.1), reported in the paragraph III.3.2. The vitamin B12 was incorporated in the HPMC granules by pre-dissolving it in the liquid binder phase (method 1, see paragraph III.3.2). To study the impact of a different kind of loading vitamin B12 was also incorporated as powder in *HPMC* powders batch mixing at a rotation rate of impellers of 78 rpm for 10 min (method 2, see paragraph III.3.2). Only the dry suitable fraction for practical uses, 0.45–2 mm in size, was fully characterized in terms of moisture content, size and particle size distribution, flow, mechanical and release properties by using the protocols described in the paragraphs III.5 and III.6. The product yield and the manufacturing scraps (small and big scrap) were calculated in according to the eqs. ((IV.1), (IV.2) and (IV.3)), respectively, defined in the paragraph IV.1.3. The effect of the vitamin B12 payload (1 %, 2.3 %, 5 % w/w) on physicochemical, mechanical and release properties of *HPMC* granules (fraction with size between 0.45–2 mm) was evaluated by performing the characterization tests in triplicate. All the measurements were

expressed as mean values ± standard deviation and statistically compared (see paragraph III.5.6).

IV.2.4 Results and discussions

IV.2.4.1 Effect of payload on physical granules properties

In Table IV.14 were reported the values of product yield, flow indices, residual moisture content and mean particle size of unloaded granules (G_1) and vitamin B12-loaded granules (G_1-B12) at three different payloads.

Table IV.14 *Unloaded and loaded granule properties (size 0.45–2 mm) in terms of product yields, flow indices, residual moisture content and mean particle size, obtained after drying and sieving (big scrap: particle fraction with size greater than 2 mm; small scrap: particle fraction with size lower than 0.45 mm)*

	G_1 granules	G_1-B12 (payload 1 %)	G_1-B12 (payload 2.3 %)	G_1-B12 (payload 5 %)
y_p [%]±SD	752±5.5	70.6±6.1	78.6±2.7	$60.6\pm6.6\times10^{-1}$
B_p [%]±SD	20.5±5.2	28.5±5.9	21.1±2.7	$39\pm7.9\times10^{-1}$
S_p [%]±SD	$4.2\pm3.4\times10^{-1}$	$8.9\times10^{-1}\pm6.8\times10^{-1}$	$3.5\times10^{-1}\pm8.3\times10^{-2}$	$3.8\times10^{-1}\pm1.2\times10^{-1}$
HR [-]±SD	$1.1\pm8.2\times10^{-3}$	$1.1\pm9\times10^{-2}$	$1.2\pm1.9\times10^{-2}$	$1.1\pm8.7\times10^{-3}$
CI [%]±SD	$8.3\pm6.7\times10^{-1}$	8.5±2.9	16±1.3	$8.6\pm7.3\times10^{-1}$
Moisture [%]±SD	$3.3\pm2.5\times10^{-1}$	$5\pm5\times10^{-1}$	$4.4\pm4.7\times10^{-1}$	$4.1\pm6.6\times10^{-1}$
Mean size [%]±SD	$7.9\times10^{-1}\pm3.6\times10^{-1}$	$8.4\times10^{-1}\pm3.9\times10^{-1}$	$1.2\pm5\times10^{-1}$	$8.9\times10^{-1}\pm4.2\times10^{-1}$

The results have highlighted that the incorporation of a load at 5 % of B12 in the *HPMC* powders produces a lower product yield ($60.6\pm6.6\times10^{-1}$ %) and a higher big scrap ($39\pm7.9\times10^{-1}$ %) compared to the unloaded granules and those loaded with 1 % and 2.3 % of B12. Thus, a high amount of vitamin B12 perturbs the features of *HPMC* granules in terms of granule formation size, demonstrating also that the semi-empirical correlations described in the paragraph IV.1.4.3 are limited to low loads of vitamin B12.

Instead, the presence of vitamin B12 (1 %, 2.3 % and 5 %) in the granules does not alter the small scrap fractions of loaded granules ($p > 0.05$), but a decrease of the small scrap of loaded granules compared to the unloaded granules was obtained ($p < 0.05$).

By comparing the residual moisture content of the unloaded and loaded granules after drying, no significant difference statistically was found ($p > 0.05$), except for the loaded granules with 1 % of B12, which appear to be more damp. Anyway, their water content is in usual industrial range, as well as reported in literature (Scala-Bertola et al., 2009).

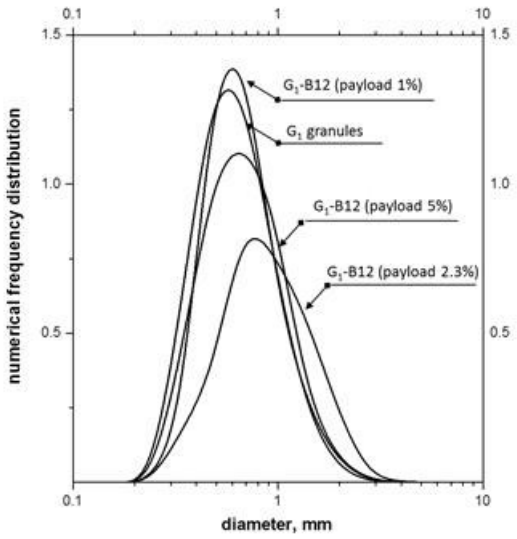

Figure IV.5 *Particle Size Distributions (PSDs) of unloaded and loaded dry granules with size between 0.45–2 mm*

The granules flow abilities were estimated by characterizing the solid material in terms of Hausner Ratio and Compressibility Index. In agreement with U.S. Pharmacopeia (see paragraph III.5.2), the values for Carr Index and Hausner Ratio obtained for all granule types indicates better flow properties for the unloaded granules and those loaded with 1 % and 5 % of B12 than granules loaded at 2.3 % of B12. The *PSDs* are in accordance with these results (see Figure IV.5). In fact, the loaded granules at 2.3 % of B12 have a wider broad granule size distribution ranging from 0.45 mm to 2 mm and thus there are particles less uniform in size, suggesting the reason of a different flowability of this product ($p < 0.05$).

IV.2.4.2 Effect of payload on mechanical granules properties

Unloaded and loaded granule mechanical properties were determined by compression tests, using the *ad hoc* built procedure, describe in the paragraph III.6.1. By compression analysis the force-deformation curves

were obtained, the maximum value of the force were determined, as plotted in Figure IV.6, and the granule strength was calculated according to eq. (III.9) and reported in Figure IV.7.

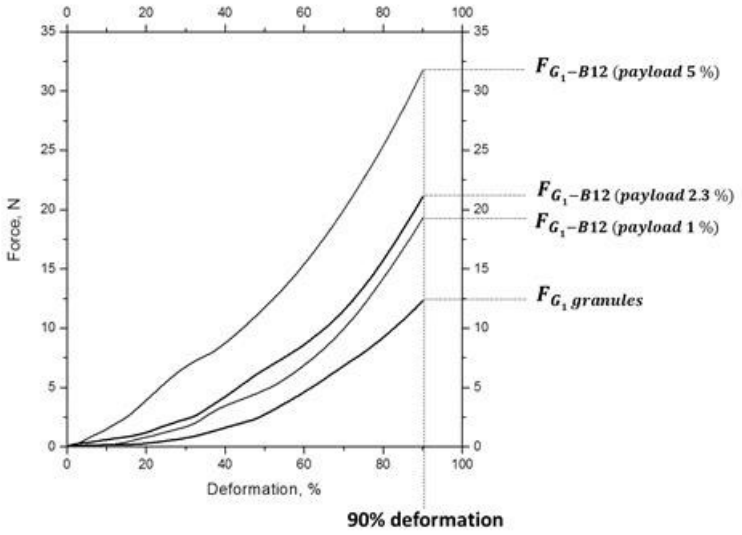

Figure IV.6 *Typical force-deformation curves obtained for loaded and unloaded dry granules with size between 0.71–1 mm*

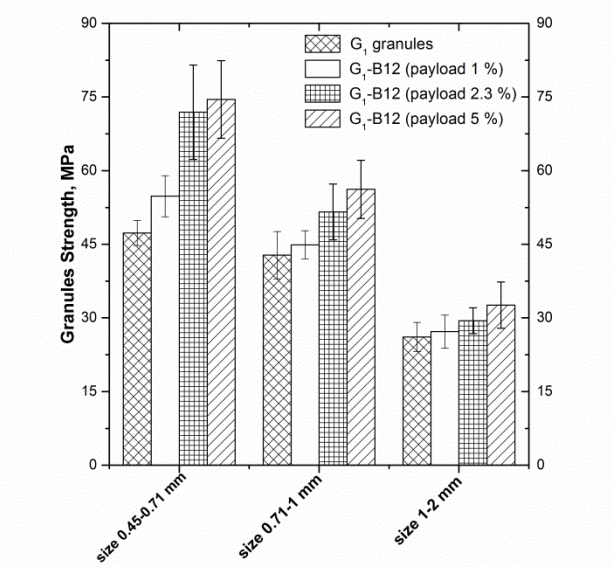

Figure IV.7 *Compression analyses: strength of unloaded and loaded dry granule for the three particle fractions (0.45-0.71 mm, 0.71–1 mm, 1–2 mm)*

Results showed that the presence of vitamin B12 in the granules with size 1–2 mm does not alter the hardness of loaded granules compared to unloaded granules ($p > 0.05$): similar granule strength value in corresponding to 90 % deformation was obtained. In granules with size 0.45–0.71 mm, the vitamin B12 presence increases the strength of loaded granules respect with unloaded granules ($p < 0.05$). In particular, the granules with a payload at 5 % of B12 have a greater hardness compared to those unloaded and loaded at 1 % of B12, result also found for the granule with size 0.71–1 mm. This means that the granules at 5 % of B12 are harder.

Some literature studies have suggested that the granules, as any solid, could to exhibit an elastoplastic deformation. About that, Hertz equation (see eq. (III.10)) was used to determine the granule elastic modulus by the force-deformation curves. In according to the work of Mangwandi et al. (2007), the gradient of F^2 vs Δ^3 was monitored and the mean young modulus of unloaded and loaded granules was calculated from the slopes of the elastic portion.

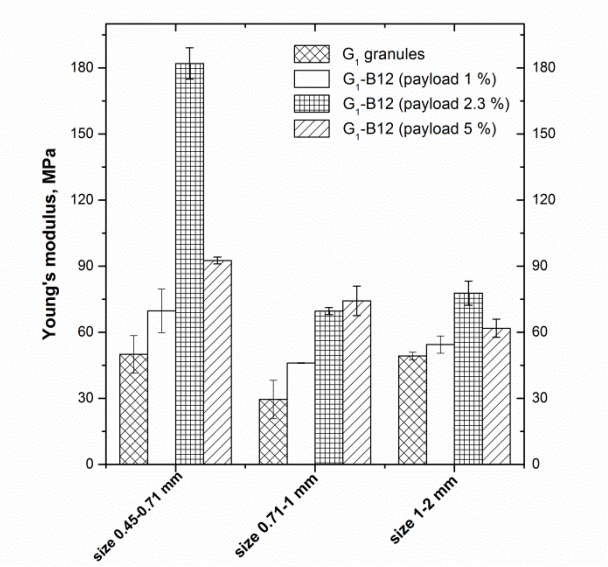

Figure IV.8 *Compression analyses: young modulus of unloaded and loaded dry granule for three particle fractions (0.45-0.71 mm, 0.71–1 mm, 1–2 mm)*

Results of mechanical properties in terms of young modulus are shown in Figure IV.8. It was observed that the loaded granules at 5 % of B12, with size 0.45-0.71 mm and 0.71–1 mm, beyond to be more hard were also less elastic ($p < 0.05$) than those unloaded and loaded at 1 % of B12, suggesting perhaps a different structural arrangement, i.e. a different granule porosity at 5 % of B12, as will be described in the paragraph IV.2.4.3. Thus, the presence of vitamin B12 has an influence on the elastic properties, in particular elastic modulus increases with increasing payload of vitamin B12

in the granules. For the granules at 2.3 % of B12, independently of the range size, granules more elastic were obtained compared to those unloaded and loaded at 1 % of B12.

It is worth noting that, overall, during the compression tests, no fragmentation of unloaded and loaded granules was observed because their morphology is quite compact, as investigated by *SEM* analysis (see paragraph IV.2.4.3).

IV.2.4.3 Effect of payload on morphological granule properties

Morphological features of pure *HPMC* powders, unloaded and loaded granules were investigated by using Scanning Electron Micropy (*SEM*), describe in the paragraph III.5.3. The morphological investigations of the *HPMC* powders (Figure IV.9 (a)) shown thin and elongated particles and some polymer spheres, as similarly found in Albertini et al. (2008). These primary filaments can still be identified in the agglomerates of *HPMC*: some of them protrude out from the surface of the unloaded and loaded granule, as can be seen in Figure IV.9 (b) and Figure IV.9 (d), respectively.

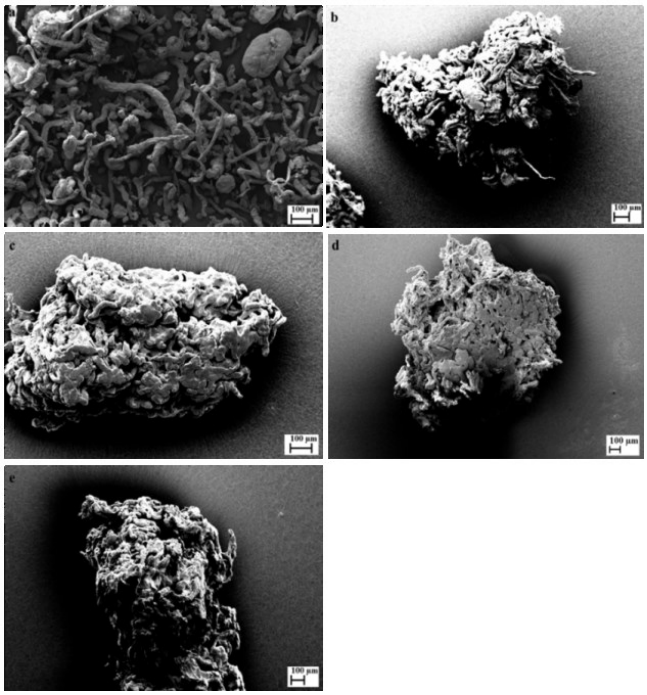

Figure IV.9 *Scanning Electron Microscope: a) HPMC powders; b) HPMC granule; c) vitamin B12-loaded HPMC granule (payload 1 %); d) vitamin B12-loaded HPMC granule (payload 2.3 %); e) vitamin B12-loaded HPMC granule (payload 5 %)*

Granules' *SEM* images (from Figure IV.9 (b) to Figure IV.9 (e)) shown a quite irregular shape and a fairly rough and porous surface, as also reported in Herder et al. (2006). The structure of the granules appears altered by the load procedure. The *SEM* images shown that the presence of vitamin B12 increases the porosity of the agglomerates. Particularly, with a payload at 5 % of B12 granules with a more porous surface were achieved (Figure IV.9 (e)). In this case, it was possible that the binder phase was more sequestered by the vitamin B12 and lends itself less to agglomerate the *HPMC* powders. Instead, a somewhat rough surface was observed in the granules loaded at 2.3 % of B12 (Figure IV.9 (d)) and this could be the reasons of the low flow properties of these granules, as described above (see paragraph IV.2.4.1). At last, for all the kinds of prepared loaded granules, no needle shaped crystals of active molecule were found on the surface and this result is in agreement with *DSC* investigation.

IV.2.4.4 Effect of payload on thermal granule properties

To evaluate if the granulation process has changed the solid state of the vitamin B12, Differential Scanning Calorimetry (*DSC*) analysis was carried out by using the technique reported in the paragraph III.5.4. *DSC* thermograms of pure vitamin B12, pure *HPMC* powders, physical mixture of *HPMC* and vitamin B12, unloaded and loaded dry granules were illustrated in Figure IV.10.

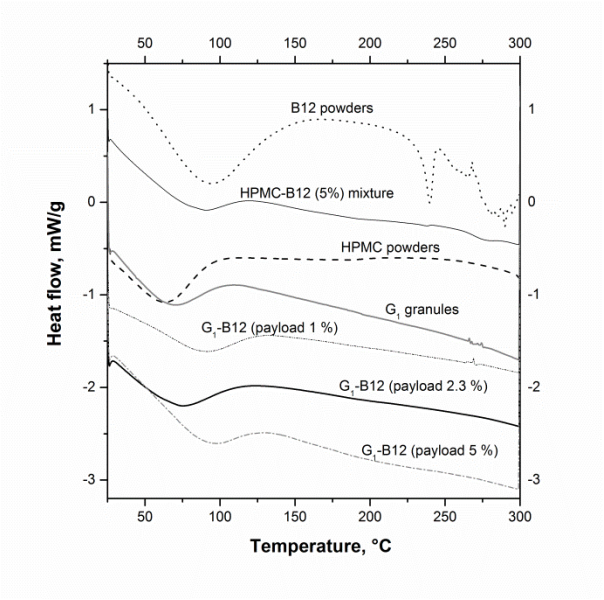

Figure IV.10 *DSC scans of pure vitamin B12, pure HPMC powders, HPMC-vitamin B12 (payload 5 %) mixture, pure HPMC granules, HPMC granules with vitamin B12 (payloads 1 %, 2.3 %, 5 % w/w)*

The thermal behaviour of the pure vitamin B12 shown a crystalline structure, exhibiting a broad endothermic peak in the range 60–120 °C, due to the loss of volatile components, and others three endothermic effects at about 231, 249, 257 °C, due to the decomposition of ligands coordinated to the cobalt atom, as reported in the work of Knyazev et al. (2014). The pure *HPMC* powders shown only one broad endothermic dehydration peak between 80 and 120 °C, related to the evaporation of moisture content. This result is in agreement with the literature data of Reverchon et al. (2008). The same *HPMC* peak can be seen in both unloaded and loaded granules. The physical mixture of *HPMC* and vitamin B12 at the highest payload (5 %) showed the endothermic peak at about 231 °C of crystalline vitamin B12, even not so pronounced due to the low concentration of vitamin itself. In the loaded granules no endothermic peak corresponding to vitamin B12 was detected. The absence of the endothermic peak of B12 in the granules emphasizes that the solid state properties of active molecule were modified by the wet granulation technique, showing an amorphous dispersion of vitamin B12 in the granules.

IV.2.4.5 Effect of payload on release granule properties

In literature, several methods have been applied to load an active molecule into solid carriers. In this work two loading methods were assayed, as reported in the paragraph III.3.2. In order to evaluate the effect of vitamin loading procedures on granules' features, vitamin solution spray in *HPMC* powders (method 1) and vitamin powders in *HPMC* bulk powders (method 2) were tested. Granulation tests were performed loading 1 % of vitamin B12; the loaded granules were dried, collected and sieved. Only the fraction with size between 0.45–2 mm was characterized and 1 g of them was dissolved in 1000 ml of distilled water at room conditions and 50 rpm, as described in the paragraph III.5.5.1. Product yield, Carr Index and Hausner Ratio were calculated and reported in Table IV.15.

Table IV.15 *Product yield, Hausner Ratio and Carr Index of vitamin B12-loaded granules (payload 1 %, size 0.45-2 mm) obtained predissolving of vitamin B12 in binder phase volume) and method 2 (pre-mixing of vitamin B12 with the powders of HPMC at 78 rpm for 10 min)*

	G_1-B12 (payload 1 %) method 1	G_1-B12 (payload 1 %) method 2
y_p [%]±SD	70.6±6.1	70.9 ± 3.4
HR [-]±SD	1.1±0.04	1.1 ± 0.07
CI [%]±SD	8.1 ± 3.4	10.8 ± 5.9

Results showed that the loading method does not create statistically significant effects on the granule properties (yield and flow index values were kept constant), but it influences the vitamin B12 distribution inside the *HPMC* polymer matrix, as observed from photos in Figure IV.11, captured by using a digital camera (Canon IXUS 850 IS). The image analysis showed that the loaded *HPMC* granules coloration (B12 imparts a rose-colour to *HPMC* granules, which unloaded, instead, were white) is more uniform in the *HPMC* granules achieved by method 1 (see Figure IV.11 (a.)). This perhaps is reasonably due to the high solubility of vitamin B12 in the binder phase and to its uniform spray by the ultrasonic atomization device.

a. b.

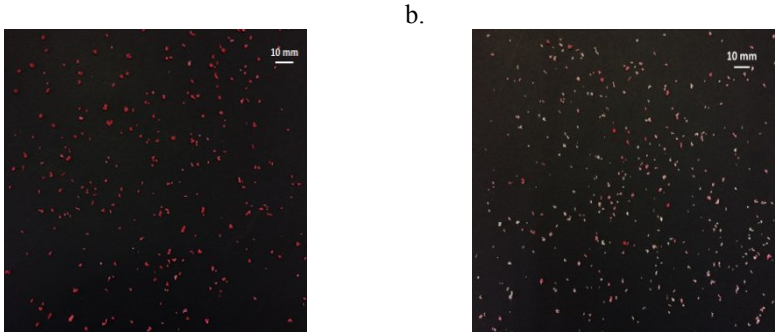

Figure IV.11 *Photos of vitamin B12 loaded HPMC granules (payload 1 %, size 0.45-2 mm) prepared by method 1 (predissolving of vitamin B12 in binder phase volume) and method 2 (pre-mixing of vitamin B12 with the powders of HPMC at 78 rpm for 10 min)*

As performed for the studies of the general and mechanical properties of loaded granules, loading method 1 was also applied to prepare batches for dissolution tests. The same three different payloads of vitamin B12 (1 %, 2.3 % and 5 % w/w) were considered to investigate if the *HPMC* granules are able to retain the vitamin B12.

Release studies were thus performed in agreement with the procedure described in the paragraph III.5.5.1; results are presented in Figure IV.12. In general, in Li et al. (2005) was reported that the drug release from hypromellose matrices and the hydration rate of the polymer depend on the hypromellose particle size and size distribution. However, in this work it was observed that all batch of loaded granules (size 0.45–2 mm) have the same mean diameter ($p > 0.05$) and thus the particle size does not influence the vitamin B12 release. Overall, it was observed that the release curves, achieved by simplified release tests as previously discussed in paragraph III.5.5.1, with the payload at 2.3 % and 5 % of B12 are not significantly different from each other ($p > 0.05$). As it is previously emphasized (paragraph IV.2.4.1) the high vitamin payload of B12 (5 % w/w) produces a large amount of big scrap and porous structures. This suggested the why there are not difference in the percentage of vitamin B12 released at 2.3 %

and 5 %: part of the B12 was in the big scrap which was not assayed. For a payload at 1 %, a slower release with respect to 2.3 % and 5 % was obtained. In particular, results showed that already at 15 min, granules with a payload at 1 % of B12 exhibits lower release profiles with respect to those loaded at 2.3 % and 5 % of B12 ($p < 0.05$); after 2 h the amount of B12 released was around 60 % for a payload with 1 % of B12, while, for a payload at 2.3 % and 5 % of B12 was about 90 %.

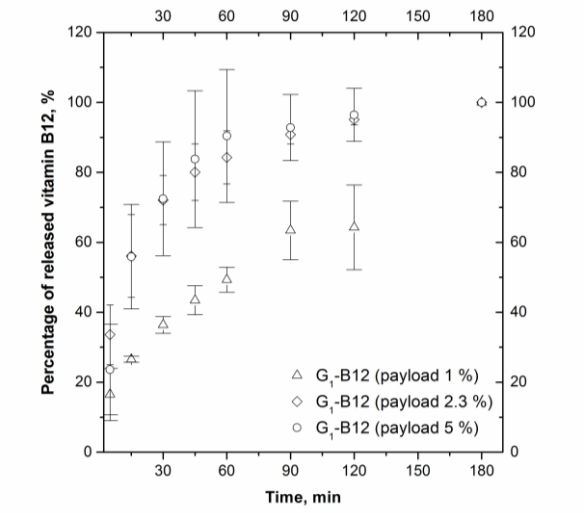

Figure IV.12 *Percentage of vitamin B12 released from HPMC granules (granules size 0.45–2 mm; payloads 1 %, 2.3 % and 5 % w/w)*

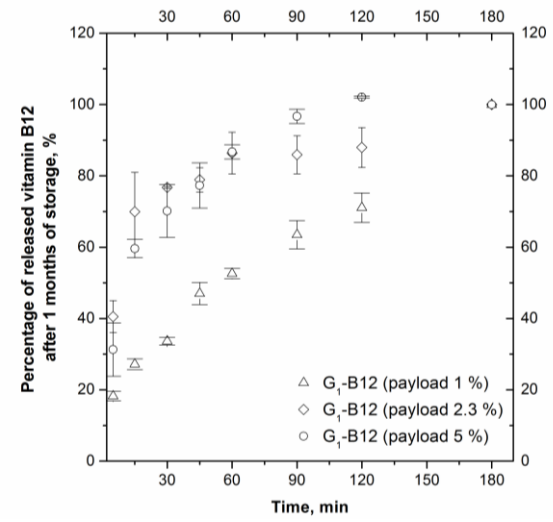

Figure IV.13 *Percentage of vitamin B12 released from HPMC granules (granules size 0.45–2 mm; payloads 1 %, 2.3 % and 5 % w/w) after 1 months of storage at room conditions*

Finally, to investigate the vitamin stability in the granules, release tests were carried out after 1 months of storage at room conditions, always adopting the procedure reported in the paragraph III.5.5.1. The vitamin B12 release profiles are presented in Figure IV.13.

The results showed that there are not relevant differences in terms of release properties between aged and fresh-prepared granules, suggesting a physical stability of the aged granules, at least for the examined time. This has confirmed the achievement of stable loaded granules.

It is important to note that already at 1 % of vitamin B12, a small amount of loaded granules, 100 mg, contains the recommended dose for oral administration by food supplementations (1 mg to day).

IV.3 Effect of binder phase and active molecule solubility on granules properties

IV.3.1 Generalities

Hydroxypropyl methylcellulose (*HPMC*) is one of the most important hydrophilic ingredients used in hydrogel matrices preparation in the form of tablets or granules. Drug release from *HPMC* matrix involves complex mechanisms (swelling, erosion, diffusion), which depend on the substitution pattern, content and viscosity of the polymer (Ghimire et al. (2010), Cheong et al., 1992, Gao et al., 1996, Jain et al., 2014, Ishikawa et al., 2000), solubility and particle size of the drug (Craig, 2002, Tahara et al., 1996), drug concentration in the gel layer (Bettini et al., 2001), presence of other polymers and excipients in addition to *HPMC* (Levina and Rajabi-Siahboomi, 2004), surface area and shape of the tablets (Caccavo et al., 2017a), method of incorporating of the materials, mixing time, compression force, and dissolution conditions (Velasco et al., 1999, Fuertes et al., 2010, Ohara et al., 2005). Several researchers reported that molecules with high solubility in water follow the diffusion release mechanism, whilst, poorly water soluble molecules are mainly released by an erosion mechanism (Li et al., 2005, Maderuelo et al., 2011, Viridén et al., 2009, Sung et al., 1996). In general, it is known that *HPMC* can be easily incorporated to form tablets by direct compression of its powder, by accommodating high levels of drug loading (Ghimire et al., 2010, Li et al., 2005). However, the drug-*HPMC* mixtures do not always have suitable compressibility degree and flow properties. Thus, compression of loaded *HPMC* granules is preferred before tableting. Wet granulation can be a good choice to produce granular forms and the selection of the proper wetting phase is important to assure reproducibility of *HPMC* based granules (McConville et al., 2004, Cao et al., 2005, Darunkaisorn et al., 2009).

Therefore, due to the importance of obtaining granular products with good physical, mechanical and release properties for the production of suitable pharmaceutical/nutraceutical dosage forms, aim of the following study was to investigate the effects of a hydrophilic (vitamin B12) model molecule and a lipophilic (vitamin D2) one on *HPMC* granules features. Because of the different hydrophilicity the effect of binder phase on granules physical, mechanical and release properties was also investigated.

IV.3.2 Materials

Hydroxypropyl methylcellulose (*HPMC* 20, supplied by Pentachem Srl, San Clemente RN-Italy) was used as polymeric powder forming granules, whose properties were described in the paragraph IV.1.2.1. Vitamin B12 (hydrophilic molecule, CAS n. 68-19-9, purchased from Sigma-Aldrich Srl,

Milan-Italy), whose properties were presented in the paragraph IV.2.2.1, and vitamin D2 (lipophilic molecule, CAS n. 50-14-6, supplied by Alfa Aesar Thermo Fisher (Kandel) GmbH, Germany) were incorporated, as model molecules, in HPMC powders by means of the wetting phase. All the powders were used as received. Distilled water and ethanol (CAS n. 64-17-5, purchased from Sigma-Aldrich Srl, Milan-Italy) were used to prepare the binder phases. Phenol (CAS n. 108-95-2, supplied by Sigma Aldrich Srl, concentration≥99% v/v) and sulfuric acid (CAS n. 7664-93-9, supplied by Sigma-Aldrich Srl, concentration 95–98 % v/v) were used for the quantitative colorimetric micro-determination of sugars (*HPMC*) in order to investigate the *HPMC* erosion rate of granules (Dubois et al., 1956).

IV.3.2.1 Vitamin D2

Vitamin D is a lipophilic molecule able to adjust the in vivo metabolization of calcium and phosphorus. Its deficiency causes an increased risk of many diseases, including some cancers, type 1 diabetes, cardiovascular disease, and osteoporosis (Barba et al., 2015). Ergocalciferol (vitamin D2, lipophilic molecule, solubility in water at 25 °C=12.6*10-9 g/l, solubility in ethanol at 25 °C=20 g/l) is one of the two common forms of vitamin D, synthesized in plants in presence of sunlight. Generally, the vitamin D is provided as an oil preparation or as a stabilized powder containing an antioxidant, such as a-tocopherol, because alone shows decomposition after only a few days of storage in air at room temperature: it is subjected to oxidation by the atmospheric oxygen and also isomerized in presence of light and under acidic conditions (Patel and San Martin-Gonzalez, 2012, Barba et al., 2015). Moreover, these preparations are typically provided in lightproof containers with inert gas flushing (Barba et al., 2015, Skibsted et al., 2010). Thus, new techniques for enhancing vitamins content, stability and bioavailability are currently developed. However, in several encapsulation methods, solvents, that are often not allowed by Pharmacopeia, are needed to solubilize hydrophobic polymers, and can cause vitamins degradation (Moebus et al., 2012, Barba et al., 2015).

IV.3.3 Methodologies

Unloaded *HPMC* granules (G_2) and vitamin D2-loaded *HPMC* granules (G_2-D2) with size of 0.45-2 mm were prepared by the wet granulation technique applying the same procedure, the same operating conditions and the same dedicated protocols of stabilization and separation used with the production of unloaded *HPMC* granules (G_1) and vitamin B12 loaded *HPMC* granules (G_1-B12) (see paragraph IV.2.3). The vitamin was incorporated in the *HPMC* granules by pre-dissolving it in the binder phase, because it was demonstrated that this loading method allowed a better degree of dispersion of the active molecule inside granules (see paragraph IV.2.4.5). The payload percentages investigated were: 1 % and 2.3 % w/w of active molecule,

calculated in agreement with eq. (III.1), reported in the paragraph III.3.2. Due to the different solubility of the two model molecules in water (B12 is hydrophilic and D2 is lipophilic), two different binder phase were used: distilled water for G_1 and G_1-B12, as already seen in the paragraph IV.2.3, and a solution of ethanol and water with a 75/25 v/v ratio for G_2 and G_2-D2. In particular, the vitamin B12 was directly dissolved in 100 ml of distilled water (G_1-B12 granules), while, the vitamin D2 was first dissolved in 75 ml of ethanol for its lipophilic feature and then diluted with 25 ml of distilled water (G_2-D2 granules). The unloaded granules (G_1 and G_2) were used as control. Only the size fraction 0.45-2 mm was characterized in terms of moisture content, size and particle size distribution, flow, mechanical and release properties by using the protocols described in the paragraphs III.5 and III.6. The product yield and the manufacturing scraps (small and big scrap) were calculated in according to the eqs. ((IV.1), (IV.2) and (IV.3)), respectively, defined in the paragraph IV.1.3. The effects of two formulation variables, molecule solubility and binder type, on physical, mechanical and release properties were investigated by performing the characterization tests in triplicate. All the measurements were expressed as mean values ± standard deviation and statistically compared (see paragraph III.5.6).

IV.3.4 Results and discussions

IV.3.4.1 Effect of binder phase and vitamin solubility on physical granule properties

Results of the product yield of control (G_1 and G_2) and loaded granules (G_1-B12 and G_2-D2) are shown in Table IV.16. The use of ethanol in granulation liquid (for the control granules G_2) reduces the granulation performance. A large amount of fine particles (size lower than 0.45 mm) was obtained (small scrap 31.2 %±0.2), thus causing a product yield (57.9 %±0.9) lower than the one obtained with the G_1 granules (75.2 %±5.5). Moreover, the mean size (d_g) in the useful fraction was reduced: d_g was about 0.8 mm and 0.5 mm for G_1 and G_2, respectively. Influence of the granulation liquid on size and agglomeration of *HPMC* granules could be explained on the basis of the wetting efficiency and the degree of granulation liquid saturation among the granule particles during the granulation process. In particular, a higher degree of granulation liquid saturation is associated with a larger amount of granulation liquid on the granule surface, producing a larger granules size due to enhanced compaction and coalescence (Cao et al., 2005). Therefore, the use of water alone as a granulation liquid induces a higher saturation for G_1 granules, tending to a larger plastic deformation as a result of the large number of collisions. These latter lead to the formation of larger and compact granules, as visible in Figure IV.14 (G_2-a).

Table IV.16 *Physical properties of the unloaded granules (G_1 and G_2) and of those loaded with vitamin B12 and vitamin D2, obtained after drying and sieving (granule size 0.45-2 mm), in terms of product yields, manufacturing scrap (big scrap and small scrap) and flow indices. Data were expressed as mean value ± standard deviation (SD)*

	G_1 granules (water as binder)	G_1-B12 (payload 1 %)	G_1-B12 (payload 2.3 %)
y_p (%) ± SD	75.2±5.5	70.6±6.1	78.6±2.7
B_p (%) ± SD	20.5±5.1	28.5±5.9	21.1±2.7
S_p (%) ±SD	4.2±0.3	0.9±0.7	0.4±0.1
ρ_b (kg/m^3) ± SD	197.0±4.7	213.3±8.6	227.3±13.9
ρ_t (kg/m^3) ± SD	214.0±5.3	233.3±9.9	270.4±12.4
HR (-) ± SD	1.09±0.01	1.09±0.03	1.19±0.02
CI (%) ± SD	8.3±0.7	8.5±2.9	16.0±1.3
d_g (mm) ± SD	0.79±0.36	0.84±0.39	1.16±0.51
Moisture (%) ± SD	3.3±0.2	5.0±0.5	4.4±0.5
	G_2 granules (ethanol-water as binder)	G_2-D2 (payload 1 %)	G_2-D2 (payload 2.3 %)
y_p (%) ± SD	57.9±0.9	54.0±1.3	58.5±3.6
B_p (%) ± SD	10.9±1.1	5.72±4.4	10.7±3.9
S_p (%) ±SD	31.2±0.2	40.3±5.7	30.7±0.3
ρ_b (kg/m^3) ± SD	148.3±4.2	166.2±7.7	173.9±1.1
ρ_t (kg/m^3) ± SD	171.0±0.8	192.5±7.7	203.7±3.8
HR (-) ± SD	1.15±0.03	1.16±0.01	1.17±0.01
CI (%) ± SD	13.2±2.1	13.7±0.5	14.6±1.1
d_g (mm) ± SD	0.49±0.21	0.51±0.21	0.49±0.21
Moisture (%) ± SD	3.8±0.1	4.4±0.2	4.3±0.3

On the contrary, the lower saturation degree in G_2 granules causes less collisions, preserving the filamentous structure of the *HPMC* powder, with a high intraparticle porosity (Figure IV.14 (G_2-b)). However, in G_2 granules there is a little fraction of larger, perhaps more saturated particles (Figure IV.14 (G_2-a)), that are similar in shape to G_1 granules (Figure IV.14 (G_1-a)).

Thus, as G_1 granule mean size is larger than the G_2 one, the shape of the smaller fraction of G_1 granules (Figure IV.14 (G_1-b)) is more defined than that of mean size fraction of G_2 granules (Figure IV.14 (G_2-b)).

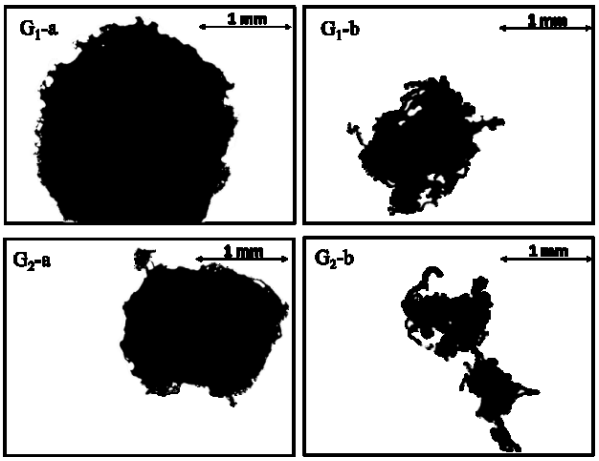

Figure IV.14 *Microscope (Leica DM-LP) photos of G_1 and G_2 granules (a, larger size; b, smaller size). 4 X magnification*

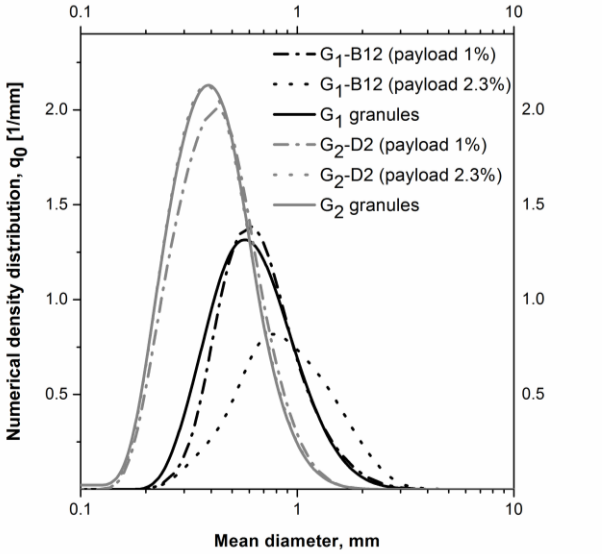

Figure IV.15 *Particle Size Distributions (PSDs) of granules (0.45-2 mm in size) unloaded (G_1, G_2) and loaded with 1 % and 2.3 % of vitamins (G_1-B12, G_2-D2)*

G_2 granules had bulk and tapped densities smaller than the G_1 granules, i.e. the G_2 granule mass occupied a greater volume than G_1 granules. This

confirms that ethanol in the binder produces granules with a less defined shape (as already shown in Figure IV.14).

The granule flowability was "excellent", in accordance with US Pharmacopeia, only for G_1 granules (1 < HR < 1.11; CI < 10 %), as reported in Table IV.16: CI and HR (13.2 %, 1.15, respectively) of G_2 granules were larger than CI and HR values (8.3 %, 1.09, respectively) of G_1. The smaller mean size and the less defined shape of G_2 granules gave them thus a worse flowability.

Presence of the lipophilic molecule did not influence neither size nor size distribution of the loaded granules (Table IV.16 and Figure IV.15, respectively): for G_2 granules the size remained unchanged after the loading procedure. In fact, as can be noted in Figure IV.15, the particle size distribution (*PSD*) of the useful fraction (0.45-2 mm) of G_2 granules is similar for both loaded and unloaded granules. Instead, the presence of the hydrophilic molecule altered both the size and the size distribution of the G_1 granules, especially at high payloads (2.3 % of B12), causing a worse flowability, as already observed in a previous work (see paragraph IV.2.4.1), a flowability worse than the one of G_2-D2 granules. In addition, increase in loading of active molecules (both vitamin B12 and vitamin D2). In addition, as it can be seen in Table IV.16, the increase in loading of active molecules (both vitamin B12 and vitamin D2) caused an increase of bulk and tapped density, due to a larger filling of voids in the solid particulate, obtaining thus matrices with more compact structures. Moreover, B12 had an impact on the granules physical properties, larger than to D2, due to its larger molecular weight and, consequently larger hydrodynamic radius (MW: B12=1355.4 g/mol, D2=396.7 g/mol; Stokes radius: B12=0.85 nm, D2=0.47 nm), causing a higher steric hindrance and a relevant higher filling of the void degree.

The residual moisture was almost the same for all types of granule ($p>0.05$) even if a little increase was observed when the active molecule was loaded, perhaps for the more compact structure keeping more water inside.

IV.3.4.2 Effect of binder phase and vitamin solubility on mechanical granule properties

Similar results were obtained from mechanical tests, as reported in Figure IV.16. Granules were compressed by a probe, recording the force required for deformation (see paragraph III.6.1). Granule strength (i.e. granule hardness) was defined as the maximum force value acting on the granule surface, according to eq. (III.9): the greater the granule strength, the harder the particles. Therefore, for the same particle size range (0.45-0.71 mm, 0.71-1 mm, 1-2 mm), G_1 granules required a greater force than the G_2 ones, to attain the same deformation, confirming that G_1 granules had a harder structure and a more defined shape. Vitamins loading increased the granule strength owing to a more compact structure, in agreement with Chevalier et al. (2010), that observed the ibuprofen loading effect on mechanical

properties of calcium phosphate granules. The results confirmed that the final mechanical properties of the granules depend on both the product composition and the individual components, as already suggested by other researchers (Caccavo et al., 2017b, Mangwandi et al., 2014).

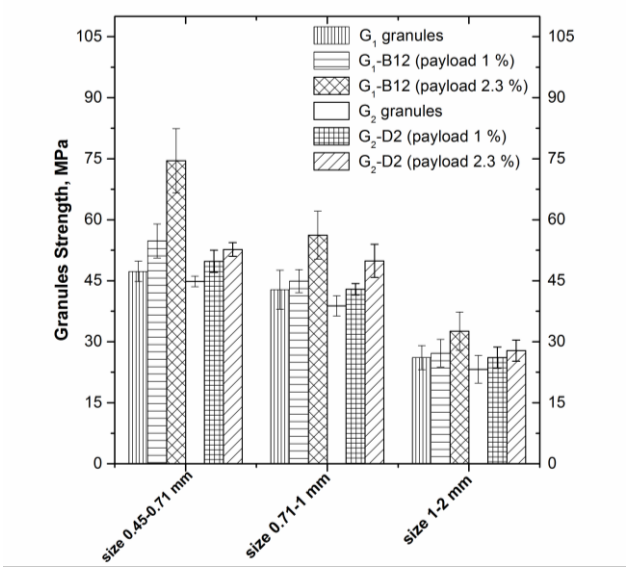

Figure IV.16 *Mechanical properties of the unloaded and loaded granules with size between 0.45-0.71 mm, 0.71-1 mm and 1-2 mm, in terms of granule strength. Data are shown as mean value ± standard deviation (SD)*

IV.3.4.3 Effect of binder phase and vitamin solubility on release and erosion granule properties

Dissolution tests of *HPMC* granules loaded with hydrophilic and lipophilic molecules (G_1-B12 and G_2-D2) were performed by using the procedure reported in the paragraph III.5.5.1, in order to investigate the effect of the vitamin solubility on the release mechanism from swellable and erodible hydrophilic matrices of *HPMC* in granules form. Released vitamin percentage from granules was defined in according to the eq. (III.7) and release profiles were reported in Figure IV.17. The lipophilic molecule (vitamin D2) was more slowly released than the hydrophilic one (vitamin B12). Actually, water-insoluble molecules tend to have slower release rates (Maderuelo et al., 2011). Moreover, the payloads influences the release rate for G_1-B12 granules: the higher the payload (2.3 % than 1 %) the greater the release rate. For example, after 60 min the G_1-B12-2.3% granules had already released 80% of vitamin B12, whereas granules loaded at 1 % showed a release of about 45 %. G_2 granules exhibit a slower vitamin release than the G_1 ones. After 3 hours, B12 was fully released from the G_1-B12 granules, while only the 14-15 % of D2 was released from G_2-D2 granules

(for both payloads). The main mechanism responsible for the molecule release is thus the outer layer erosion of the *HPMC* granules for vitamin D2, while for vitamin B12 this is attributed to the diffusion of the dissolved molecule through the matrix gel layer (Maderuelo et al., 2011, Fuertes et al., 2010).

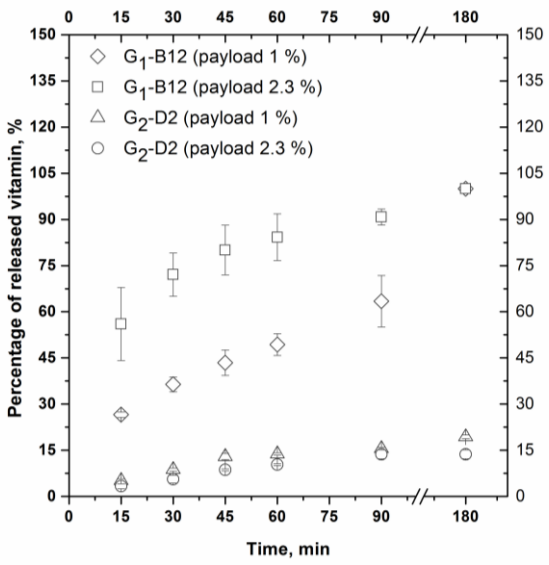

Figure IV.17 *Time profiles of the vitamin B12 and vitamin D2 percentage released from G_1 and G_2 granules, respectively. The experiments were performed in distilled water at room temperature, pH 6.5 and under 50 rpm stirring. Data are shown as mean ± standard deviation (repeatability 3)*

To confirm the hypothesis, measurements of the released *HPMC* from unloaded granules (G_1 and G_2) into the same dissolution medium were performed (see paragraph III.5.5.2). Eroded *HPMC* percentage from granules was defined in according to the eq. (III.8) and the erosion profiles of the *HPMC* granules-matrices were plotted in Figure IV.18. The results showed that the polymer erosion rate was slightly slower for the G_1 granules, due to their greater mean size and the more compact and harder structure. However, the percentage of eroded matrix of both types of *HPMC* granules was globally of about 7 % at 15 min and between 13-14 % at 180 min during the dissolution test.

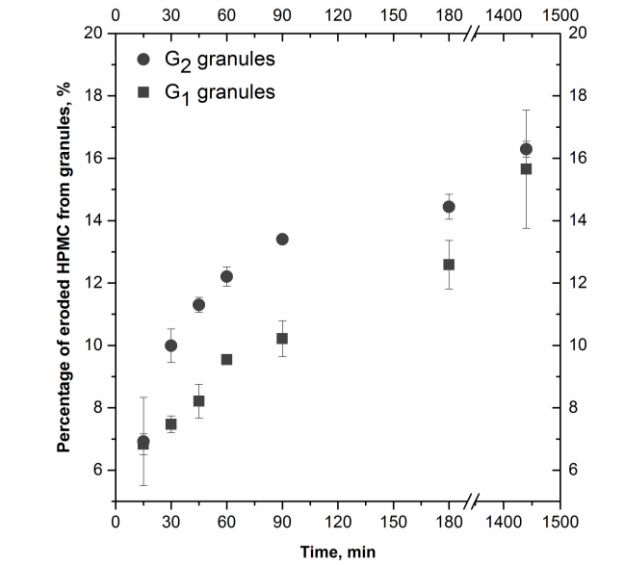

Figure IV.18 *Time profiles of the eroded HPMC percentage from G_1 and G_2 granules. The experiments were performed in distilled water at room temperature, pH 6.5 and under 50 rpm stirring. Data are shown as mean ± standard deviation (repeatability 3)*

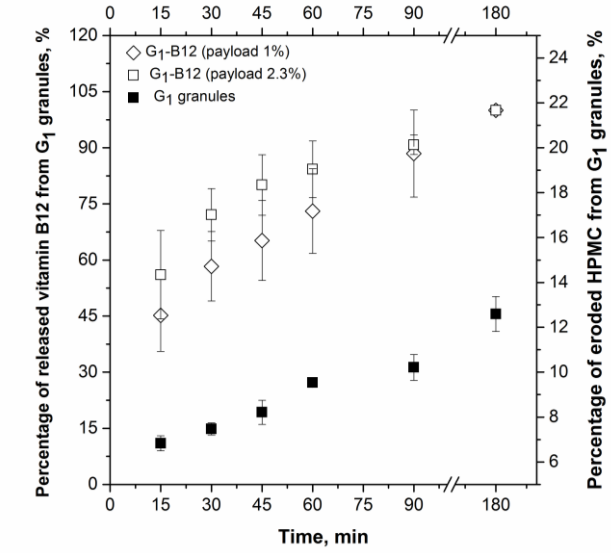

Figure IV.19 *Time profiles of the eroded HPMC and released vitamin B12 percentage from G_1 granules (payloads 1 % and 2.3 %)*

In Figure IV.19 the time profiles of the eroded *HPMC* and released vitamin B12 percentage from G_1 granules (payloads 1 % and 2.3 %) was

plotted. Instead, in Figure IV.20 are reported those of the eroded *HPMC* and released vitamin D2 percentage from G_1 granules (payloads 1 % and 2.3 %).

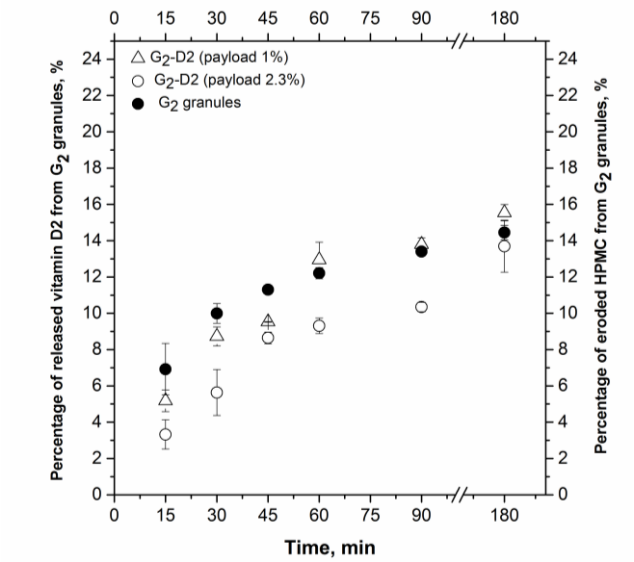

Figure IV.20 *Time profiles of the eroded HPMC and released vitamin D2 percentage from G_2 granules (payloads 1 % and 2.3 %)*

By comparing vitamins release to *HPMC* erosion data from matrices in granular form (Figure IV.19 and Figure IV.20), it was observed that the *HPMC* erosion rate of G_2 granules was similar to the vitamin D2 release rate from the same granules G_2-D2 ($p > 0.05$), confirming that the water-insoluble molecules mainly tend to follow a release mechanism based on a polymeric matrix erosion process (see Figure IV.20). On the contrary, the vitamin B12 release rate from G_2-B12 granules was faster than the unloaded granules erosion (see Figure IV.19), demonstrating that the water-soluble molecules dissolve and diffuse through the hydrated gel layer.

To quantify the different contributions of erosion and diffusion in the B12 release shown in Figure IV.19, a mechanistic model accounting for drug release, diffusion and erosion should be adopted (see for example studies reported in Siepmann and Peppas (2001), Lamberti et al. (2011), and Siepmann and Peppas (2000)).

IV.4 Chapter IV remarks

Nowadays, for both marketing reasons and technological aspects, the granules are the final products of a wide range of industrial transformations in pharmaceutical, nutraceutical, food, cosmetic, and zootechnical fields. Indeed, granules improve several properties of the powders, such as size, flowability and compressibility and can constitute a good delivery system for drug/functional molecules for oral administrations/food preparations.

The impact that the formulation and process variables have on final granule properties is continuously studied to predict the final product quality in order to achieve granules with toiled features. Despite that, in literature, experimental data and related mathematical correlations giving the combined effect of impeller rotation speed, binder to powder ratio, and binder phase flow rate on product yield and on flow index are not available, at least for granulation systems similar to that used in this work.

In this study, hydroxypropyl methylcellulose (*HPMC*) powder was agglomerated in a bench scale low-shear granulator apparatus by wet granulation process, spraying distilled water as binder phase by ultrasonic atomization device. Unloaded and loaded granulated are produced and characterized.

The Central Composite Design (*CCD*) statistical protocol was applied for planning the experimental campaign of *HPMC* granules production with sizes between 0.45-2 mm (sizes suitable for food, pharmaceutical and zootechnical applications). Three process variables (impeller rotation speed, binder to powder ratio, and binder phase flow rate), each at three intensities, were varied to assay their impact on the resulting dry granulated, in terms of product yield (% w/w of dry granules with sizes between 0.45 mm and 2 mm), residual moisture content, compressibility and flowability properties.

The performed tests have confirmed that the granule properties depend on the formulation and process variables. There are process operating conditions, which combined together cause failure of the aggregation phenomena; others instead, achieve clusters of powder and binder, i.e., overwetting phenomena, that is a condition to avoid. The best conditions of granulation, able to produce granules with a defined size (450–2000 mm) and good flowability together with a high product yield, to reduce manufacturing scrap, were obtained by working with a high impeller rotation speed, i.e., 112 rpm, a high binder phase volume, i.e., 100 ml, and a low binder flow rate, i.e., 17 ml/min. Then, mathematical correlations between granule properties and process parameters were developed by describing the experimental data with several model equations. Akaike information criterion and R-square calculations showed that the best comparison between experimental data and model predicted values was attained by using the second-order polynomial equation. The proposed correlations were then validated by new granulation tests, not included in the work plan provided

by *CCD* method, underlining their ability to predict the granule final properties in terms of flowability and product yield.

HPMC, thanks its versatile properties, is the most employed excipient in the formulation of hydrogel-based matrices in form of tablets or granules in order to obtain controlled release oral solid dosage systems. Therefore, the found combination of process parameters (for granules better final properties) was thus used in the production of loaded granules, with the aim to evaluate the effect of three formulation variables, molecule payload, molecule solubility and binder type, on their physical, mechanical, and release properties. First of all, the best loading method for a hydrophilic molecule, vitamin B12, in *HPMC* granules was investigated. Vitamin B12 was incorporated in the *HPMC* granules by two different loading methods: according to the method 1, it was dissolved in the liquid binder phase (here, the binder was a solution of water and vitamin B12); according to the method 2, the vitamin B12 was premixed with *HPMC* powders at an impeller rotation rate of 78 rpm for 10 min. It was observed that the loading method did not have significant effects on either the granules flowability or the yield, but a better dispersion of vitamin B12 inside the *HPMC* polymer matrix was achieved by the method 1, perhaps thanks to the high solubility of this vitamin in the binder and the relevant uniform spray by the ultrasonic atomization device. Thus, by exploiting the most successful method 1, three different payloads of B12 (1 %, 2.3 %, and 5% w/w) were tested. It was observed that a high vitamin payload (5%) reduces the product yield and brought to the formation of granules with a harder and less elastic structure if compared to unloaded ones and those loaded at 1 % and 2.3 % of B12. Vitamin release kinetics was slower when it was added with 1 % payload, thus suggesting a better incorporation. Moreover, the fresh and one month-aged granules showed release kinetics similar, thus no effect of the storage on release properties of loaded granules was observed. Moreover, the effect of the incorporation of a lipophilic molecule, vitamin D2, was also tested by using the loading method 1. Due to its lipophilic properties, a binder composed of a solution of ethanol and water with a 75/25 v/v ratio was used. Results showed that the use of ethanol give a reduced product yield and granules with a less defined shape, a smaller dimensions, a less hard structure, a worse flowability, and slightly faster polymer erosion if compared to granules produced using only distilled water as binder phase. It was demonstrated that the molecule solubility does not affect either granules' physical or mechanical properties, but it has effect on the molecule release mechanism (diffusion for the hydrophilic molecule and erosion for the lipophilic one).

Main results of this chapter are presented in:

De Simone V., Dalmoro A., Lamberti G., Barba A.A., "Design of Experiment's approach in granulation processes", national conference GRICU 2016, 12-14/09/2016, Anacapri (NA), Italy

De Simone V., Dalmoro A., Lamberti G., d'Amore M., Barba A.A, "Central composite design in HPMC granulation and correlations between product properties and process parameters", New Journal of Chemistry, 41 (2017) 6504-6513

Barba A.A., d'Amore M., Dalmoro A., **De Simone V.**, Lamberti G., "Production of granulates of hydroxypropyl methylcellulose loaded with vitamin B12 by wet granulation process", 8th International Granulation Workshop-Granulation Conference, 28-30/06/2017, Sheffield (UK), England

De Simone V., Dalmoro A., Lamberti G., Caccavo D., d'Amore M., Barba A.A, "HPMC granules by wet granulation process: Effect of vitamin load on physicochemical, mechanical and release properties", Carbohydrate Polymers, 181 (2018) 939-947

De Simone V., Dalmoro A., Caccavo D., Lamberti G., d'Amore M., Barba A.A., "Vitamins-loaded HPMC granules by wet granulation process: impact of liquid binder/vitamin solubility on HPMC granules properties", 23rd International Congress of Chemical and Process Engineering CHISA 2018, 25-29/08/2018, Prague (CZ), Czech Republic

De Simone V., Caccavo D., Dalmoro A., Lamberti G., d'Amore M.; Barba A.A., "Inside the phenomenological aspects of wet granulation: role of process parameters", chap. X in "Granularity in Materials Science", InTech Ed., 2018, ISBN 978-953-51-6821-8

De Simone V., Dalmoro A., Lamberti G., Caccavo D., d'Amore M., Barba A.A., "Effect of binder and load solubility properties on HPMC granules produced by wet granulation process", Journal of Drug Delivery Science and Technology, 49 (2019) 513-520

Chapter V

Phenomenological analysis for process parameters optimization in wet granulation

V.1 Generalities

For many years and still to a certain extent currently, granulation process is still based on practical experience. In general, the majority of literature is concerned experimentally with the role of material properties and process conditions on the properties of the product granules. However, phenomena taking place in granulators are still not well understood, and it is difficult to successfully produce a product with tailored features (in terms of size, morphology, hardness, release properties, etc.) without extensive experimental tests. This constitutes a great problem for industries exploiting many and frequently changing formulations with widely varying properties (e.g. food, pharmaceuticals and agricultural chemicals). Thus, new formulations always need expensive and lengthy laboratory and pilot scale testing. Moreover, even when pilot scale testing is ok, there is still a significant failure rate during scale up to the industrial production (Iveson and Litster, 1998b). In a wet granulation process, these phenomena normally occur simultaneously in granulator vessel and depend on formulation variables (feed-materials properties, i.e.: binder viscosity, liquid-solid surface tension, particle size distribution, and binder adhesive properties) and on process variables (equipment type and operating conditions, i.e.: binder volume, binder flow rate, method of binder addition, impeller rotation speed and process time) (Iveson et al., 2001a, Chitu et al., 2011, Litster, 2003a, Litster et al., 2001). Thus, only by a deep understanding of phenomena involved during granules formation suitable predictive tools can be developed with the aim to choose right process conditions to be used in developing new formulations by avoiding or reducing costs for new tests.

Studies on Particles Size Distribution (*PSD*) during the granulation process can offer a good initial understanding of both phenomena and effects of variables on granules size and shape (Rajniak et al., 2007, Ramachandran et al., 2008, Hu et al., 2008).

To light of knowledges acquired on the process through the experimental campaigns performed, in the following study, the understanding of the process (phenomenological analysis) for the process optimization was carried out, which constitute the novelty of this study. Phenomenological analysis for process parameters optimization was carried out by exploiting the *PSD* of *HPMC* granules at different granulation times. *PSD* measurements were obtained using an *ad hoc* built device based on Dynamic Image Analysis (*DIA*). Optimization studies on process time, binder phase flow rate, and impeller rotation speed were performed to achieve a high granulation yield (% w/w of wet granules with size between 2000 μm and 10000 μm). In this scenary the *DIA* technique is an indispensable tool to obtain statistically reliable experimental data.

V.2 Materials

For the preparation of granules, hydroxypropyl methylcellulose (*HPMC* 20), supplied by Pentachem Srl (San Clemente, RN-Italy) was used as polymeric powder, whose properties were described in the paragraph IV.1.2.1. Distilled water was used as binder phase.

V.3 Methodologies

HPMC granule production was performed by using a laboratory scale low-shear granulator. Briefly, the *HPMC* powder was processed spraying the binder phase (distilled water) by an atomization device assisted by ultrasonic energy (see paragraph III.2). During the granulation, on the basis of preliminary studies (see paragraph IV.1), the process time (20 min), the powder mass (50 g), the binder to powder ratio (2), i.e. binder phase volume (100 ml), the frequency (20 kHz) and the ultrasonic energy amplitude (45 %) of the atomization device were kept constant, whilst the impeller rotation speed (72, 93, 112 rpm) and the binder phase flow rate (17, 34, 58 ml/min) were varied to assess their impact on the resulting granulated product. The spray time was thus given by the ration between binder phase volume and binder phase flow rate. The experimental campaign (i.e. runs number to be performed) was planned by using the Full Factorial Design (*FFD*) statistical protocol, one of the *DoE* techniques already discusses in the paragraph III.4.1. In Table V.1, the experimental work plan for two independent variables at three levels was reported. For each run, the granulation process was stopped at predetermined times (2, 3, 6, 9, 12, 15, 18, 20 min), the wet granules were withdrawn, analysed by the *DIA*-based device, method

describe in the paragraph III.6.2, and then reintroduced inside the granulator to proceed with the process. This treatment (the time and the method of analysis) does not modify the granulate properties.

Table V.1 *Work plan for two independent variables (factors, k), each at three intensities (levels, L), in agreement with Full Factorial Design protocol (*$run\ number = L^k$*)*

	Independent variables	
Runs	Impeller rotation speed [rpm]	Binder phase flow rate [ml/min]
1	72	17
2	72	34
3	72	58
4	93	17
5	93	34
6	93	58
7	112	17
8	112	34
9	112	58

The granulation yield (y_g) and the manufacturing scraps (big scrap (*BS*) and small scrap (*SS*)) were selected as the dependent variables (results of interest) and defined as the % w/w of wet granules with size between 2000 µm and 10000 µm, 10000 µm and 20000 µm and 60 µm and 2000, respectively. Such a large dimensional range for the granulation yield it was chosen in light of the conventional following industrial steps of a granulation process (i.e. milling, drying etc.) that tend to reduce the granules size bringing them to desired dimensions.

Granulation yield, big scrap and small scrap were calculated, using the outputs data of the *DIA* (saved in spreadsheets files), as the difference between the volume-weighted undersize cumulative distribution values at a fixed size ($Q_{3_{size}}$), according to eq.s ((V.1), (V.2) and (V.3)) respectively.

$$y_g = \left(Q_{3_{10000\ \mu m}} - Q_{3_{2000\ \mu m}}\right) \times 100 \quad \text{(V.1)}$$

$$BS = \left(Q_{3_{20000\ \mu m}} - Q_{3_{10000\ \mu m}}\right) \times 100 \quad \text{(V.2)}$$

$$SS = \left(Q_{3_{2000\ \mu m}} - Q_{3_{60\ \mu m}}\right) \times 100 \quad \text{(V.3)}$$

Always from the *DIA*, the Ellipse Ratio (ER) was calculated for each particle and the number of particles per unit of volume (N_i), for each particles class "i", and the volume-weighted mean particle size ($x_{1,3}$) were determined by eq.s ((V.4) and (V.5)) respectively.

$$N_i, dm^{-3} = \frac{particles\ number\ for\ class}{total\ volume\ of\ particles} = \\ = \frac{\int_{x_{i-1}}^{x_i} q_0 dx}{\int_0^{\infty} x^3 q_0 dx} \sim \frac{q_{0,i}(x_i - x_{i-1})}{\sum_i x_i^3 q_{0,i}\,(x_i - x_{i-1})} = \frac{n_i}{\sum_i n_i \times d_i^3} \quad \text{(V.4)}$$

$$x_{1,3}, \mu m = \frac{\int_0^{\infty} x\, q_3 dx}{\int_0^{\infty} q_3 dx} \quad \text{(V.5)}$$

The number of particles per unit of volume is particularly useful to analyse the phenomenological behaviour of a process that involves *PSD* modifications. For example:

- agglomeration phenomena produce a shift of the *PSD* in terms of N_i toward higher dimensions with a lowering of the distribution function due to the lowering of particles density (smaller particles coalesce to form bigger particles, lowering the number of particles in the system);
- breakage phenomena produce a shift of the *PSD* in terms of N_i toward lower dimensions with an increasing of the distribution function due to the increasing of particles density (bigger particles break down in smaller particles, increasing the number of particles in the system);
- nucleation produces an increase of the *PSD* in terms of N_i in the size range interested by this phenomenon. For a granulation process, nucleation is generated by the formation of granules by particles with dimensions smaller than the smaller class (first class), producing an increase in the total number of particles.

Response Surface Methodology (*RSM*), statistical approach discusses in the paragraph III.4, was employed to optimize the process parameters in terms of binder phase flow rate and impeller rotation speed in order to obtain the maximum granulation yield.

All experimental batches (the 9 possible combinations) were performed in triplicate to reduce the possibility of erroneous results and to increase the confidence in the resulting empirical relationships derived using *RSM*.

V.4 Results and discussions

V.4.1 Phenomenology through the analysis of the time evolution of the PSDs

The analyses of *PSDs* evolution during the wet granulation process were particularly useful to understand the ongoing phenomenology of the process. In the following the results of the run 5 (central point of the work plan matrix (Table V.1): 93 rpm, 34 ml/min) will be discussed as example. All the other runs showed similar behaviour but at different times depending on the setting operating conditions (impeller rotation speed and binder flow rate). In Figure V.1 the undersize cumulative distribution by number (Figure V.1 (a.)) and by volume (Figure V.1 (b.)) were reported during the evolution of the granulation process. As it is known the numeric distribution emphasizes the presence of the more numerous particles, while the volume (or mass) distribution emphasizes the presence of particle with the greater volume/mass: the observation of both the distributions is indispensable to correctly interpret the results. The curves at time 0 min represent the *PSDs* of the *HPMC* powder. It has also to be considered that for this run (run 5) the spray time (the process time employed to spray the 100 ml of binder phase) is about 3 min (176 s).

It can be seen that for process times lower than the spray time (2 and 3 min) the distribution is strongly bimodal, with a large presence in number of small particles (Figure V.1 (a.)) as well as the presence of few and big agglomerates (better emphasized in Figure V.1 (b.)). This demonstrates that during the spray time the agglomeration phenomenon leads to the production of big aggregates: during the water adding phase the saturation of the granule increases, a higher fraction of the void space within the granules is filled with liquid, reducing the interstitial volume (Salman et al., 2006a). The granules become more easily deformable and more liquid is available on their surface. Therefore, the probability of a successful coalescence in case of granule collision is greater (Liu et al., 2000), with consequent increase in the particles mean size. Moreover, also the physical nature of the *HPMC* can be responsible for this behaviour: the *HPMC* is a physical hydrogel forming polymer, thanks to hydrophobic interaction between the polymeric chains (Caccavo et al., 2017c). Once the polymeric powders are reached by the water droplets, they can start to agglomerate also thanks to these weak bonds, forming large aggregates of gel-like nature.

However, as the granulation proceeds this large aggregates are broken apart thanks to the shear forces (the breakage phenomenon) and the *PSDs* move toward lower dimensions. After the spray time, as the granulation proceeds, an equilibrium is reached between agglomeration and breakage and the *PSDs* stabilize.

a. b.

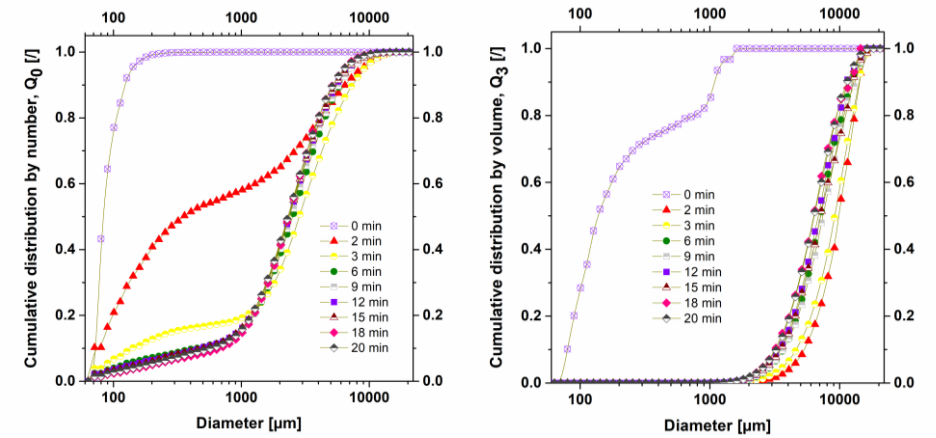

Figure V.1 *Undersize cumulative distribution of the HPMC particles at the process times of 0, 2, 3, 6, 9, 12, 15, 18 and 20 min: a. undersize cumulative distribution by number* (Q_0)*; b. undersize cumulative distribution by volume,* (Q_3)*. The illustrated tests were carried out granulating 50 g of HPMC 20 powder with 93 rpm, 100 ml of binder, and a flow rate of 34 ml/min*

The same reasoning can be done on the *PSDs* in terms of particle numeric density (see Figure V.2).

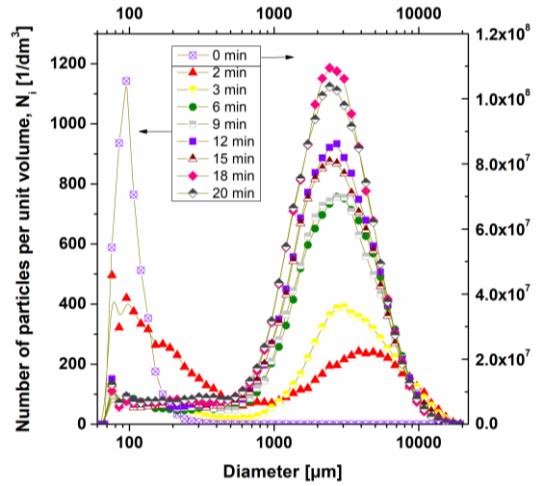

Figure V.2 *Number of particles per unit volume (axis y, right for 0 min and left for the others) with a given diameter (axis x) at different times of the granulation process. The data shown were obtained working 50 g of HPMC 20 powder with an impeller rotation speed of 93 rpm and a distilled water volume and flow rate of 100 ml and 34 ml/min respectively. Each experimental point represents a mean value from three independent experiments*

At 2 min, a bimodal curve can be observed due to the presence of both very small particles (peak at 100 μm) and agglomerates (peak at about 4500 μm with the distribution tail reaching 1 cm). At 3 min, the peak for small particles is highly lowered, but it does not disappear, even for longer times, for the permanence of the nucleation phenomenon. Indeed it is highly probable that fine particles (lower than 60 μm) continuously coalesce and form small granules that enter within the range of interest. In the first minutes (at process times lower than the spray time) the coalescence phenomenon (due to effective impact and gel forming tendency) prevails and small particles are agglomerated to form big structures.
After that all the binder is added, the breakage starts to be competitive with the agglomeration and the numeric particle density peak increases and moves towards lower dimensions.

Therefore, from the analysis of *PSDs* data in terms of Q_0, Q_3 and N_i, it can be highlighted the simultaneous presence of nucleation, agglomeration and breakage phenomena during all the process time, with an initial and strong presence of agglomeration (during the binder spraying) that is later balanced by the breakage phenomenon.

a. b.

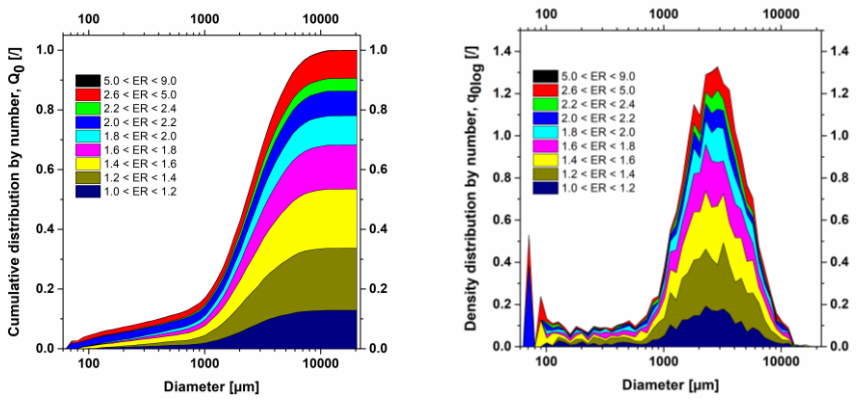

Figure V.3 *Particle Size Distribution cumulated with ellipse ratio (ER): a. the cumulative numeric undersize distribution (Q_0); b. the density distribution by number ($q_0 log$)*

Beside the dimension of the particles, from *DIA* data the ellipse ratio was determined for each particle to quantify their morphology. As example, in Figure V.3 ((a.) and (b.)) are respectively reported the cumulative and frequency distribution functions of the run 5 (central point of the work plan matrix: 93 rpm, 34 ml/min) cumulated with the ellipse ratio information. As it can be seen most of the particles present an elliptic shape (an image useful to individuate the impact of the *ER* value on the shape of the particle is provided in the paragraph III.6.2) and almost all are represented by an *ER* between 1 and 2.6.

V.4.2 Optimization of the process time

In a granulation process the variable of interest is the amount of product (in mass) that has a desired dimension. In this study, in the eq. V.1, it has been defined a granulation yield, which represents the percentage in mass of wet product with dimensions between 2000 μm and 10000 μm. Thanks to the phenomenological analysis, which allows a better understanding of the granulation phenomena, it is also possible to optimize the key parameters of the process. Before analysing the impact of the impeller rotation speed and the binder flow rate on the granulation yield via the *RSM* (see paragraph III.4), the process time can also be optimized, optimizing as well the production costs. Time evolution of the granulation yield and of the big scrap were investigated for all runs illustrated in the work plan matrix (Table V.1) in order to optimize the process time. Granulation yield and big scrap were calculated by volume-weighted undersize cumulative distribution according to eqs. ((V.1) and (V.2), respectively) showed above. The granulation yield is reported in Figure V.4 (a.) and the big scrap in Figure V.4 (b.) as mean values ± standard deviations (repeatability 3).

a. b.

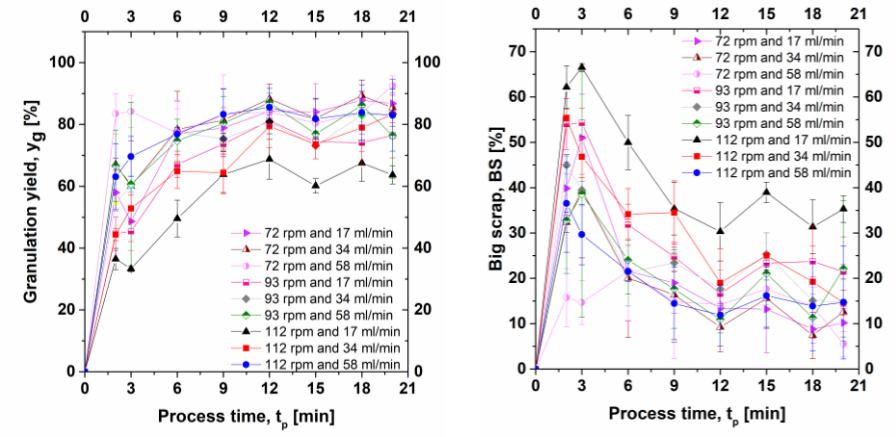

Figure V.4 *a. Granulation yield (% w/w of wet granules with size between 2000 μm and 10000 μm) during the wet granulation process; b. big scrap (% w/w of wet granules with size between 10000 μm and 20000 μm). Data are illustrated as mean values ± standard deviations (repeatability 3)*

Under all granulating conditions, a clear trend in terms of process time impact on the granulation yield is shown: a consistent growth of the granulation yield up to a plateau value. It can be noted that the plateau values, at constant impeller rotation speed, are reached sooner as the binder flow rate increases (Figure V.4 (a.)): the more the amount of binder phase added at a given time, the less the amount of big agglomerates (above 10000 μm) (Figure V.4 (b.)). At lower quantity of binder phase there is the

formation of big aggregates with the presence of ungranulated powders (in number) (as shown in Figure V.4 (b.)). However, these last are not relevant in terms of mass and therefore the resulting product has a consistent amount of big scrap: i.e. looking at the 112 rpm runs, at 3 min, the run with the lower flow rate (and therefore the lower amount of binder) shows the major presence of big scrap. Increasing the amount of binder (proceeding with the granulation time), the big aggregates are broken apart to form granules with the desired dimensions. The amount of 100 ml of binder seems to be necessary to reach its homogenous distribution within the systems so that all the powder mass can take part to the agglomeration process.

The impeller rotation speed, at constant flow rate, does not show a particular impact on the time required to reach the plateau value.

To consider the process at the best of its capabilities, in terms of granulation yield, an optimum process time of 12 min was chosen for all the runs to analyse the impact of the impeller rotation speed and of the binder flow rate. This represents a first important result, obtained thanks to the use of the Dynamic Image Analysis (*DIA*), since it optimizes the process time (of 8 min out of 20 min) with respect to that used in the previous studies (see Chapter IV), allowing faster and cheaper granulation processes.

V.4.3 Optimization of binder flow rate and impeller rotation speed

To optimize the effect of the impeller rotation speed (x_1) and binder phase flow rate (x_2) on the granulation yield, Response Surface Methodology (*RSM*) was applied.

In particular, the optimum values of the independent variables were identified by using the data of dependent variables (responses), in terms of granulation yield, manufactured big scrap and volume-weighted mean size, at the optimized process time (12 min) (reported in Table V.2).

Experimental results (9 values for each analysed dependent variable) were analysed with Design-Expert® 11 (a commercial software) to determine the statistical significance of the factors with analysis of variance (ANOVA) and to assess the correlation of the factors with the responses. The model used in the following will have the general form of a second-degree polynomial equation (see eq. (V.6)).

$$f(x_1, x_2) = p_{00} + p_{10} \times x_1 + p_{01} \times x_2 + p_{20} \times x_1^2 + p_{11} \times x_1 \times x_2 + p_{02} \times x_2^2 \quad \text{(V.6)}$$

In eq. V.6 p_{ii} are constants to be determined by fitting the experimental data. According to the Withcomb score (a heuristic scoring system) the best model to describe the relation between the factors and the yield is a quadratic model.

Table V.2 *Results of the run in terms of granulation yield, big scrap and volume-weighted mean particle size at the optimized process time (12 min)*

	Independent variables		
Runs	Granulation yield	Big scrap	Volume-weighted mean size
	y_g	BS	$x_{1,3}$
	[%]	[%]	[µm]
1	84.0	13.4	6555
2	88.3	9.2	6750
3	84.0	14.2	7252
4	81.2	16.6	7262
5	81.8	17.6	7266
6	87	10.9	6466
7	68.8	30.3	8378
8	79.4	19	7236
9	85.6	11.9	6383

Table V.3 *Fitting parameters for the polynomial fitting equation and the coefficient of determination*

$f(x_1, x_2)$	y_g,%	*BS*, %	$x_{1,3}$, µm
p_{00}	91.44	-33.38	1131
p_{10}	0.09	0.61	71.00
	p < 0.0001	p = 0.0001	p = 0.0008
p_{01}	-0.37	0.90	134.64
	p < 0.0001	p < 0.0001	p < 0.0001
p_{20}	-3.50×10^{-3}	0	0
	p=0.16180	/	/
p_{11}	1.02×10^{-2}	-1.18×10^{-2}	-1.64
	p < 0.0001	p < 0.0001	p < 0.0001
p_{02}	-5.12×10^{-3}	0	0
	p = 0.0387	/	/
R^2	0.95	0.9	0.95
$p-value$	p < 0.0001	p < 0.0001	p < 0.0001
$F-value$	32.27	38.1	79.37

Performing the analysis of variance, whose results in terms of coefficients and scores are reported in Table V.3, it can be seen that the whole quadratic model is, with an F-value of 37.27, significant. There is only a 0.01 % chance that an F-value this large could occur due to noise. The p-values of the model coefficients less than 0.05 indicate that the model terms are significant, whereas p_{20}, the quadratic coefficient associated with the first factor (rpm), with a $p > 0.05$ is statistically insignificant and the model could be reduced to neglect this term.

a.

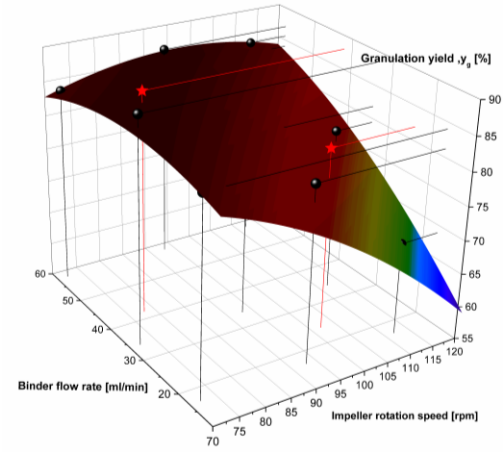

b.

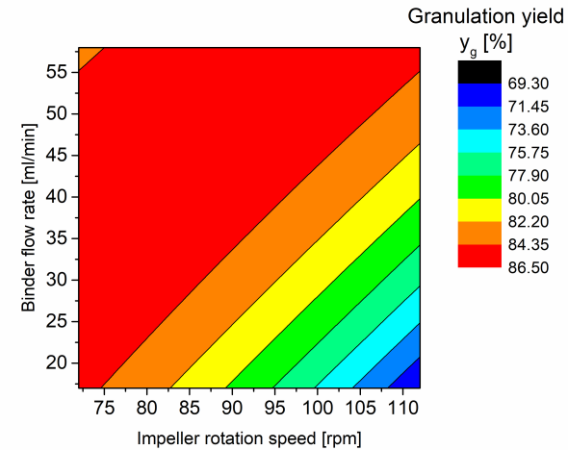

Figure V.5 *a. Response surface of granulation yields (% w/w of wet granules with size between 2000 µm and 10000 µm) at the optimized process time (12 min), calculated by varying rpm and binder flow rate. Black balloons represent the experimental results of run 1-9, red stars represent the validation runs (102 rpm and 24 ml/min and 78 rpm and 42 ml/min). b. Response surface in a 2D contour plot representation*

In Figure V.5 the effect of binder phase flow rate and impeller rotation speed (rpm) on granulation yield is shown. The response surface, better highlighted in Figure V.5 (b.), indicates that for low values of rpm the flow rate does not influence the granulation yield. The higher the rpm the stronger is the impact of the flow rate on the granulation yield. This is due to the fact that at higher rpm the energy transferred to the particles increases, and both the agglomeration and breakage phenomena become more relevant and more susceptible to the variations of other parameters. In particular, at the higher investigated impeller rotation speed (112 rpm), a binder flow rate of 17 ml/min brought to a granulation yield of 69 %, whilst a binder flow rate of 58 ml/min gave a granulation yield of 85 %. This demonstrates that the binder flow rate (i.e. its spray time) is crucial in the granulation process. The big aggregates formed in the first minutes, especially at high rpm, can consolidate ((Chevalier et al. (2009)) showed that at higher rpm the granules tend to have an higher density and a lower friability) and can be less subjected to breakage phenomena, resulting in an over granulated product.

From the study of the derivatives of the fitting equation (eq. (V.6)) of the granulation yield, which is a continuous function, the maximum value of the granulation yield (86 %) is obtained at 92 rpm and 55 ml/min, which is really close to the operative condition of run 6 (see Table V.1). The design space to optimize the granulation yield results is the red zone in the contour plot in Figure V.5 (b.).

To have a complete understanding of the process it useful to look also to the big scrap produced. According to the Withcomb score the best model to describe the relation between the factors and the big scrap is a two factor interaction model (in which the pure quadratic terms are set to zero). As it can be seen in Table V.3, the whole model as well as the coefficients is statistically significant. In Figure V.6 the resultant response surface (as 3D surface plot and contour plot) is reported. At the worst operative conditions (112 rpm and 17 ml/min) the amount of big scrap reaches the 30 % w/w, sign of an over agglomeration, whereas at the optimal conditions (92 rpm and 55 ml/min) the big scrap is only 11 %. This result could seem not in agreement with the findings of the previous study (see paragraph IV.1), where the optimum product yield, defined as mass percentage of particles between 450 μm and 2000 μm after the drying step, was find to be at 112 rpm and 17 ml/min. It is highly probable that during the drying process, the breakage phenomenon produces the translation of the *PSD* toward lower dimensions and therefore, an over agglomeration in the granulation step ensures the desired *PSD* at the end of the entire process. Despite this is not of interest in this study, the monitoring of the *PSD* during all process could be useful to optimize the single steps as well as the global industrial granulation processes.

a.

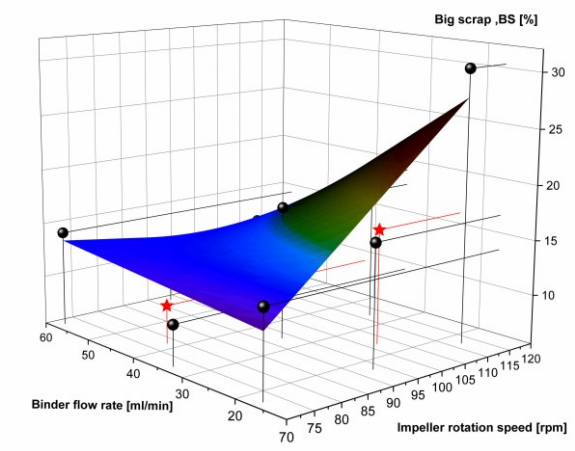

b.

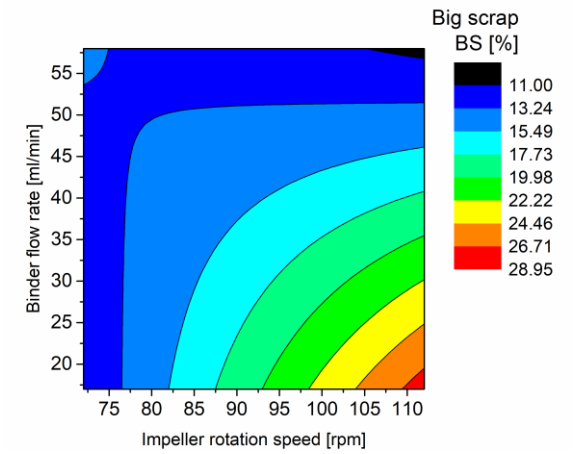

Figure V.6 *a. Response surface of big scrap (% w/w of wet granules with size between 10000 μm and 20000 μm) at the optimized process time (12 min) determined by varying rpm and binder flow rate. Black balloons represent the experimental results of run 1-9, red stars represent the validation runs (102 rpm and 24 ml/min and 78 rpm and 42 ml/min). b. Response surface in a 2D contour plot representation*

In Figure V.7 the impact of the impeller rotation speed and binder flow rate on the volume-weighted mean particle size ($x_{1,3}$) after granulation is reported (in Table V.3 the best fit parameters for eq. (V.6)). Also in this case the best model resulted to be the two factor interaction model and both the model and the coefficient results to be statistically significant. The Figure V.7 confirms the previous considerations: at the best operating conditions for granulation yield the mean size is about 6400 μm (well between the range of

interest), whereas it increases up to 8400 μm (closer to the upper limit of the defined granulation yield) at the worst operative conditions.

a.

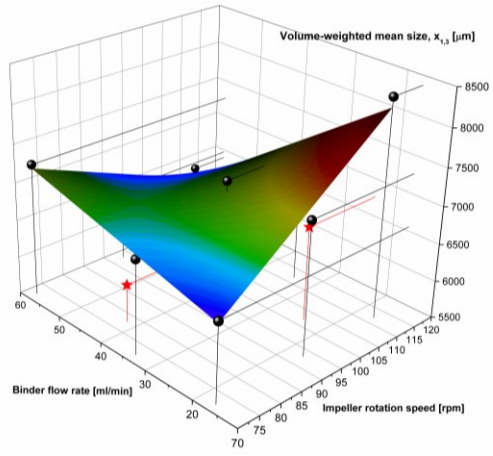

b.

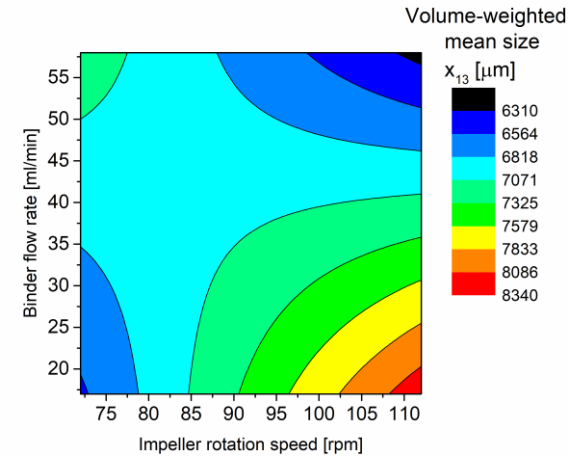

Figure V.7 *a. Response surface of weighted mean particle size of the volume distribution density vs binder flow rate and rpm. Black balloons represent the experimental results of run 1-9, red stars represent the validation runs (102 rpm and 24 ml/min and 78 rpm and 42 ml/min). b. Response surface in a 2D contour plot representation*

The fitting equations (eq. (V.6)) were validated comparing their predictions with respect to the results of granulation tests performed at two different intensities of the granulation parameters: 102 rpm and 24 ml/min and 78 rpm and 42 ml/min. The comparisons are reported in Table V.4 and the experimental results are reported in Figure V.5 (a.), Figure V.6 (a.) and Figure V.7 (a.) as stars.

Table V.4 *Comparison between experimental results and modeling predictions*

	102 rpm and 24 ml/min				78 rpm and 42 ml/min			
	Exp	Mod	Err abs	Err %	Exp	Mod	Err abs	Err %
y_g, %	82	78	4	5.8	88	86	2	2.3
BS, %	16	20	4	29.6	9	11	2	38.8
$x_{1,3}$, μm	7589	7589	831	160	5925	6951	1026	148

The modeling predictions, despite a slightly overestimation of the agglomeration phenomena (more evident in the volume weighted mean particle size) satisfactorily describe the experimental results considering the limited dimension of the *DoE* matrix used in this work (data driven models in general become more accurate increasing the number of data (runs) on which the model is trained). Therefore, with the eq. (V.6) and the parameter reported in Table V.3, it is possible to choose the operative conditions (rpm and impeller rotation speed) that provide the desired *PSD* with a certain granulation yield.

V.5 Chapter V remarks

In spite of its great importance and over 50 years of research, granulation process is still based on practical experience, i.e. there is a quantitative understanding of the process variables effects on agglomeration phenomena but a qualitative understanding of the granule growth mechanisms. A modern and rational approach in the production of granular structures with tailored features (in terms of size and size distribution, flowability, mechanical and release properties, etc.) requires a deep understanding of phenomena involved during granules formation. By this knowledge, suitable predictive tools can be developed with the aim to choose right process conditions to be used to improve the system performance, obtaining the maximum benefit from it without increasing the process costs.

Therefore, in this chapter, the phenomenological aspects involved in the formation of the granules with respect to the main process parameters and the operating conditions optimization are presented by experimental demonstration. In particular, a 3^2 Full Factorial Design approach was used to plan the experimental activities, considering impeller rotation speed and binder phase flow rate as independent variables (factors). *HPMC* granules behaviour, in terms of *PSD*, was investigated using an *ad hoc* built Dynamic Image Analysis (*DIA*) device, based on the free falling particle scheme. The process parameters optimization was carried out using Response Surface Methodology (*RSM*) and using the granulation yield (% w/w of wet granules within the size range 2000-10000 μm) as the main variable of interest, determined by *PSD* data. *PSD* measurements at different process times until 20 min showed that nucleation, agglomeration and breakage phenomena influence the wet granules size and occur simultaneously in the granulator, with the dominance of the agglomeration during the binder addition phase, later balanced by the breakage. It was shown that the granulation yield increases until 12 min, after which a steady state condition is reached. Moreover, response surface have highlighted that the interaction between the impeller rotation speed and the binder flow rate has a significant influence on the granulation yield (and in general on the granules *PSD*), especially at high rpm.

In conclusion, the coupling of statistical techniques (*DoE* and *RSM*) with the *PSD* analysis method (*DIA*) revealed to be a powerful tool to understand the phenomenology of the granulation process and thus allows the process conditions optimization.

Main results of this chapter are presented in:

De Simone V., Caccavo D., Lamberti G., d'Amore M., Barba A.A., "Phenomenological analysis, process parameters optimization and mathematical modeling of a low-shear wet granulation process", 23rd International Congress of Chemical and Process Engineering CHISA 2018, 25-29/08/2018, Prague (CZ), Czech Republic

De Simone V., Caccavo D., Dalmoro A., Lamberti G., d'Amore M.; Barba A.A., "Inside the phenomenological aspects of wet granulation: role of process parameters", chap. V in "Granularity in Materials Science", InTech Ed., 2018, ISBN 978-1-78984-308-8

De Simone V., Caccavo D., Lamberti G., d'Amore M., Barba A.A., "Wet-granulation process: phenomenological analysis and process parameters optimization", Powder Technology, 340 (2018) 411-419

De Simone V., Caccavo D.; Lamberti G., d'Amore M., Barba A.A., Dalmoro A., Low-shear wet granulation process: a new strategy in design and manufacturing of granular materials, to be presented to 3rd European Conference on Pharmaceutics, 25-26/03/2019, Bologna, Italy

Chapter VI
Mathematical modeling of the low-shear wet granulation

VI.1 Generalities

Mathematical modeling of the granulation process can play a dual role: can help to understand and to underline the observed physical phenomena and can predict properties (size and size distribution) of granular materials. It is important to note that the predictive ability is a powerful way to drive towards suitable process conditions, minimizing costs of experimental tests.

As already discussed in the state of art (see paragraph II.5), the Population Balance (*PB*) is the most used approach to modeling the wet granulation process: nowadays, the mathematical description of systems, where nucleation, agglomeration and breakage occur, is still performed by Population Balances, despite the complexity of the involved equations (integro-differential) (Salman et al., 2006a, Lister et al., 1995). *PB* form was initially publicized by Hulburt and Katz (1964), Randolph (1964), and Fredrickson et al. (1967) and it has been discussed at length by Ramkrishna (2000). The analytic solution of the Population Balance Equations (*PBEs*) is not trivial (Salman et al., 2006a). Several numerical methods have been developed to "easily" solve the *PBEs*. Among them the Discretization of the *PBEs* (*DPBEs*) in classes (multi-class method) is the most used method to describe the evolution of the entire *PSD*, including all the phenomena that cause variation of the distribution (Yang and Mao, 2014, J. et al., 1988, Kumar and Ramkrishna, 1996a, Kumar and Ramkrishna, 1996b, Kumar and Ramkrishna, 1997, Lister et al., 1995, Hounslow, 1990, Hounslow et al., 1988). The *DPBE* has been developed by Gelbard and Seinfeld (1980), Batterham et al. (1981), Marchal et al. (1988) and Landgrebe and Pratsinis (1990). By using *DPBEs*, the differentials are replaced with the Ordinary Differential Equations (*ODEs*), the integrals with the summation, and the

density distribution function with the number of particles in a certain interval.

Usually, in literature, the approach to the granulation process is based on either experimental tests (to study granules properties) or on modeling studies. In this study, an integrated approach was applied. In particular, a physical mathematical model based on the one-dimensional (one internal coordinate: particle size) discretized *PBEs* (*DPBEs*) was proposed and compared with experimental data. These models were implemented and numerically solved in MATLAB® 2014b in collaboration with researchers of TPP group. Nucleation, agglomeration, and breakage phenomena were considered in the formation of the granules. The *PBEs* was discretized in 60 classes, ranging from 60 to 20000 μm with a geometrical progression of $2^{1/6}$, therefore, the resulting model was a system of 60 *ODEs*, one for each class. Experimental data, i.e. number of particles per unit volume, were obtained from the tests already presented in the chapter V, by using a laboratory scale low-shear granulator.

VI.2. From the continuous to the discretized form of *PBEs*

Considering the entire granulator as control volume, the *PBEs* do not depend on spatial variables (external coordinates), and a general one-dimensional (one internal coordinate: particle size) *PBEs* for a mixed system can be written in agreement with eq. (VI.1).

$$\frac{\partial n(v,t)}{\partial t} = \frac{\dot{Q}_{in}}{V} n_{in}(v) - \frac{\dot{Q}_{out}}{V} n_{out}(v) - \frac{\partial[(G-A)n(v,t)]}{\partial v} + B_{Nuc}(v,t) + B_{Agg}(v,t) - D_{Agg}(v,t) + B_{Br}(v,t) - D_{Br}(v,t) \quad \text{(VI.1)}$$

$$I.C.\ n(v,0) = n_0(v)$$

$$B.C.\ n(0,t) = 0$$

In the eq. (VI.1), $n(v,t)$ is the probability density function $[b^{-1}\, x^{-1}]$, with "b" basis of calculation that can be the total mass of powder $[kg]$ or the total volume $[m^3]$, and x the particle volume $[m^3]$ or the particle diameter $[m]$, depending on the internal coordinate chosen. Indeed, this last v $[x]$ can be the particles volume v [m^3] or the particles diameter l $[m]$. $\dot{Q}_{in}$ and $\dot{Q}_{out}$ are the inlet and outlet flow rates from the system $[b\ t^{-1}]$, V is the volume or mass in the granulator $[b]$, G and A are the growth as layering and the attrition $[x\ t^{-1}]$, respectively. The terms *Nuc*, *Agg*, and *Br* are the abbreviations for nucleation, aggregation and breakage, respectively. In particular, B_{Nuc} is the birth by nucleation $[b^{-1}x^{-1}t^{-1}]$, which creates particles within the *PSD* of interest. B_{Agg} and D_{Agg} are the birth and death by

agglomeration of particle of size *v*, and analogously B_{Br} and D_{Br} are the birth and death by breakage phenomena of particle of size *v*.

For a batch granulator, where there are not inflow or outflow of particles, the only growth mechanism is coalescence and the attrition phenomenon can be disregarded (Litster and Ennis, 2013, Kumar et al., 2008), the eq. (VI.1) becomes:

$$\frac{\partial n(v,t)}{\partial t} = B_{Nuc}(v,t) + B_{Agg}(v,t) - D_{Agg}(v,t) + B_{Br}(v,t) - D_{Br}(v,t) \quad \text{(VI.2)}$$

$$I.C.\ n(v,0) = n_0(v)$$

In the eq. (VI.2) the birth and death by nucleation, agglomeration and breakage phenomena are expressed with the eqs. ((VI.3), (VI.4), (VI.5), (VI.6), and (VI.7), respectively).

$$B_{Nuc}(v,t) = k\delta(v) \quad \text{(VI.3)}$$

$$B_{Agg}(v,t) = \frac{1}{2}\int_0^v \beta(u, v-u)n(u,t)n(v-u,t)du \quad \text{(VI.4)}$$

$$D_{Agg}(v,t) = \int_0^\infty \beta(u,v)n(u,t)n(v,t)du \quad \text{(VI.5)}$$

$$B_{Br}(v,t) = \int_v^\infty b(u,v)S(u)n(u,t)du \quad \text{(VI.6)}$$

$$D_{Br}(v,t) = S(v)n(v,t) \quad \text{(VI.7)}$$

In these equations, *k* is a constant that multiply a function of the internal coordinate *v* ($\delta(v)$: Dirac delta function); β is the coalescence kernel [$b\ t^{-1}$], which describes both the frequency of collision between particles of internal coordinate *u* and *v* and the influence of the internal coordinates on the efficiency of agglomeration; *b* is the breakage function [x^{-1}], which describes the probability of formation of particles of internal coordinates v from the collision and breakage of particles of internal coordinates u ($u > v$); *S* is a selection function [t^{-1}], which describes the frequency at which particles of a given internal coordinates are broken.

The eq. (VI.2) was solved adopting a numerical method: the classes methods of zero-order (Salman et al., 2006b). According to the zero-order method, the probability density function ($n(v)$) is discretised in classes with characteristic size v_i: $v_i' \leq v_i \leq v_{i+1}'$. With the zero-order methods, the

PSD is approximated by a histogram and the particles are assumed to be uniformly distributed in each class. Therefore, the number of particles per unit base [b^{-1}], N_i, within a class with size range $[v'_i, v'_{i+1}]$, is determined in agreement with eq. VI.8.

$$N_i = \int_{v'_i}^{v'_{i+1}} n(v)dv = n_i(v'_{i+1} - v'_i) \quad \text{(VI.8)}$$

With this approach, instead of solving for a continuous (particle size) distribution, a system of ordinary differential equations (ODEs) is generated to describe the evolution of the number of particles within the classes. Increasing the number of classes, the number of ODEs increases as well as the computational power requirements: the most used discretization is based on a geometric progression with common ratio $v'_{i+1}/v'_i = 2^{1/q}$ (or equivalently $l'_{i+1}/l'_i = \sqrt[3q]{2}$), where q is an integer ≥ 1.

VI.3 Equations discretization

VI.3.1 Agglomeration phenomena

The most used discretized form of the agglomeration phenomena is the one proposed by Hounslow et al. (1988), where the PSD is broken up into discrete size intervals using a geometric discretization with $q = 1$ ($v'_{i+1}/v'_i = 2$). This approach was updated by Lister et al. (1995) to consider geometric progression with $q \geq 1$ ($v'_{i+1}/v'_i = 2^{1/q}$).

In this study, the agglomeration phenomenon was modelled by discretized form of Lister et al. (1995). In particular, the described agglomeration phenomenon is binary (interaction between two particles) and the birth terms are due to the collisions and coalescence between particles of lower dimensions with respect to the considered class. The death terms account for the interactions and coalescence of particles belonging to the considered class, producing their disappearance (and their birth in upper classes).

Generally, five possible types of interaction that change the number of particles in the *i*th interval can be established. Three type of interaction add particles larger than the *i*th interval (type 1, type 2 and type 3). The other two remove particle from the *i*th interval (type 4 and type 5). In particular, according to the type 1 some of the interactions give particles in the *i*th interval and some give particles smaller in the *i*th interval; according to the type 2, all the interactions give particles in the *i*th interval; according to the type 3 some interactions give particles in the *i*th interval and some give particles larger than the *i*th interval; according to the type 4 some interactions remove particles from the *i*th interval; according to the type 5 all interactions remove particles from the *i*th interval (Lister et al., 1995). The

total birth and death terms due to agglomeration phenomena are reported in eq. (VI.9).

$$
\begin{aligned}
&B_{Agg_i}(t) - D_{Agg_i}(t) = \\
&\sum_{j=1}^{i-S(q)-1} \frac{2^{\frac{j-i+1}{q}}}{2^{\frac{1}{q}}-1}\,\beta(i-1,j)\;N_{i-1}N_j \;+ \\
&+\sum_{k=2}^{q}\sum_{j=i-S(q-k+2)-k+1}^{i-S(q-k+1)-k} \frac{2^{\frac{j-i+1}{q}}-1+\;2^{\frac{-k+1}{q}}}{2^{\frac{1}{q}}-1}\beta(i-k,j)\;N_{i-1}N_j \\
&+ \\
&+0.5\,\beta(i-q,i-q)N_{i-q}^2 + \\
&+\sum_{k=2}^{q}\sum_{j=i-S(q-k+2)-k+2}^{i-S(q-k+1)-k+1} \frac{2^{\frac{j-i}{q}}-\;2^{\frac{-k+1}{q}}+2^{\frac{1}{q}}}{2^{\frac{1}{q}}-1} \\
&\beta(i-k+1,j)\;N_{i-k+1}N_j + \\
&-\sum_{j=1}^{i-S(q)} \frac{2^{\frac{j-i}{q}}}{2^{\frac{1}{q}}-1}\,\beta(i,j)\;N_iN_j \;-\sum_{j=1-S(q)+1}^{h}\beta(i,j)N_iN_j
\end{aligned}
\tag{VI.9}
$$

where $S(q)=\sum_{p=1}^{q}p$. For $q=1$ the Hounslow discretization can be obtained.

VI.3.1.1 The kernel of coalescence

The coalescence kernel is the most important parameter when describing granulation processes. A body of literature is present on this kernel, proposing several expressions ranging from purely empirical, semi-empirical and model-based kernels. In general, the coalescence kernel is split into two parts (see eq. VI.10): the first ($\beta_0(t)$) is the "aggregation rate" term and the latter ($\beta(u,v)$) expresses the influence of granule size on the likelihood of coalescence.

$$\beta(u,v,t)=\beta_0(t)\cdot\beta(u,v) \tag{VI.10}$$

In the first term of the eq. (VI.10), various system parameters are incorporated, such as the granulator operating conditions (i.e. granulator geometry, operating conditions) and the formulation properties (average primary particle size, binder viscosity, etc.) (Iveson, 2002, Abberger, 2007).

In this study, the first term of the coalescence kernel $\left(\beta_0(t)\right)$ was described on mathematical basis by a step function, depending on the spray time, as reported in the eq. (VI.11).

$$@\ t \geq t_{spray} \quad \beta_0 = \beta_\infty$$
$$@\ t \geq t_{spray} \quad \beta_0 = \beta_{in} \tag{VI.11}$$

The second term ($\beta(u,v)$) of the eq. (VI.10) determines the shape of resulting *PSD* and in it the assumption that each collision leads to coalescence is implicit (Abberger, 2007, Iveson, 2002). The nature of $\beta(u,v)$, most of the time an homogeneous function, establishes how the agglomeration modifies the internal coordinate, in particular whether or not the transformation is self-preserving in *PSD* and whether or not a gelling behaviour should be expected. Analysing the degree of homogeneity Λ ($\beta(cu,cv) = c^{\Lambda}\beta(u,v)$), which expresses the strength of the dependence of $\beta(u,v)$ on its argument, it is possible to distinguish between non-gelling and leading to a self-preserving size distribution kernels ($\Lambda \leq 1$) and gelling (and non self-preserving *PSD*) kernels ($\Lambda > 1$) (Abberger, 2007). Several empirical and theoretical expressions for $\beta(u,v)$ were proposed and used in the literature (see Table VI.1).

Table VI.1 *Examples of* $\beta(u,v)$ *and degrees of homogeneity*

Kernel	**Equation**	Λ
Constant kernel	$\beta(u,v) = 1$	0
Sum kernel	$\beta(u,v) = u + v$	1
Product kernel	$\beta(u,v) = u\,v$	2
Coagulation kernel	$\beta(u,v) = u^{\frac{2}{3}} + v^{\frac{2}{3}}$	2/3
Equi kinetic energy kernel	$\beta(u,v) = \left(u^{\frac{1}{3}} + v^{\frac{1}{3}}\right)^2 \sqrt{\frac{1}{u} + \frac{1}{v}}$	1/6

In this study, these $\beta(u,v)$ were implemented in Excel to get an idea of the behaviour of each function for a binary process. It was defined a matrix of 50 classes for *u* (rows of the matrix) and 50 classes for *v* (columns of the matrix), and each value was normalized with respect to the maximum value. In Figure VI.1, the (normalized) coalescence kernels are reported. As it can be seen, for a (normalized) sum kernel, a (normalized) product kernel and a (normalized) coagulation kernel, the maximum probability of coalescence in a binary process is between two big particles (high classes). Instead, for a (normalized) Equi Kinetic Energy (*EKE*) kernel the maximum probability of coalescence in a binary process is between a big particle (high classes) and a small particle (low classes).

The most used kernel in literature is the *EKE* kernel, which is a non-gelling and leading to a self-preserving size distribution kernels, as it can be seen from homogeneity degree, reported in the (see Table VI.1). Therefore, in this study *EKE* kernel was used for the second part ($\beta(u,v)$) of the kernel of coalescence.

a.

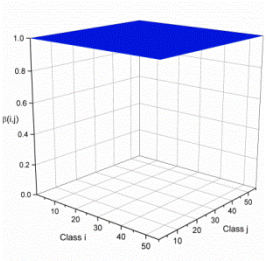

b.

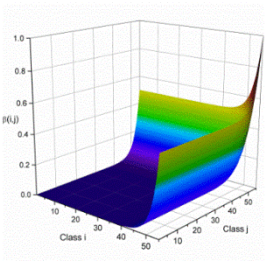

c.

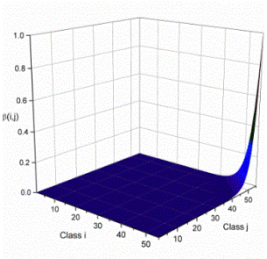

d.

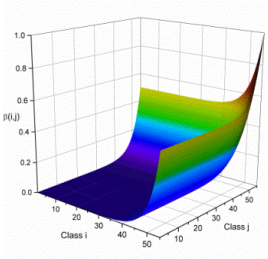

e.

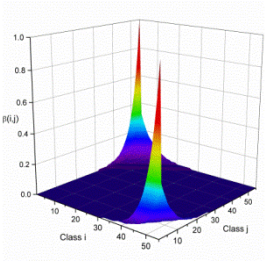

Figure VI.1 *Normalized coalescence kernel: (a) constant kernel; (b) sum kernel; (c) product kernel; (d) coagulation kernel;(e) Equi Kinetic Energy kernel*

VI.3.2 Breakage phenomena

The discretized form of the breakage phenomena is reported in the eq. (VI.12).

$$B_{Br_i}(t) - D_{Br_i}(t) = \sum_{j=i+1}^{\infty} b(v_i, v_j) S(v_j) N_j \Delta v'_j - S_i N_i \quad \text{(VI.12)}$$

However, as suggested in Vanni (2000), to satisfy the mass conservation (valid for both agglomeration and breakage), for all the possible discretizations (i.e. for a geometric progression of the type $v'_{i+1}/v'_i = 2^{1/q}$), the equation has to be corrected with the parameter *C* (see eq. (VI.X13)).

$$B_{Br_i}(t) - D_{Br_i}(t) = \sum_{j=i+1}^{\infty} \Gamma_{i,j} S_j N_j C_j^{(1)} - C_i^{(2)} S_i N_i \quad \text{(VI.13)}$$

where:

$$C_i^{(1)} = \frac{v_i}{\sum_{j=1}^{i-1} v_j \Gamma_{ji}} C_i^{(2)} \quad \text{(VI.14)}$$

$$C_i^{(2)} = 1 - \frac{1}{v'_{i+1} - v'_i} \int_{v'_i}^{v'_{i+1}} \left[\int_{v}^{v'_{i+1}} b(v, q) dq \right] dv \quad \text{(VI.15)}$$

$$\Gamma_{ij} = \int_{v'_i}^{v'_{i+1}} b(v_i, v_j) dv \quad \text{(VI.16)}$$

Where *S* is the selection function and *b* the breakage function, already described in the paragraph VI.2, with $C_1^{(2)} = 0$ and v_i the characteristic size *x* of the class in volume $[m^3]$. In this case, the distribution density function has been obtained ($n(l,t)$) and discretized ($N_i = n_i(l'_{i+1} - l'_i)$) with the diameter l_i as characteristic size. The relation $v_i \sim l_i^3$ can be used to adapt eqs. ((VI.14), (VI.15), and (VI.16)).

In this study, the breakage phenomenon was described by discretized form of Vanni (2000).

VI.3.2.1 The selection and breakage functions

Several functions can be chosen for the selection function and breakage function (continuous or discrete), usually of semi empirical nature: the breakage theory is not well developed as the agglomeration theory (Vanni, 2000).

In this study, the selection function was described by the power law expression, reported in eq. (VI.17), because it is the form usually adopted when more accurate predictions are sought, with exponent values (γ) taking in the range from $1/3$ to 2 (Vanni, 2000). In particular, it was considered $\gamma = 1/3$, and the first term of the selection function (k(t)) was defined on

mathematical basis by a step function, that depends on the spray time (see eq. (VI.18)).

$$S_i(t) = k(t) \cdot v_i^{\gamma} \tag{VI.17}$$

$$@\ t \geq t_{spray} \quad k = k_{i\infty}$$
$$@\ t \geq t_{spray} \quad k = k_{i0} \tag{VI.18}$$

Instead, in this study, the breakage function was described by the parabolic distribution, reported in eq. (VI.19), because it resumes many of the features of continuous fragment distribution functions (Vanni, 2000).

$$b(v_i, v_j) = \frac{c}{v_j - 1} + \left(1 - \frac{c}{2}\right)\left[\frac{8\,(3v_i^2 - 3v_i + 1)}{(v_j - 1)^3} - \frac{12(2v_i - 1)}{(v_j - 1)^2} + \frac{6}{v_j - 1}\right] \tag{VI.19}$$

The parabolic form, depending on *c,* can simulate different behaviors: with a concave parabola (*0≤c<2*), it is more likely the formation of unequal fragments; with a convex parabola (*2<c<3*), it is more likely the formation of equal fragments; with (*c=2*), the equation simplifies to the case of uniform breakage, in which it is equally likely to form a child particle of any size (Vanni, 2000). In this study, $c = 0.5$ was used.

VI.3.3 Nucleation phenomena

Nucleation phenomena occurs because small particles lower than the considered minimum size class can suddenly form granules (i.e. due to the action of binder droplets) within the considered size range. In light of this, it is clear that nucleation is not a mass conservative mechanism. It can be modeled considering the eq. (VI.20), in which $\eta(t)$ is a function of time and describes for how long this phenomenon is present, and $f(i)$ is a function of the size class and it individuates the class interested by nucleation.

$$B_{Nuc_i}(t) = \eta(t) \cdot f(i) \tag{VI.20}$$

In this study, it was assumed that the nucleation rate was firstly high (when the amount of powder is large it is much more likely that a drop will fall on the powder and form an aggregate) and then decreased gradually until it reached a steady state value.

$$\left(\eta_0\left(e^{-\frac{t}{t_{nuc}}}\right) + \eta_\infty\right) \cdot \left(\frac{1}{\delta\sqrt{2\pi}}\, e^{\frac{1}{2}\left(\frac{x_i - \mu}{\delta}\right)^2}\right) \tag{VI.21}$$

In particular, the birth by nucleation ($B_{Nuc_i}(t)$) was mathematically represented with a continue function (see eq. (VI.21)), given by the product of a decreasing exponential function, which depends on the nucleation time (t_{nuc}) and has asymptotic value η_∞, and a normal distribution (with

maximum unit height, mean (μ) and standard deviation (σ) of 90 μm). The mean value of the distribution was chosen equal at 90 μm since this was the average size of the drops generated by the atomizer.

VI.3.4 Models implementation

In this study, a pure agglomeration model, an agglomeration and breakage model, and a complete model with agglomeration, breakage and nucleation, were implemented and solved numerically in MATLAB® 2014b to describe the experimental results and find the best fitting parameters. The discretization was performed in 60 classes, ranging from 60 μm to 20000 μm with a geometrical progression of $2^{1/6}$ (i.e. $q = 2$). Thus, the resulting *DPBEs* were a system of 60 Ordinary Differential Equations (*ODEs*), one for each class. The *PSD* of the *HPMC* powders, obtained by *DIA*-device (see chapter V), and a time range of [0 min, 20 min] were used as initial condition and extremes of integration, respectively. The *DPBEs* for the three models mentioned above with corresponding parameters are shown below.

<u>*Pure agglomeration model*</u>

The pure agglomeration model (see eq. (VI.22)) disregards the breakage and nucleation phenomena and considers only the agglomeration one in the formation of granules. The model parameters are two: β_{in} and β_{∞}, explicated in the first term of the kernel of coalescence (see eqs. ((VI.10) and (VI.11))).

$$\begin{aligned}\frac{dN_i}{dt} = & \sum_{j=1}^{i-S(q)-1} \frac{2^{\frac{j-i+1}{q}}}{2^{\frac{1}{q}}-1}\beta(i-1,j,t) * N_{i-1}N_j \; + \\ & + \sum_{k=2}^{q} \sum_{j=i-S(q-k+1)-k+1}^{i-S(q-k+2)-k} \frac{2^{\frac{j-i+1}{q}} - 1 + 2^{\frac{-k+1}{q}}}{2^{\frac{1}{q}}-1}\beta(i-k,j,t)N_{i-1}N_j + \\ & + 0.5\beta(i-q,i-q,t)N_{i-q}^2 + \\ & + \sum_{k=2}^{q} \sum_{j=i-S(q-k+1)-k+1}^{i-S(q-k+2)-k+2} \frac{2^{\frac{j-i}{q}} - 2^{\frac{-k+1}{q}} + 2^{\frac{1}{q}}}{2^{\frac{1}{q}}-1}\beta(i-k+1,j,t)N_{i-k+1}N_j \\ & + \\ & - \sum_{j=1}^{i-S(q)} \frac{2^{\frac{j-i}{q}}}{2^{\frac{1}{q}}-1}\beta(i,j,t)\,N_iN_j \; - \sum_{j=1-S(q)+1}^{h} \beta(i,j,t) * N_iN_j\end{aligned} \tag{VI.22}$$

Agglomeration and breakage phenomena

The agglomeration and breakage model (see eq. (VI.23)) disregards only nucleation phenomena in the formation of granules. The model parameters are four: β_{in}, β_{∞}, k_{i0}, and $k_{i\infty}$. The last two (k_{i0}, and $k_{i\infty}$) are shown in the first term of the selection function of the breakage phenomena (see eqs. ((VI.17) and (VI.18))).

$$\frac{dN_i}{dt} = \sum_{j=1}^{i-S(q)-1} \frac{2^{\frac{j-i+1}{q}}}{2^{\frac{1}{q}}-1}\beta(i-1,j,t) * N_{i-1}N_j \; + \\ + \sum_{k=2}^{q} \sum_{j=i-S(q-k+2)-k+1}^{i-S(q-k+1)-k} \frac{2^{\frac{j-i+1}{q}} - 1 + 2^{\frac{-k+1}{q}}}{2^{\frac{1}{q}}-1}\beta(i-k,j,t)N_{i-1}N_j + \\ +0.5\beta(i-q,i-q,t)N_{i-q}^2 + \\ + \sum_{k=2}^{q} \sum_{j=i-S(q-k+2)-k+2}^{i-S(q-k+1)-k+1} \frac{2^{\frac{j-i}{q}} - 2^{\frac{-k+1}{q}} + 2^{\frac{1}{q}}}{2^{\frac{1}{q}}-1}\beta(i-k+1,j,t)N_{i-k+1}N_j \qquad \text{(VI.23)} \\ + \\ - \sum_{j=1}^{i-S(q)} \frac{2^{\frac{j-i}{q}}}{2^{\frac{1}{q}}-1}\beta(i,j,t)\,N_iN_j \; - \sum_{j=1-S(q)+1}^{h} \beta(i,j,t) * N_iN_j \; + \\ -C_i^{(2)}S_i(t) * N_i + \sum_{j=i+1}^{N_{classi}} b(i,j)S_i(t)\,N_jC_i^{(1)}\Gamma(i,j)$$

Agglomeration, breakage and nucleation model

The complete model (see eq. (VI.24)) considers all the three phenomena (agglomeration, breakage and nucleation) in the formation of granules. The model parameters are seven: β_{in}, β_{∞}, k_{i0}, $k_{i\infty}$, η_0, η_{∞}, and t_{nuc}. Therefore, three further parameters (η_0, η_{∞}, and t_{nuc}), compared to the agglomeration and breakage model, were considered with the introduction of the nucleation phenomena.

$$\frac{dN_i}{dt} = \sum_{j=1}^{i-S(q)-1} \frac{2^{\frac{j-i+1}{q}}}{2^{\frac{1}{q}}-1}\beta(i-1,j,t) * N_{i-1}N_j \; +$$

$$+\sum_{k=2}^{q}\sum_{j=i-S(q-k+2)-k+1}^{i-S(q-k+1)-k} \frac{2^{\frac{j-i+1}{q}}-1+2^{\frac{-k+1}{q}}}{2^{\frac{1}{q}}-1}\beta(i-k,j,t)N_{i-1}N_j +$$

$$+0.5\beta(i-q,i-q,t)N_{i-q}^2 +$$

$$+\sum_{k=2}^{q}\sum_{j=i-S(q-k+2)-k+2}^{i-S(q-k+1)-k+1} \frac{2^{\frac{j-i}{q}}-2^{\frac{-k+1}{q}}+2^{\frac{1}{q}}}{2^{\frac{1}{q}}-1}\beta(i-k+1,j,t)N_{i-k+1}N_j \qquad \text{(VI.24)}$$

$$+$$

$$-\sum_{j=1}^{i-S(q)} \frac{2^{\frac{j-i}{q}}}{2^{\frac{1}{q}}-1}\beta(i,j,t)\,N_iN_j \; - \sum_{j=1-S(q)+1}^{h} \beta(i,j,t) * N_iN_j \; +$$

$$-C_i^{(2)}S_i(t) * N_i + \sum_{j=i+1}^{N_{classi}} b(i,j)S_i(t)\,N_jC_i^{(1)}\Gamma(i,j) +$$

$$+\left(\eta_0\left(e^{-\frac{t}{t_{nuc}}}\right)+\eta_\infty\right)\cdot\left(\frac{1}{\delta\sqrt{2\pi}}\,e^{\frac{1}{2}\left(\frac{x_i-\mu}{\delta}\right)^2}\right)$$

VI.4 Modeling results

The different modeling structures above described (the pure agglomeration model, the agglomeration and breakage model, and the complete model with agglomeration, breakage and nucleation, discussed above, see eqs. ((VI.22), (VI.23) and (VI.24)), were then validated by comparison with experimental data achieved in this work (see chapter V).

In Figure VI.2, the comparison between the experimental and modelling results, in terms of number of particles per unit volume (axis *y*) with a given diameter (axis *x*), is reported at different granulation times (3-6-9-12-15-20 min). The experimental data were obtained working with 50 g of HPMC powder, with an impeller rotation speed of 93 rpm and a distilled water volume and flow rate of 100 ml and 34 ml/min respectively, which are the operating conditions of the central run of the *FFD* matrix (see paragraph V.3). Each experimental point represents a mean value from three independent experiments.

As it can be seen, a pure agglomeration model (see red squares in Figure VI.2) overestimates the granules formation. This modeling result represents a reasonable physical phenomenon: only the agglomeration in the granules formation leads to the lowering of the peak of N_i and its translation toward

higher dimension of the *PSD* (particles decrease in number increasing their size).

The insertion of the descriptive function of the breaking phenomenon (see green spheres in Figure VI.2) reflects more accurately the physics found with the experimental activities: breakage phenomena lead to an increase of the number of particles per unit volume, with a translation toward lower dimensions of the *PSD*.

The complete model with agglomeration, breakage and nucleation (blue triangles in Figure VI.2) seems to describe also the presence of small particles due to embryonic nuclei or powder clusters.

Globally, achieved results prove that the developed modeling structures respond to physical observed phenomena.

In the Table VI.2 parameters values of fitting resulting from the optimization considering the pure agglomeration model, the agglomeration and breakage model, and the complete model with agglomeration, breakage and nucleation were shown.

Table VI.2 *Parameters values of fitting*

	Agglomeration (A)	Agglomeration and breakege (A+B)	Agglomeration, breakage and nucleation (A+B+N)
$\beta_{in} \times 10^{10}\ [m^3/s]$	60.2	133	1.7 x 10^4
$\beta_{\infty} \times 10^{10}\ [m^3/s]$	1	18.5	15
$k_0 \times 10^6\ [1/s]$	-	3.8	494
$k_{\infty} \times 10^6\ [1/s]$	-	2	2
$\eta_0[1/m^3 s]$	-	-	3.9 x 10^6
$\eta_{\infty}[1/m^3 s]$	-	-	13
$t_{nuc}[s]$	-	-	14

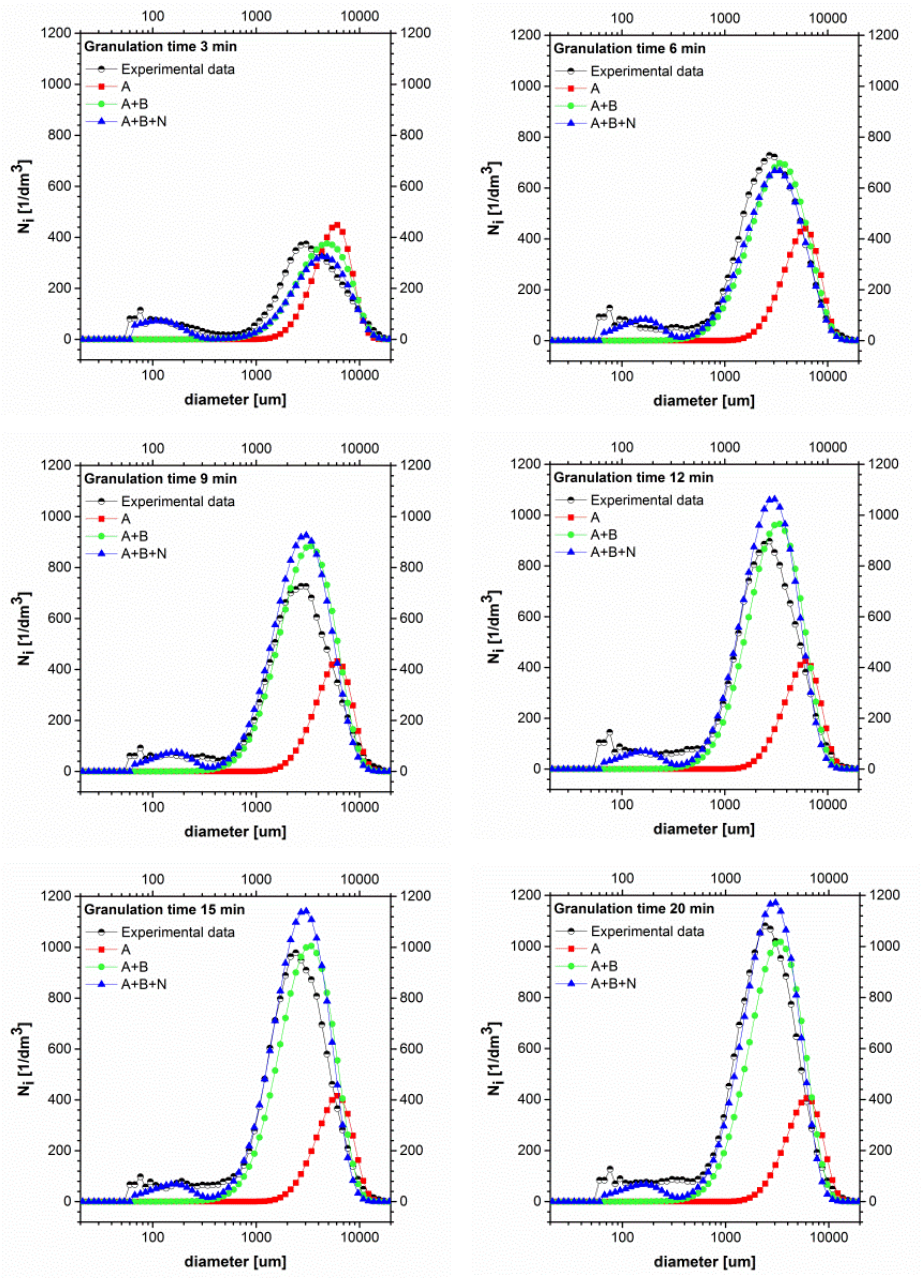

Figure VI.2 *Comparison between model predictions and experimental data of PSDs at different times of wet granulation process, performed with an impeller rotation speed of 93 rpm and a binder phase flow rate of 34 ml/min. A: Agglomeration; B: Breakage; N: Nucleation. A indicates the pure agglomeration model; A+B the agglomeration and breakage model; A+B+N the agglomeration, breakage and nucleation model*

VI.5 Towards scale-up approaches for the wet granulation process

The results from phenomenological analysis and the main physical aspects description by mathematical equations constitute milestones towards wet granulation process scale–up.

A rational approach to scale-up in the field of granulation is the "*dimensional analysis"*, procedure applied first time by Rayleigh (1915). Dimensional analysis develops dimensionless numbers and derives functional relationships among them that completely characterize any given process (Faure et al., 1999, Faure et al., 2001, Landin et al., 1996). This analysis is based on the principle of similarity, according to which, two processes are considered similar if there is a geometrical, kinematic, and dynamic similarity (Leuenberger, 1983). Two systems are called geometrically similar if they have the same ratio of characteristic linear dimensions (for example, two cylindrical mixing vessels are geometrically similar if they have the same ratio of height to diameter). Two geometrically similar systems are called kinematically similar if they have the same ratio of rates between corresponding points. Two kinematically similar systems are dynamically similar if they have the same ratio of forces between corresponding points (Levin, 2005, Yadav et al., 2010).

For two dynamically similar systems, scale up is carried out by keeping constant the dimensionless numbers necessary to describe the process (Kayrak-Talay et al., 2013, Levin, 2005).

Dimensionless numbers depend on the process parameters, the properties of the materials and the apparatus geometry. For a wet granulation process performed in an agitate apparatus with power consumption *P*, containing a powder of specific density ρ_s and dynamic viscosity η_s, mixed by an impeller of diameter *D* and rotation speed *N*, the dimensionless numbers most commonly used are: Newton, Froude and Reynolds. Newton number ($N_e = P/\rho_s N^3 D^5$) is a measure of required power to overcome friction in fluid flow in a stirred reactor and it relates the drag force acting on a unit area of the impeller and the inertial stress. Froude number ($F_r = N^2 D/g$) relates the inertial stress to the gravitational force per unit area acting on the material and it has been suggested both as criterion for dynamic similarity and scale up parameter in wet granulation process. Reynold number ($R_e = D^2 N\rho_s/\eta_s$) relates the inertial force to the viscous force (Landin et al., 1996, Levin, 2005, Yadav et al., 2010).

It is obvious that the key process parameter in the scale up is the impeller rotation speed (*N*), whose best value could be found "in-silico", i.e. thanks to the model predictability, able to reduce or completely delete experimental tests.

VI.6 Chapter VI remarks

Granules size distributions were mathematically described by using the Population Balance Equations (*PBEs*) approach. MATLAB® 2014b was used to implement and to solve the equations' discretization and their solution.

Nucleation, agglomeration, and breakage phenomena, experimentally observed for a batch wet granulation process with a low shear granulator, were described by appropriate mathematical functions selected from literature or purposely developed in this work.

In particular, three models with increasing complexity were considered: a pure agglomeration model that disregards all the other phenomena; an agglomeration and breakage model; a complete model with agglomeration, breakage and nucleation. The different modeling structures were then validated by comparison with experimental data. As overall result, it was observed that a pure agglomeration model overestimates the granules formation and, despite the presence of the breakage factor improves the model capabilities, the best matching with experimental evidences was obtained using the complete model, which takes into account also the nucleation phenomena. Achieved results prove that the developed modeling structures respond to physical observed phenomena.

Main results of this chapter are presented in:

De Simone V., Caccavo D., Lamberti G., d'Amore M., Barba A.A., "Phenomenological analysis, process parameters optimization and mathematical modeling of a low-shear wet granulation process", 23rd International Congress of Chemical and Process Engineering CHISA 2018, 25-29/08/2018, Prague (CZ), Czech Republic

De Simone V., Caccavo D., Dalmoro A., Lamberti G., d'Amore M.; Barba A.A., "Inside the phenomenological aspects of wet granulation: role of process parameters", chap. V in "Granularity in Materials Science", InTech Ed., 2018, ISBN 978-1-78984-308-8

De Simone V.; Caccavo D.; Lamberti G; d'Amore M.; Barba A.A.; Dalmoro A.; Low-shear wet granulation process: a new strategy in design and manufacturing of granular materials, to be presented to 3rd European Conference on Pharmaceutics, 25-26/03/2019, Bologna (Italia)

Chapter VII
Concluding remarks

Wet granulation is a size enlargement process used in many fields, such as pharmaceutical, nutraceutical, zootecnichal, etc., due its ability to improve technological properties of the final product, compared to the powder form, and/or to realize suitable delivery systems for drug/functional molecules for oral administrations/food preparations and/or to produce intermediate processing products. In spite of its widespread use, economic importance and almost 50 years of research, in literature the approach to the granulation process is still based on either experimental tests (to study the impact of formulation and process variables on granules properties) or on modeling studies (mathematical description of the phenomena). The two approaches, experimental and theoretical, are rarely applied together. Moreover, phenomena involved in powders aggregation are not well understood, and thus it is difficult to successfully obtain a product with tailored features without extensive experimental tests.

In light of these literature findings, this research project was based on the investigation of the role of the phenomenological aspects, and their connection with the main operating parameters in granulation process, on granules final properties, in order to develop physical-mathematical descriptions of the size enlargement unit operation, which can constitute a starting point for scale up studies. The integrated approach, exploiting experimental studies and modeling aspects together, constitutes the main novelty of this Ph.D. research activity.

To this scope, it was firstly carried out the design and realization of a bench scale experimental set up, with the innovative feature of using an ultrasonic atomizer for spraying the wetting phase in order to improve the degree of binder phase dispersion on the surface of powder bed. Then, granular structures with tailored features (in terms of size and size distribution, flowability, mechanical and release properties, etc.) were produced and characterized by standard and *ad hoc* innovative protocols. In

particular, a new procedure for analysing the mechanical properties of granules, and an *ad hoc* built Dynamic Image Analysis (*DIA*) device, based on the free falling particle scheme, for monitoring the evolution of the Particle Size Distribution (*PSD*) during the solids processing, were developed.

For the preparation of granules with sizes between 0.45-2 mm (sizes suitable for food, pharmaceutical and zootechnical applications), hydroxypropyl methylcellulose (*HPMC*) was used as powder model material due to its versatile properties. It is an easy to handle, available at low cost, odourless, hypoallergenic, biocompatible, and not toxic polymer, which nowadays continues to be the most employed excipient in the formulation of hydrogel-based matrices in form of tablets or granules, in order to provide controlled release of oral solid dosage systems. Distilled water was used as binder phase.

The experiments were planned by using the techniques of the Design of Experiments (*DoEs*), i.e. statistical approaches applied to minimize the number of experiments to be performed and maximize the information on the system behaviour and operating variables, avoiding loss of time and resources. Three process variables (impeller rotation speed (rpm), binder to powder ratio, and binder phase flow rate) were varied to assay their impact on granules properties. The results were used to find the best process operating conditions to obtain a product with tailored features, i.e. high product yield (% w/w of dry granules with size between 0.45 mm and 2 mm), low residual moisture content, and good flowability and compressibility properties. Under phenomenological point of view, it was observed that low rpm with high binder phase flow rate and low binder to powder ratio, or, high rpm with lower binder phase flow rate and binder to powder ratio produce failure of the aggregation phenomena, i.e. high amount of fine particles with size lower than requested one (0.45-2 mm). Low rpm with high binder phase flow rate and high added binder phase amount achieve clusters of powder and binder, i.e. over wetting phenomena, which is a condition to avoid. High rpm with high binder to powder ratio and low binder phase flow rate give a high product yield.

To fully understanding the behaviour of *HPMC* granules as active ingredient delivery systems, the intensities of process parameters which are found to give the better product yield were used in the production of loaded granules. In particular, the effect of three formulation variables, i.e. molecule payload, molecule solubility and binder type, on physical and mechanical properties of granules were investigated and, moreover, analysis of release mechanisms (by diffusive phenomena or due to polymer erosion) were speculated. A hydrophilic compound, vitamin B12, and a lipophilic one, vitamin D2, were employed as model molecules. Due to the different solubility of the two molecules in water, two different binder phases were

used: distilled water for vitamin B12 loaded *HPMC* granules, and a composed solution of ethanol and water with a 75/25 v/v ratio for vitamin D2 loaded *HPMC* granules. First of all, the best loading method in *HPMC* granules was investigated using the hydrophilic molecule. Vitamin B12 was either dissolved in the binder phase (method 1) or dispersed in powder phase (method 2). It was observed that the loading method does not have significant effects on either the granules flowability or the yield, but a better dispersion of vitamin B12 inside the *HPMC* polymer matrix was achieved by the method 1, perhaps thanks to the high solubility of this vitamin in the binder and the relevant uniform spray by the ultrasonic atomization device. Thus, by exploiting the most successful method 1, two different payloads of B12 and D2 (1 % and 2.3 % w/w) were tested. Results showed that the use of ethanol reduces product yield and produces granules with less defined shape, smaller dimensions, less hard structure, worse flowability, and slightly faster polymer erosion. The increase of payload both for the hydrophilic and lipophilic molecule leads to the formation of granules with a harder and more compact structure. It was demonstrated that the molecule solubility plays a relevant role in their release mechanism: diffusion for the hydrophilic molecule and erosion for the lipophilic one.

Due to the relevance of size granules distributions in practical uses of granulates (the process yield is based on this parameter), attention was focused on the way to evaluate, by a dynamic manner, the growing of powder agglomerates. Thus, the statistical techniques (*DoEs* and *RSM*) were coupled with the *PSD* analysis method (*DIA*) to understand phenomenological aspects involved in the formation of the granules always to achieve process conditions optimization. To this aim, the process parameters optimization was carried out using the granulation yield (% w/w of wet granules within the size range 2-10 mm) as the main variable of interest, determined by *PSD* data. *PSD* measurements at different process times, obtained by using the *ad hoc* built *DIA* device, showed that nucleation, agglomeration and breakage phenomena influence the wet *HPMC* granules size and occur simultaneously in the granulator, with the dominance of the agglomeration during the binder addition phase, later balanced by the breakage. Thanks to this initial phenomenological analysis, process time was optimized. At last, response surface studies indicated that the interaction between the impeller rotation speed and the binder flow rate have a significant influence on the granulation yield (and in general on the granules *PSD*), especially at high rpm.

Granules size distributions were mathematically described by using the Population Balance Equations (*PBEs*) approach. MATLAB® 2014b was used to implement and to solve the equations' discretization. The *PBEs* were discretized in 60 classes, ranging from 60 to 20000 μm with a geometrical progression of $2^{1/6}$, therefore, the resulting model was a system of 60

Ordinary Differential Equations (*ODEs*), one for each class. Suitable mathematical functions to describe phenomena and parameters were selected from literature or purposely developed in this work. In particular, three models with increasing complexity were considered: a pure agglomeration model that disregards all the other phenomena; an agglomeration and breakage model; a complete model with agglomeration, breakage and nucleation. The different modeling structures were then validated by comparison with experimental data achieved in this study.

As overall result, the comparison between the experimental and modeling results showed that a pure agglomeration model (disregarding all the other phenomena) overestimates the granules formation, the presence of the breakage improves the model capabilities, and the complete model (agglomeration, breakage and nucleation) seems to describe well the presence of small particles due to embryonic nuclei or powder clusters. Achieved results thus prove that the developed modeling structures respond to physical observed phenomena.

An integrated approach based on a rational planning of experimental tests and the availability of a predictive tool can constitute an efficacious strategy to optimize or to implement a new granulation process starting from powder materials of interest, from the bench scale to the industrial scale.

References

ABBERGER, T. 2007. Chapter 24 Population balance modelling of granulation. *In:* SALMAN, A. D., HOUNSLOW, M. J. & SEVILLE, J. P. K. (eds.) *Handbook of Powder Technology.* Elsevier Science B.V.

ACHARYA, S., PATRA, S. & PANI, N. R. 2014. Optimization of HPMC and carbopol concentrations in non-effervescent floating tablet through factorial design. *Carbohydrate polymers,* 102**,** 360-368.

ADETAYO, A. & ENNIS, B. 2000. A new approach to modeling granulation processes for simulation and control purposes. *Powder technology,* 108**,** 202-209.

ADETAYO, A., LITSTER, J., PRATSINIS, S. E. & ENNIS, B. 1995. Population balance modelling of drum granulation of materials with wide size distribution. *Powder technology,* 82**,** 37-49.

AGRAWAL, A. M., NEAU, S. H. & BONATE, P. L. 2003. Wet granulation fine particle ethylcellulose tablets: effect of production variables and mathematical modeling of drug release. *Aaps Pharmsci,* 5**,** 48-60.

AGRAWAL, R. & NAVEEN, Y. 2011. Pharmaceutical processing–A review on wet granulation technology. *International journal of pharmaceutical frontier research,* 1**,** 65-83.

AKAIKE, H. 1970. Statistical predictor identification. *Annals of the institute of Statistical Mathematics,* 22**,** 203-217.

AKAIKE, H. 1974. A new look at the statistical model identification. *IEEE transactions on automatic control,* 19**,** 716-723.

ALBERTINI, B., CAVALLARI, C., PASSERINI, N., GONZÁLEZ-RODRıGUEZ, M. & RODRIGUEZ, L. 2003. Evaluation of β-lactose, PVP K12 and PVP K90 as excipients to prepare piroxicam granules using two wet granulation techniques. *European journal of pharmaceutics and biopharmaceutics,* 56**,** 479-487.

ALBERTINI, B., CAVALLARI, C., PASSERINI, N., VOINOVICH, D., GONZÁLEZ-RODRıGUEZ, M. L., MAGAROTTO, L. & RODRIGUEZ, L. 2004. Characterization and taste-masking evaluation of acetaminophen granules: comparison between different preparation methods in a high-shear mixer. *European journal of pharmaceutical sciences,* 21**,** 295-303.

ALBERTINI, B., PASSERINI, N., GONZÁLEZ-RODRÍGUEZ, M., CAVALLARI, C., CINI, M. & RODRIGUEZ, L. 2008. Wet granulation as innovative and fast method to prepare controlled

release granules based on an ion-exchange resin. *Journal of pharmaceutical sciences,* 97**,** 1313-1324.

ALEKSIĆ, I., ĐURIŠ, J., ILIĆ, I., IBRIĆ, S., PAROJČIĆ, J. & SRČIČ, S. 2014. In silico modeling of in situ fluidized bed melt granulation. *International Journal of Pharmaceutics,* 466**,** 21-30.

ASGHARNEJAD, M., DRAPER, J., DUBOST, D., KAUFMAN, M. & STOREY, D. 2000. Wet granulation formulation of a growth hormone secretagogue. Google Patents.

ASLAN, N. 2008. Application of response surface methodology and central composite rotatable design for modeling and optimization of a multi-gravity separator for chromite concentration. *Powder Technology,* 185**,** 80-86.

BADAWY, S. I., NARANG, A. S., LAMARCHE, K., SUBRAMANIAN, G. & VARIA, S. A. 2012. Mechanistic basis for the effects of process parameters on quality attributes in high shear wet granulation. *International journal of pharmaceutics,* 439**,** 324-333.

BADAWY, S. I. F. & HUSSAIN, M. A. 2004. Effect of starting material particle size on its agglomeration behavior in high shear wet granulation. *AAPS PharmSciTech,* 5**,** 16-22.

BADAWY, S. I. F., MENNING, M. M., GORKO, M. A. & GILBERT, D. L. 2000. Effect of process parameters on compressibility of granulation manufactured in a high-shear mixer. *International journal of pharmaceutics,* 198**,** 51-61.

BARBA, A. A., D'AMORE, M., CASCONE, S., LAMBERTI, G. & TITOMANLIO, G. 2009a. Intensification of biopolymeric microparticles production by ultrasonic assisted atomization. *Chemical Engineering and Processing: Process Intensification,* 48**,** 1477-1483.

BARBA, A. A., D'AMORE, M., CHIRICO, S., LAMBERTI, G. & TITOMANLIO, G. 2009b. Swelling of cellulose derivative (HPMC) matrix systems for drug delivery. *Carbohydrate Polymers,* 78**,** 469-474.

BARBA, A. A., DALMORO, A. & D'AMORE, M. 2013. Microwave assisted drying of cellulose derivative (HPMC) granular solids. *Powder technology,* 237**,** 581-585.

BARBA, A. A., DALMORO, A., D'AMORE, M. & LAMBERTI, G. 2015. Liposoluble vitamin encapsulation in shell–core microparticles produced by ultrasonic atomization and microwave stabilization. *LWT-Food Science and Technology,* 64**,** 149-156.

BARESCHINO, P., MARZOCCHELLA, A. & SALATINO, P. 2017. Fluidised bed drying of powdered materials: Effects of operating conditions. *Powder Technology,* 308**,** 158-164.

BAŞ, D. & BOYACı, I. H. 2007. Modeling and optimization I: Usability of response surface methodology. *Journal of food engineering,* 78**,** 836-845.

BATTERHAM, R., HALL, J. & BARTON, G. 1981. Pelletizing kinetics and simulation of full scale balling circuits.

BELLOCQ, B., CUQ, B., RUIZ, T., DURI, A., CRONIN, K. & RING, D. 2018. Impact of fluidized bed granulation on structure and functional properties of the agglomerates based on the durum wheat semolina. *Innovative Food Science & Emerging Technologies,* 45**,** 73-83.

BENALI, M., GERBAUD, V. & HEMATI, M. 2009. Effect of operating conditions and physico–chemical properties on the wet granulation kinetics in high shear mixer. *Powder Technology,* 190**,** 160-169.

BERTÍN, D., COTABARREN, I. M., VELIZ MORAGA, S., PIÑA, J. & BUCALÁ, V. 2018. The effect of binder concentration in fluidized-bed granulation: Transition between wet and melt granulation. *Chemical Engineering Research and Design,* 132**,** 162-169.

BETTINI, R., CATELLANI, P., SANTI, P., MASSIMO, G., PEPPAS, N. & COLOMBO, P. 2001. Translocation of drug particles in HPMC matrix gel layer: effect of drug solubility and influence on release rate. *Journal of Controlled Release,* 70**,** 383-391.

BEUSELINCK, L., GOVERS, G., POESEN, J., DEGRAER, G. & FROYEN, L. 1998. Grain-size analysis by laser diffractometry: comparison with the sieve-pipette method. *Catena,* 32**,** 193-208.

BEZERRA, M. A., SANTELLI, R. E., OLIVEIRA, E. P., VILLAR, L. S. & ESCALEIRA, L. A. 2008. Response surface methodology (RSM) as a tool for optimization in analytical chemistry. *Talanta,* 76**,** 965-977.

BIKA, D., TARDOS, G., PANMAI, S., FARBER, L. & MICHAELS, J. 2005. Strength and morphology of solid bridges in dry granules of pharmaceutical powders. *Powder Technology,* 150**,** 104-116.

BJÖRN, I. N., JANSSON, A., KARLSSON, M., FOLESTAD, S. & RASMUSON, A. 2005. Empirical to mechanistic modelling in high shear granulation. *Chemical engineering science,* 60**,** 3795-3803.

BOUWMAN, A., HENSTRA, M., WESTERMAN, D., CHUNG, J., ZHANG, Z., INGRAM, A., SEVILLE, J. & FRIJLINK, H. 2005. The effect of the amount of binder liquid on the granulation mechanisms and structure of microcrystalline cellulose granules prepared by high shear granulation. *International journal of pharmaceutics,* 290**,** 129-136.

BRUNS, R. E., SCARMINIO, I. S. & DE BARROS NETO, B. 2006. *Statistical design-chemometrics*, Elsevier.

BU, X., XIE, G., PENG, Y. & CHEN, Y. 2016. Kinetic modeling and optimization of flotation process in a cyclonic microbubble flotation

column using composite central design methodology. *International Journal of Mineral Processing,* 157**,** 175-183.

BUTENSKY, M. & HYMAN, D. 1971. Rotary drum granulation. An experimental study of the factors affecting granule size. *Industrial & Engineering Chemistry Fundamentals,* 10**,** 212-219.

CACCAVO, D., BARBA, A., D'AMORE, M., DE PIANO, R., LAMBERTI, G., ROSSI, A. & COLOMBO, P. 2017a. Modeling the modified drug release from curved shape drug delivery systems–Dome Matrix®. *European Journal of Pharmaceutics and Biopharmaceutics,* 121**,** 24-31.

CACCAVO, D., CASCONE, S., APICELLA, P., LAMBERTI, G. & BARBA, A. 2017b. HPMC-based granules for prolonged release of phytostrengtheners in agriculture. *Chemical Engineering Communications,* 204**,** 1333-1340.

CACCAVO, D., LAMBERTI, G., BARBA, A. A., ABRAHMSÉN-ALAMI, S., VIRIDÉN, A. & LARSSON, A. 2017c. Effects of HPMC substituent pattern on water up-take, polymer and drug release: An experimental and modelling study. *International journal of pharmaceutics,* 528**,** 705-713.

CAMERON, I., WANG, F., IMMANUEL, C. & STEPANEK, F. 2005. Process systems modelling and applications in granulation: A review. *Chemical Engineering Science,* 60**,** 3723-3750.

CANTOR, S. L., KOTHARI, S. & KOO, O. M. 2009. Evaluation of the physical and mechanical properties of high drug load formulations: Wet granulation vs. novel foam granulation. *Powder Technology,* 195**,** 15-24.

CAO, Q.-R., CHOI, Y.-W., CUI, J.-H. & LEE, B.-J. 2005. Effect of solvents on physical properties and release characteristics of monolithic hydroxypropylmethylcellulose matrix granules and tablets. *Archives of pharmacal research,* 28**,** 493-501.

CAPES, C. 1965. Granule formation by the agglomeration of damp powders: Part 1. The mechanism of granule growth. *Trans. Inst. Chem. Eng.,* 43**,** 116-124.

CASCONE, S., LAMBERTI, G., TITOMANLIO, G., D'AMORE, M. & BARBA, A. A. 2014. Measurements of non-uniform water content in hydroxypropyl-methyl-cellulose based matrices via texture analysis. *Carbohydrate polymers,* 103**,** 348-354.

CHAKRABORTY, S., KHANDAI, M., SHARMA, A., PATRA, C., PATRO, V. & SEN, K. 2009. Effects of drug solubility on the release kinetics of water soluble and insoluble drugs from HPMC based matrix formulations. *Acta Pharmaceutica,* 59**,** 313-323.

CHEN, Y.-C., HO, H.-O., CHIOU, J.-D. & SHEU, M.-T. 2014. Physical and dissolution characterization of cilostazol solid dispersions prepared by hot melt granulation (HMG) and thermal adhesion granulation

(TAG) methods. *International journal of pharmaceutics,* 473**,** 458-468.
CHEONG, L. W. S., HENG, P. W. S. & WONG, L. F. 1992. Relationship between polymer viscosity and drug release from a matrix system. *Pharmaceutical research,* 9**,** 1510-1514.
CHEVALIER, E., VIANA, M., CAZALBOU, S. & CHULIA, D. 2009. Comparison of low-shear and high-shear granulation processes: effect on implantable calcium phosphate granule properties. *Drug development and industrial pharmacy,* 35**,** 1255-1263.
CHEVALIER, E., VIANA, M., CAZALBOU, S., MAKEIN, L., DUBOIS, J. & CHULIA, D. 2010. Ibuprofen-loaded calcium phosphate granules: Combination of innovative characterization methods to relate mechanical strength to drug location. *Acta biomaterialia,* 6**,** 266-274.
CHITU, T. M., OULAHNA, D. & HEMATI, M. 2011. Wet granulation in laboratory scale high shear mixers: Effect of binder properties. *Powder technology,* 206**,** 25-33.
CHOUINARD, F. & JACQUES, W. 1999. Pharmaceutical controlled release tablets containing a carrier made of cross-linked amylose and hydroxypropylmethylcellulose. Google Patents.
CONDRA, L. 2001. *Reliability improvement with design of experiment*, CRC Press.
COSTA, S., MORIS, V. S. & ROCHA, S. 2011. Influence of process variables on granulation of microcrystalline cellulose in vibrofluidized bed. *Powder Technology,* 207**,** 454-460.
CRAIG, D. Q. 2002. The mechanisms of drug release from solid dispersions in water-soluble polymers. *International journal of pharmaceutics,* 231**,** 131-144.
DAHIRU, T. 2008. P-value, a true test of statistical significance? A cautionary note. *Annals of Ibadan postgraduate medicine,* 6**,** 21-26.
DALMORO, A., BARBA, A. A., D'AMORE, M. & LAMBERTI, G. 2014. Single-pot semicontinuous bench scale apparatus to produce microparticles. *Industrial & Engineering Chemistry Research,* 53**,** 2771-2780.
DARELIUS, A., RASMUSON, A., BJÖRN, I. N. & FOLESTAD, S. 2005. High shear wet granulation modelling—a mechanistic approach using population balances. *Powder Technology,* 160**,** 209-218.
DARUNKAISORN, W., MAHADLEK, J. & PHAECHAMUD, T. 2009. HPMC matrix granule formation: selection of suitable granulating fluid. *Thai Pharmaceutical and Health Science Journal-วารสาร ไทย เภสัชศาสตร์ และ วิทยาการ สุขภาพ,* 4**,** 29-45.
DUBOIS, M., GILLES, K. A., HAMILTON, J. K., REBERS, P. T. & SMITH, F. 1956. Colorimetric method for determination of sugars and related substances. *Analytical chemistry,* 28**,** 350-356.

ENNIS, B. & LITSTER, J. 1997. Particle size enlargement. *Perry's Chemical Engineers' Handbook. 7th edition, McGraw-Hill, New York,* 20.

ENNIS, B. J., TARDOS, G. & PFEFFER, R. 1991. A microlevel-based characterization of granulation phenomena. *Powder Technology,* 65**,** 257-272.

ENNIS, B. J., WITT, W., WEINEKOTTER, R., SPHAR, D., COMMERAN, E., SNOW, R., ALLEN, T., RAYMUS, C. & LISTER, J. 2007. Solid-solid operations and processing. *Perry's chemical engineers' handbook.* McGraw-Hill, New York.

EUSSEN, S. J., DE GROOT, L. C., CLARKE, R., SCHNEEDE, J., UELAND, P. M., HOEFNAGELS, W. H. & VAN STAVEREN, W. A. 2005. Oral cyanocobalamin supplementation in older people with vitamin B12 deficiency: a dose-finding trial. *Archives of Internal Medicine,* 165**,** 1167-1172.

FAN, X., YANG, Z., PARKER, D. J., NG, B., DING, Y. & GHADIRI, M. 2009. Impact of surface tension and viscosity on solids motion in a conical high shear mixer granulator. *AIChE journal,* 55**,** 3088-3098.

FAO 2017. World fertilizer trends and outlook to 2020.

FAURE, A., GRIMSEY, I. M., ROWE, R. C., YORK, P. & CLIFF, M. J. 1999. Applicability of a scale-up methodology for wet granulation processes in Collette Gral high shear mixer-granulators. *European journal of pharmaceutical sciences,* 8**,** 85-93.

FAURE, A., YORK, P. & ROWE, R. 2001. Process control and scale-up of pharmaceutical wet granulation processes: a review. *European Journal of Pharmaceutics and Biopharmaceutics,* 52**,** 269-277.

FRANCESCHINI, G. & MACCHIETTO, S. 2008. Model-based design of experiments for parameter precision: State of the art. *Chemical Engineering Science,* 63**,** 4846-4872.

FREDRICKSON, A. G., RAMKRISHNA, D. & TSUCHIYA, H. M. 1967. Statistics and dynamics of procaryotic cell populations. *Mathematical Biosciences,* 1**,** 327-374.

FU, J., REYNOLDS, G. K., ADAMS, M. J., HOUNSLOW, M. J. & SALMAN, A. D. 2005. An experimental study of the impact breakage of wet granules. *Chemical Engineering Science,* 60**,** 4005-4018.

FUERTES, I., CARABALLO, I., MIRANDA, A. & MILLÁN, M. 2010. Study of critical points of drugs with different solubilities in hydrophilic matrices. *International journal of pharmaceutics,* 383**,** 138-146.

GAIKWAD, V. L., BHATIA, N. M., DESAI, S. A. & BHATIA, M. S. 2016. Quantitative structure property relationship modeling of excipient properties for prediction of formulation characteristics. *Carbohydrate polymers,* 151**,** 593-599.

GAO, P., SKOUG, J. W., NIXON, P. R., ROBERT JU, T., STEMM, N. L. & SUNG, K. C. 1996. Swelling of hydroxypropyl methylcellulose matrix tablets. 2. Mechanistic study of the influence of formulation variables on matrix performance and drug release. *Journal of pharmaceutical sciences,* 85**,** 732-740.

GELBARD, F. & SEINFELD, J. H. 1980. Simulation of multicomponent aerosol dynamics. *Journal of colloid and Interface Science,* 78**,** 485-501.

GHAFARI, S., AZIZ, H. A., ISA, M. H. & ZINATIZADEH, A. A. 2009. Application of response surface methodology (RSM) to optimize coagulation–flocculation treatment of leachate using poly-aluminum chloride (PAC) and alum. *Journal of hazardous materials,* 163**,** 650-656.

GHIMIRE, M., HODGES, L. A., BAND, J., O'MAHONY, B., MCINNES, F. J., MULLEN, A. B. & STEVENS, H. N. 2010. In-vitro and in-vivo erosion profiles of hydroxypropylmethylcellulose (HPMC) matrix tablets. *Journal of Controlled Release,* 147**,** 70-75.

GUIGON, P., SIMON, O., SALEH, K., BINDHUMADHAVAN, G., ADAMS, M. & SEVILLE, J. 2007. Handbook of Powder Technology, 11, Granulation. Elsevier Science BV.

HAMMER, K. 1984. Steam granulation apparatus and method. Google Patents.

HAPGOOD, K. P. 2000. Nucleation and binder dispersion in wet granulation.

HAPGOOD, K. P., LITSTER, J. D., BIGGS, S. R. & HOWES, T. 2002. Drop penetration into porous powder beds. *Journal of Colloid and Interface Science,* 253**,** 353-366.

HAPGOOD, K. P., LITSTER, J. D. & SMITH, R. 2003. Nucleation regime map for liquid bound granules. *AIChE Journal,* 49**,** 350-361.

HERDER, J., ADOLFSSON, Å. & LARSSON, A. 2006. Initial studies of water granulation of eight grades of hypromellose (HPMC). *International journal of pharmaceutics,* 313**,** 57-65.

HOLM, P. 1987. Effect of impeller and chopper design on granulation in a high speed mixer. *Drug Development and Industrial Pharmacy,* 13**,** 1675-1701.

HOORNAERT, F., WAUTERS, P. A., MEESTERS, G. M., PRATSINIS, S. E. & SCARLETT, B. 1998. Agglomeration behaviour of powders in a Lödige mixer granulator. *Powder technology,* 96**,** 116-128.

HOUNSLOW, M., RYALL, R. & MARSHALL, V. 1988. A discretized population balance for nucleation, growth, and aggregation. *AIChE Journal,* 34**,** 1821-1832.

HOUNSLOW, M. J. 1990. A discretized population balance for continuous systems at steady state. *AIChE journal,* 36**,** 106-116.

HU, X., CUNNINGHAM, J. C. & WINSTEAD, D. 2008. Study growth kinetics in fluidized bed granulation with at-line FBRM. *International Journal of Pharmaceutics,* 347**,** 54-61.

HUICHAO, W., SHOUYING, D., YANG, L., YING, L. & DI, W. 2014. The application of biomedical polymer material hydroxy propyl methyl cellulose (HPMC) in pharmaceutical preparations. *Journal of Chemical and Pharmaceutical Research,* 6**,** 155-160.

HULBURT, H. M. & KATZ, S. 1964. Some problems in particle technology: A statistical mechanical formulation. *Chemical Engineering Science,* 19**,** 555-574.

HUSSEIN, K., TÜRK, M. & WAHL, M. A. 2008. Drug loading into β-cyclodextrin granules using a supercritical fluid process for improved drug dissolution. *european journal of pharmaceutical sciences,* 33**,** 306-312.

ISHIKAWA, T., WATANABE, Y., TAKAYAMA, K., ENDO, H. & MATSUMOTO, M. 2000. Effect of hydroxypropylmethylcellulose (HPMC) on the release profiles and bioavailability of a poorly water-soluble drug from tablets prepared using macrogol and HPMC. *International journal of pharmaceutics,* 202**,** 173-178.

IVESON, S. & LITSTER, J. 1998a. Fundamental studies of granule consolidation part 2: quantifying the effects of particle and binder properties. *Powder technology,* 99**,** 243-250.

IVESON, S. & LITSTER, J. 1998b. Growth regime map for liquid-bound granules. *AIChE journal,* 44**,** 1510-1518.

IVESON, S., LITSTER, J. & ENNIS, B. 1996. Fundamental studies of granule consolidation Part 1: Effects of binder content and binder viscosity. *Powder Technology,* 88**,** 15-20.

IVESON, S. M. 2002. Limitations of one-dimensional population balance models of wet granulation processes. *Powder Technology,* 124**,** 219-229.

IVESON, S. M., LITSTER, J. D., HAPGOOD, K. & ENNIS, B. J. 2001a. Nucleation, growth and breakage phenomena in agitated wet granulation processes: a review. *Powder technology,* 117**,** 3-39.

IVESON, S. M., WAUTERS, P. A., FORREST, S., LITSTER, J. D., MEESTERS, G. M. & SCARLETT, B. 2001b. Growth regime map for liquid-bound granules: further development and experimental validation. *Powder Technology,* 117**,** 83-97.

J., H. M., L., R. R. & R., M. V. 1988. A discretized population balance for nucleation, growth, and aggregation. *AIChE Journal,* 34**,** 1821-1832.

JAIN, A. K., SÖDERLIND, E., VIRIDÉN, A., SCHUG, B., ABRAHAMSSON, B., KNOPKE, C., TAJAROBI, F., BLUME, H., ANSCHÜTZ, M. & WELINDER, A. 2014. The influence of hydroxypropyl methylcellulose (HPMC) molecular weight,

concentration and effect of food on in vivo erosion behavior of HPMC matrix tablets. *Journal of Controlled Release,* 187**,** 50-58.
JAMZAD, S. & FASSIHI, R. 2006. Development of a controlled release low dose class II drug-Glipizide. *International journal of pharmaceutics,* 312**,** 24-32.
JOHANSEN, A. & SCHÆFER, T. 2001. Effects of interactions between powder particle size and binder viscosity on agglomerate growth mechanisms in a high shear mixer. *European Journal of Pharmaceutical Sciences,* 12**,** 297-309.
JONA, J., KANAPURAM, S. & DAURIO, D. 2007. Wet granulation process. Google Patents.
KAPUR, P. 1978. Balling and granulation. *Advances in Chemical Engineering,* 10**,** 55-123.
KATDARE, A. V. & KRAMER, K. A. 2004. Wet granulation formulation for bisphosphonic acids. Google Patents.
KAYRAK-TALAY, D., DALE, S., WASSGREN, C. & LITSTER, J. 2013. Quality by design for wet granulation in pharmaceutical processing: assessing models for a priori design and scaling. *Powder technology,* 240**,** 7-18.
KENINGLEY, S., KNIGHT, P. & MARSON, A. 1997. An investigation into the effects of binder viscosity on agglomeration behaviour. *Powder Technology,* 91**,** 95-103.
KETTERHAGEN, W. R., AM ENDE, M. T. & HANCOCK, B. C. 2009. Process modeling in the pharmaceutical industry using the discrete element method. *Journal of pharmaceutical sciences,* 98**,** 442-470.
KHURI, A. I. & CORNELL, J. A. 1996. *Response surfaces: designs and analyses*, CRC press.
KIM, J., CHOI, I., SHIN, W.-K. & KIM, Y. 2015. Effects of HPMC (Hydroxypropyl methylcellulose) on oil uptake and texture of gluten-free soy donut. *LWT-Food Science and Technology,* 62**,** 620-627.
KNIGHT, P. 1993. An investigation of the kinetics of granulation using a high shear mixer. *Powder technology,* 77**,** 159-169.
KNIGHT, P., INSTONE, T., PEARSON, J. & HOUNSLOW, M. 1998. An investigation into the kinetics of liquid distribution and growth in high shear mixer agglomeration. *Powder Technology,* 97**,** 246-257.
KNIGHT, P., JOHANSEN, A., KRISTENSEN, H., SCHAEFER, T. & SEVILLE, J. 2000. An investigation of the effects on agglomeration of changing the speed of a mechanical mixer. *Powder Technology,* 110**,** 204-209.
KNYAZEV, A., SMIRNOVA, N., PLESOVSKIKH, A., SHUSHUNOV, A. & KNYAZEVA, S. 2014. Low-temperature heat capacity and thermodynamic functions of vitamin B 12. *Thermochimica Acta,* 582**,** 35-39.

KODRE, K., ATTARDE, S., YENDHE, P., PATIL, R. & BARGE, V. 2014. Research and Reviews: Journal of Pharmaceutical Analysis.
KRYCER, I., POPE, D. G. & HERSEY, J. A. 1983. An evaluation of tablet binding agents part I. Solution binders. *Powder Technology,* 34**,** 39-51.
KUMAR, J., PEGLOW, M., WARNECKE, G. & HEINRICH, S. 2008. An efficient numerical technique for solving population balance equation involving aggregation, breakage, growth and nucleation. *Powder Technology,* 182**,** 81-104.
KUMAR, S. & RAMKRISHNA, D. 1996a. On the solution of population balance equations by discretization—I. A fixed pivot technique. *Chemical Engineering Science,* 51**,** 1311-1332.
KUMAR, S. & RAMKRISHNA, D. 1996b. On the solution of population balance equations by discretization—II. A moving pivot technique. *Chemical Engineering Science,* 51**,** 1333-1342.
KUMAR, S. & RAMKRISHNA, D. 1997. On the solution of population balance equations by discretization—III. Nucleation, growth and aggregation of particles. *Chemical Engineering Science,* 52**,** 4659-4679.
LADE, P. V. & NELSON, R. B. 1987. Modelling the elastic behaviour of granular materials. *International journal for numerical and analytical methods in geomechanics,* 11**,** 521-542.
LAGUNA, L., PRIMO-MARTÍN, C., VARELA, P., SALVADOR, A. & SANZ, T. 2014. HPMC and inulin as fat replacers in biscuits: Sensory and instrumental evaluation. *LWT-Food Science and Technology,* 56**,** 494-501.
LAITINEN, N., ANTIKAINEN, O. & YLIRUUSI, J. 2003. Characterization of particle sizes in bulk pharmaceutical solids using digital image information. *Aaps Pharmscitech,* 4**,** 383-391.
LAMBERTI, G., GALDI, I. & BARBA, A. A. 2011. Controlled release from hydrogel-based solid matrices. A model accounting for water up-take, swelling and erosion. *International Journal of Pharmaceutics,* 407**,** 78-86.
LANDGREBE, J. D. & PRATSINIS, S. E. 1989. Gas-phase manufacture of particulates: interplay of chemical reaction and aerosol coagulation in the free-molecular regime. *Industrial & engineering chemistry research,* 28**,** 1474-1481.
LANDGREBE, J. D. & PRATSINIS, S. E. 1990. A discrete-sectional model for particulate production by gas-phase chemical reaction and aerosol coagulation in the free-molecular regime. *Journal of Colloid and Interface Science,* 139**,** 63-86.
LANDIN, M., YORK, P., CLIFF, M., ROWE, R. & WIGMORE, A. 1996. Scale-up of a pharmaceutical granulation in fixed bowl mixer-granulators. *International journal of pharmaceutics,* 133**,** 127-131.

LANGHAUSER, K. 2017. Long Live OSD. *Solid Dose Trends.* Pharmaceutical manufacturing.
LEE, K. F., DOSTA, M., MCGUIRE, A. D., MOSBACH, S., WAGNER, W., HEINRICH, S. & KRAFT, M. 2017. Development of a multi-compartment population balance model for high-shear wet granulation with discrete element method. *Computers & Chemical Engineering,* 99**,** 171-184.
LEUENBERGER, H. 1983. Scale-up of granulation process with reference to power monitoring. *Pharm. Acta Helv.,* 29**,** 274-280.
LEVIN, M. 2005. How to scale up scientifically. *Pharmaceutical technology,* 26**,** 4-13.
LEVINA, M. & RAJABI-SIAHBOOMI, A. R. 2004. The influence of excipients on drug release from hydroxypropyl methylcellulose matrices. *Journal of pharmaceutical sciences,* 93**,** 2746-2754.
LI, C. L., MARTINI, L. G., FORD, J. L. & ROBERTS, M. 2005. The use of hypromellose in oral drug delivery. *Journal of pharmacy and pharmacology,* 57**,** 533-546.
LIN, H.-L., HO, H.-O., CHEN, C.-C., YEH, T.-S. & SHEU, M.-T. 2008. Process and formulation characterizations of the thermal adhesion granulation (TAG) process for improving granular properties. *International journal of pharmaceutics,* 357**,** 206-212.
LINTZ, F.-C. & KELLER, M. 2006. Wet granulation process. Google Patents.
LISTER, J., SMIT, D. & HOUNSLOW, M. 1995. Adjustable discretized population balance for growth and aggregation. *AIChE Journal,* 41**,** 591-603.
LITSTER, J. 2003a. Scaleup of wet granulation processes: science not art. *Powder Technology,* 130**,** 35-40.
LITSTER, J. 2003b. Scaleup of wet granulation processes: science not art. *Powder Technology,* 130**,** 35-40.
LITSTER, J. & ENNIS, B. 2013. *The science and engineering of granulation processes*, Springer Science & Business Media.
LITSTER, J., HAPGOOD, K., MICHAELS, J., SIMS, A., ROBERTS, M., KAMENENI, S. & HSU, T. 2001. Liquid distribution in wet granulation: dimensionless spray flux. *Powder Technology,* 114**,** 32-39.
LIU, L., LITSTER, J., IVESON, S. & ENNIS, B. 2000. Coalescence of deformable granules in wet granulation processes. *AIChE Journal,* 46**,** 529-539.
LUNDSTEDT, T., SEIFERT, E., ABRAMO, L., THELIN, B., NYSTRÖM, Å., PETTERSEN, J. & BERGMAN, R. 1998. Experimental design and optimization. *Chemometrics and intelligent laboratory systems,* 42**,** 3-40.

LUO, G., XU, B., ZHANG, Y., CUI, X., LI, J., SHI, X. & QIAO, Y. 2017. Scale-up of a high shear wet granulation process using a nucleation regime map approach. *Particuology,* 31**,** 87-94.

MACKAPLOW, M. B., ROSEN, L. A. & MICHAELS, J. N. 2000. Effect of primary particle size on granule growth and endpoint determination in high-shear wet granulation. *Powder Technology,* 108**,** 32-45.

MADERUELO, C., ZARZUELO, A. & LANAO, J. M. 2011. Critical factors in the release of drugs from sustained release hydrophilic matrices. *Journal of Controlled Release,* 154**,** 2-19.

MAHDI, F., HASSANPOUR, A. & MULLER, F. 2018. An investigation on the evolution of granule formation by in-process sampling of a high shear granulator. *Chemical Engineering Research and Design,* 129**,** 403-411.

MAHOURS, G. M., SHAABAN, D. E. Z., SHAZLY, G. A. & AUDA, S. H. 2017. The effect of binder concentration and dry mixing time on granules, tablet characteristics and content uniformity of low dose drug in high shear wet granulation. *Journal of Drug Delivery Science and Technology,* 39**,** 192-199.

MANGWANDI, C., ALBADARIN, A. B., AL-MUHTASEB, A. A. H., ALLEN, S. J. & WALKER, G. M. 2013a. Optimisation of high shear granulation of multicomponent fertiliser using response surface methodology. *Powder Technology,* 238**,** 142-150.

MANGWANDI, C., ALBADARIN, A. B., ALA'A, H., ALLEN, S. J. & WALKER, G. M. 2013b. Optimisation of high shear granulation of multicomponent fertiliser using response surface methodology. *Powder technology,* 238**,** 142-150.

MANGWANDI, C., ALBADARIN, A. B., JIANGTAO, L., ALLEN, S. & WALKER, G. M. 2014. Development of a value-added soil conditioner from high shear co-granulation of organic waste and limestone powder. *Powder Technology,* 252**,** 33-41.

MANGWANDI, C., CHEONG, Y., ADAMS, M., HOUNSLOW, M. & SALMAN, A. 2007. The coefficient of restitution of different representative types of granules. *Chemical Engineering Science,* 62**,** 437-450.

MARCHAL, P., DAVID, R., KLEIN, J. & VILLERMAUX, J. 1988. Crystallization and precipitation engineering—I. An efficient method for solving population balance in crystallization with agglomeration. *Chemical Engineering Science,* 43**,** 59-67.

MARCHISIO, D. L. & FOX, R. O. 2013. *Computational models for polydisperse particulate and multiphase systems*, Cambridge University Press

MCCONVILLE, J. T., ROSS, A. C., CHAMBERS, A. R., SMITH, G., FLORENCE, A. J. & STEVENS, H. N. 2004. The effect of wet granulation on the erosion behaviour of an HPMC–lactose tablet,

used as a rate-controlling component in a pulsatile drug delivery capsule formulation. *European journal of pharmaceutics and biopharmaceutics,* 57**,** 541-549.

MIKLI, V., KAERDI, H., KULU, P. & BESTERCI, M. 2001. Characterization of powder particle morphology. *Proceedings of the Estonian Academy of Sciences: Engineering(Estonia),* 7**,** 22-34.

MILLS, P., SEVILLE, J., KNIGHT, P. & ADAMS, M. 2000. The effect of binder viscosity on particle agglomeration in a low shear mixer/agglomerator. *Powder technology,* 113**,** 140-147.

MOEBUS, K., SIEPMANN, J. & BODMEIER, R. 2012. Novel preparation techniques for alginate–poloxamer microparticles controlling protein release on mucosal surfaces. *European Journal of Pharmaceutical Sciences,* 45**,** 358-366.

MORENO-ATANASIO, R. & GHADIRI, M. 2006. Mechanistic analysis and computer simulation of impact breakage of agglomerates: effect of surface energy. *Chemical engineering science,* 61**,** 2476-2481.

MORIN, G. & BRIENS, L. 2014. A Comparison of Granules Produced by High-Shear and Fluidized-Bed Granulation Methods. *AAPS PharmSciTech,* 15**,** 1039-1048.

MORKHADE, D. M. 2017. Comparative impact of different binder addition methods, binders and diluents on resulting granule and tablet attributes via high shear wet granulation. *Powder Technology,* 320**,** 114-124.

NALESSO, S., CODEMO, C., FRANCESCHINIS, E., REALDON, N., ARTONI, R. & SANTOMASO, A. C. 2015. Texture analysis as a tool to study the kinetics of wet agglomeration processes. *International Journal of Pharmaceutics,* 485**,** 61-69.

NEWITT, D. 1958. A contribution to the theory and practice of granulation. *Tran Inst Chem Eng,* 36**,** 422-442.

NING, Z. & GHADIRI, M. 2006. Distinct element analysis of attrition of granular solids under shear deformation. *Chemical Engineering Science,* 61**,** 5991-6001.

OHARA, T., KITAMURA, S., KITAGAWA, T. & TERADA, K. 2005. Dissolution mechanism of poorly water-soluble drug from extended release solid dispersion system with ethylcellulose and hydroxypropylmethylcellulose. *International journal of pharmaceutics,* 302**,** 95-102.

OKA, S., KAŠPAR, O., TOKÁROVÁ, V., SOWRIRAJAN, K., WU, H., KHAN, M., MUZZIO, F., ŠTĚPÁNEK, F. & RAMACHANDRAN, R. 2015. A quantitative study of the effect of process parameters on key granule characteristics in a high shear wet granulation process involving a two component pharmaceutical blend. *Advanced Powder Technology,* 26**,** 315-322.

OKA, S., SMRČKA, D., KATARIA, A., EMADY, H., MUZZIO, F., ŠTĚPÁNEK, F. & RAMACHANDRAN, R. 2017. Analysis of the origins of content non-uniformity in high-shear wet granulation. *International Journal of Pharmaceutics,* 528**,** 578-585.

OSBORNE, J. D., SOCHON, R. P. J., CARTWRIGHT, J. J., DOUGHTY, D. G., HOUNSLOW, M. J. & SALMAN, A. D. 2011. Binder addition methods and binder distribution in high shear and fluidised bed granulation. *Chemical Engineering Research and Design,* 89**,** 553-559.

OULAHNA, D., CORDIER, F., GALET, L. & DODDS, J. A. 2003. Wet granulation: the effect of shear on granule properties. *Powder Technology,* 130**,** 238-246.

PANI, N. R. & NATH, L. K. 2014. Development of controlled release tablet by optimizing HPMC: Consideration of theoretical release and RSM. *Carbohydrate polymers,* 104**,** 238-245.

PARIKH, D. M. 2016. *Handbook of pharmaceutical granulation technology*, CRC Press.

PATEL, M. R. & SAN MARTIN-GONZALEZ, M. F. 2012. Characterization of ergocalciferol loaded solid lipid nanoparticles. *Journal of food science,* 77**,** N8-N13.

PATHARE, P. B. & BYRNE, E. P. 2011. Application of wet granulation processes for granola breakfast cereal production. *Food Engineering Reviews,* 3**,** 189-201.

PERRY, R. H. & GREEN, D. W. 1999. *Perry's chemical engineers' handbook*, McGraw-Hill Professional.

PHINNEY, R. 2000. Wet granulation method for generating fertilizer granules. Google Patents.

PHINNEY, R. 2001. Wet granulation method generating sulfur granules. Google Patents.

POON, J. M.-H., IMMANUEL, C. D., DOYLE III, F. J. & LITSTER, J. D. 2008. A three-dimensional population balance model of granulation with a mechanistic representation of the nucleation and aggregation phenomena. *Chemical Engineering Science,* 63**,** 1315-1329.

RAJMOHAN, T. & PALANIKUMAR, K. 2013. Application of the central composite design in optimization of machining parameters in drilling hybrid metal matrix composites. *Measurement,* 46**,** 1470-1481.

RAJNIAK, P., MANCINELLI, C., CHERN, R., STEPANEK, F., FARBER, L. & HILL, B. 2007. Experimental study of wet granulation in fluidized bed: impact of the binder properties on the granule morphology. *International journal of pharmaceutics,* 334**,** 92-102.

RAMACHANDRAN, R., POON, J. M.-H., SANDERS, C. F., GLASER, T., IMMANUEL, C. D., DOYLE III, F. J., LITSTER, J. D., STEPANEK, F., WANG, F.-Y. & CAMERON, I. T. 2008.

Experimental studies on distributions of granule size, binder content and porosity in batch drum granulation: Inferences on process modelling requirements and process sensitivities. *Powder Technology,* 188**,** 89-101.

RAMAKER, J., JELGERSMA, M. A., VONK, P. & KOSSEN, N. 1998. Scale-down of a high-shear pelletisation process: flow profile and growth kinetics. *International Journal of Pharmaceutics,* 166**,** 89-97.

RAMBALI, B., BAERT, L. & MASSART, D. 2001. Using experimental design to optimize the process parameters in fluidized bed granulation on a semi-full scale. *International Journal of Pharmaceutics,* 220**,** 149-160.

RAMKRISHNA, D. 2000. *Population Balances: Theory and Applications to Particulate Systems in Engineering*, Elsevier Science.

RANDOLPH, A. D. 1964. A population balance for countable entities. *The canadian journal of chemical engineering,* 42**,** 280-281.

RANODOLPH, A. 2012. *Theory of particulate processes: analysis and techniques of continuous crystallization*, Elsevier.

RAYLEIGH, L. 1915. The principle of similitude. *Nature,* 95**,** 66.

RESEARCH, G. V. 2017. Animal Feed Additives Market Analysis By Product (Antioxidants, Amino Acids, Enzymes (Phytase, Non-Starch Polysaccharides), Acidifiers, By Livestock (Pork/Swine, Poultry, Cattle, Aquaculture), And Segment Forecasts, 2018 - 2025. Grand View Research.

REYNOLDS, G., FU, J., CHEONG, Y., HOUNSLOW, M. & SALMAN, A. 2005. Breakage in granulation: a review. *Chemical Engineering Science,* 60**,** 3969-3992.

RITALA, M., JUNGERSEN, O., HOLM, P., SCHAEFER, T. & KRISTENSEN, H. 1986. A comparison between binders in the wet phase of granulation in a high shear mixer. *Drug Development and Industrial Pharmacy,* 12**,** 1685-1700.

SAIKH, M. A. A. 2013. A technical note on granulation technology: a way to optimise granules. *International journal of pharmaceutical sciences and research,* 4**,** 55.

SAKR, W. F., IBRAHIM, M. A., ALANAZI, F. K. & SAKR, A. A. 2012. Upgrading wet granulation monitoring from hand squeeze test to mixing torque rheometry. *Saudi Pharmaceutical Journal,* 20**,** 9-19.

SALMAN, A. D., HOUNSLOW, M. & SEVILLE, J. P. 2006a. *Granulation*, Elsevier.

SALMAN, A. D., HOUNSLOW, M. & SEVILLE, J. P. K. 2006b. *Granulation*, Elsevier Science

SANDERS, C., WILLEMSE, A., SALMAN, A. & HOUNSLOW, M. 2003. Development of a predictive high-shear granulation model. *Powder Technology,* 138**,** 18-24.

SANDERS, C. F., HOUNSLOW, M. J. & DOYLE III, F. J. 2009. Identification of models for control of wet granulation. *Powder Technology,* 188**,** 255-263.
SANNINO, A., DEMITRI, C. & MADAGHIELE, M. 2009. Biodegradable cellulose-based hydrogels: design and applications. *Materials,* 2**,** 353-373.
SARKAR, S. & CHAUDHURI, B. 2018. DEM modeling of high shear wet granulation of a simple system. *Asian Journal of Pharmaceutical Sciences*.
SASTRY, K., PANIGRAPHY, S. & FUERSTENAU, D. 1977. Effect of wet grinding and dry grinding on the batch balling behaviour of particulate materials. *Transactions of the Society of Mining Engineers,* 262**,** 325-330.
SASTRY, K. V. & FUERSTENAU, D. 1973. Mechanisms of agglomerate growth in green pelletization. *Powder Technology,* 7**,** 97-105.
SASTRY, K. V. & FUERSTENAU, D. W. 1970. Size distribution of agglomerates in coalescing dispersed phase systems. *Industrial & Engineering Chemistry Fundamentals,* 9**,** 145-149.
SCALA-BERTOLA, J., RABISKOVA, M., LECOMPTE, T., BONNEAUX, F. & MAINCENT, P. 2009. Granules in the improvement of oral heparin bioavailability. *International journal of pharmaceutics,* 374**,** 12-16.
SCHAEFER, T., HOLM, P. & KRISTENSEN, H. 1990. Melt granulation in a laboratory scale high shear mixer. *Drug Development and Industrial Pharmacy,* 16**,** 1249-1277.
SCHÆFER, T., JOHNSEN, D. & JOHANSEN, A. 2004. Effects of powder particle size and binder viscosity on intergranular and intragranular particle size heterogeneity during high shear granulation. *European journal of pharmaceutical sciences,* 21**,** 525-531.
SCHÆFER, T. & MATHIESEN, C. 1996. Melt pelletization in a high shear mixer. IX. Effects of binder particle size. *International journal of pharmaceutics,* 139**,** 139-148.
SCHÆFER, T., TAAGEGAARD, B., THOMSEN, L. J. & KRISTENSEN, H. G. 1993. Melt pelletization in a high shear mixer. V. Effects of apparatus variables. *European Journal of Pharmaceutical Sciences,* 1**,** 133-141.
SCOTT, A., HOUNSLOW, M. & INSTONE, T. 2000. Direct evidence of heterogeneity during high-shear granulation. *Powder Technology,* 113**,** 205-213.
SEN, M., BARRASSO, D., SINGH, R. & RAMACHANDRAN, R. 2014. A Multi-Scale Hybrid CFD-DEM-PBM Description of a Fluid-Bed Granulation Process. *Processes,* 2**,** 89.
SEO, A., HOLM, P. & SCHÆFER, T. 2002. Effects of droplet size and type of binder on the agglomerate growth mechanisms by melt

agglomeration in a fluidised bed. *European journal of pharmaceutical sciences,* 16**,** 95-105.
SHANMUGAM, S. 2015. Granulation techniques and technologies: recent progresses. *BioImpacts: BI,* 5**,** 55.
SIEPMANN, J. & PEPPAS, N. 2000. Hydrophilic matrices for controlled drug delivery: an improved mathematical model to predict the resulting drug release kinetics (the "sequential layer" model). *Pharmaceutical Research,* 17**,** 1290-1298.
SIEPMANN, J. & PEPPAS, N. 2012. Modeling of drug release from delivery systems based on hydroxypropyl methylcellulose (HPMC). *Advanced drug delivery reviews,* 64**,** 163-174.
SIEPMANN, J. & PEPPAS, N. A. 2001. Modeling of drug release from delivery systems based on hydroxypropyl methylcellulose (HPMC). *Advanced Drug Delivery Reviews,* 48**,** 139-157.
SINGH, J., SINGH, G. & KAUR, H. 2015. Pharmacological Efficacy of Insulin-Loaded Granules Made Up of Various Grades of Hydroxypropyl Methylcellulose in Normal Rats. *Journal of Bioequivalence & Bioavailability,* 7**,** 257.
SKIBSTED, L. H., RISBO, J. & ANDERSEN, M. L. 2010. *Chemical deterioration and physical instability of food and beverages*, Elsevier.
SMIT, D., HOUNSLOW, M. & PATERSON, W. 1995. Aggregation and gelation: III. Numerical classification of kernels and case studies of aggregation and growth. *Chemical engineering science,* 50**,** 849-862.
SNIPES, M. & TAYLOR, D. C. 2014. Model selection and Akaike Information Criteria: An example from wine ratings and prices. *Wine Economics and Policy,* 3**,** 3-9.
SOLANKI, H. K., BASURI, T., THAKKAR, J. H. & PATEL, C. A. 2010. Recent advances in granulation technology. *International Journal of Pharmaceutical Sciences Review and Research,* 5**,** 48-54.
SONI, S., CHOUDHARY, B. S., AHMAD, S. & RATHI, G. 2013. Extended Release Granules of Acetyl Salicylic Acid: Preparation and In-vitro Characterization. *Inventi Rapid: Pharm Tech*.
SRIVASTAVA, S. & MISHRA, G. 2010. Fluid bed technology: overview and parameters for process selection. *International Journal of Pharmaceutical Sciences and Drug Research,* 2**,** 236-246.
STUER, M., ZHAO, Z. & BOWEN, P. 2012. Freeze granulation: Powder processing for transparent alumina applications. *Journal of the European Ceramic Society,* 32**,** 2899-2908.
SUN, Y., LIU, J. & KENNEDY, J. F. 2010. Application of response surface methodology for optimization of polysaccharides production parameters from the roots of Codonopsis pilosula by a central composite design. *Carbohydrate polymers,* 80**,** 949-953.

SUNG, K., NIXON, P. R., SKOUG, J. W., JU, T. R., GAO, P., TOPP, E. & PATEL, M. 1996. Effect of formulation variables on drug and polymer release from HPMC-based matrix tablets. *International journal of pharmaceutics,* 142**,** 53-60.

SURESH, P., SREEDHAR, I., VAIDHISWARAN, R. & VENUGOPAL, A. 2017. A comprehensive review on process and engineering aspects of pharmaceutical wet granulation. *Chemical Engineering Journal,* 328**,** 785-815.

TAHARA, K., YAMAMOTO, K. & NISHIHATA, T. 1996. Application of model-independent and model analysis for the investigation of effect of drug solubility on its release rate from hydroxypropyl methylcellulose sustained release tablets. *International journal of pharmaceutics,* 133**,** 17-27.

TAKASAKI, H., YONEMOCHI, E., MESSERSCHMID, R., ITO, M., WADA, K. & TERADA, K. 2013. Importance of excipient wettability on tablet characteristics prepared by moisture activated dry granulation (MADG). *International journal of pharmaceutics,* 456**,** 58-64.

TAMHANE, A. C. 2009. *Statistical analysis of designed experiments: theory and applications*, John Wiley & Sons.

TAN, H. S., SALMAN, A. & HOUNSLOW, M. 2004. Kinetics of fluidised bed melt granulation: IV. Selecting the breakage model. *Powder technology,* 143**,** 65-83.

TAN, M. X. & HAPGOOD, K. P. 2011a. Foam granulation: Binder dispersion and nucleation in mixer-granulators. *Chemical engineering research and design,* 89**,** 526-536.

TAN, M. X. & HAPGOOD, K. P. 2011b. Foam granulation: Liquid penetration or mechanical dispersion? *Chemical engineering science,* 66**,** 5204-5211.

TAN, M. X. & HAPGOOD, K. P. 2012. Foam granulation: Effects of formulation and process conditions on granule size distributions. *Powder technology,* 218**,** 149-156.

TARDOS, G. I., KHAN, M. I. & MORT, P. R. 1997. Critical parameters and limiting conditions in binder granulation of fine powders. *Powder Technology,* 94**,** 245-258.

TSAPATSARIS, S. & KOTZEKIDOU, P. 2004. Application of central composite design and response surface methodology to the fermentation of olive juice by Lactobacillus plantarum and Debaryomyces hansenii. *International Journal of Food Microbiology,* 95**,** 157-168.

US, D., CHAUDHARI, P., BHAVSAR, D. & CHAVAN, R. 2013. Melt Granulation: An Alternative to Traditional Granulation Techniques. *INDIAN DRUGS,* 50**,** 03.

VAN ARNUM, P. 2015. *Evaluating Market Opportunities for Solid Dosage Products and Manufacturing* [Online]. Available: https://www.dcatvci.org/1.

VAN DEN DRIES, K. & VROMANS, H. 2002. Relationship between inhomogeneity phenomena and granule growth mechanisms in a high-shear mixer. *International journal of pharmaceutics,* 247**,** 167-177.

VANNI, M. 2000. Approximate Population Balance Equations for Aggregation–Breakage Processes. *Journal of Colloid and Interface Science,* 221**,** 143-160.

VELASCO, M. V., FORD, J. L., ROWE, P. & RAJABI-SIAHBOOMI, A. R. 1999. Influence of drug: hydroxypropylmethylcellulose ratio, drug and polymer particle size and compression force on the release of diclofenac sodium from HPMC tablets. *Journal of Controlled Release,* 57**,** 75-85.

VERSTRAETEN, M., VAN HAUWERMEIREN, D., LEE, K., TURNBULL, N., WILSDON, D., AM ENDE, M., DOSHI, P., VERVAET, C., BROUCKAERT, D., MORTIER, S. T. F. C., NOPENS, I. & BEER, T. D. 2017. In-depth experimental analysis of pharmaceutical twin-screw wet granulation in view of detailed process understanding. *International Journal of Pharmaceutics,* 529**,** 678-693.

VICENTE, G., COTERON, A., MARTINEZ, M. & ARACIL, J. 1998. Application of the factorial design of experiments and response surface methodology to optimize biodiesel production. *Industrial crops and products,* 8**,** 29-35.

VIRIDÉN, A., WITTGREN, B. & LARSSON, A. 2009. Investigation of critical polymer properties for polymer release and swelling of HPMC matrix tablets. *European journal of pharmaceutical sciences,* 36**,** 297-309.

WALKER, G., ANDREWS, G. & JONES, D. 2006. Effect of process parameters on the melt granulation of pharmaceutical powders. *Powder Technology,* 165**,** 161-166.

WASHINGTON, C. 2005. *Particle Size Analysis In Pharmaceutics And Other Industries: Theory And Practice: Theory And Practice*, CRC Press.

WATANO, S. & MIYANAMI, K. 1995. Image processing for on-line monitoring of granule size distribution and shape in fluidized bed granulation. *Powder technology,* 83**,** 55-60.

WATANO, S., NUMA, T., MIYANAMI, K. & OSAKO, Y. 2000. On-line monitoring of granule growth in high shear granulation by an image processing system. *Chemical and pharmaceutical bulletin,* 48**,** 1154-1159.

WESTERHUIS, J. A., COENEGRACHT, P. M. & LERK, C. F. 1997. Multivariate modelling of the tablet manufacturing process with wet granulation for tablet optimization and in-process control. *International journal of Pharmaceutics,* 156**,** 109-117.

WILLIAMS, R. O., SYKORA, M. A. & MAHAGUNA, V. 2001. Method to recover a lipophilic drug from hydroxypropyl methylcellulose matrix tablets. *AAPS PharmSciTech,* 2**,** 29-37.

WRIGHT, T. 2016. Solid Dosage Outsourcing Trends. *Contract Pharma*

YADAV, P., CHAUHAN, J., KANNOJIA, P., JAIN, N. & TOMAR, V. 2010. A Review: On Scale-Up Factor Determination of Rapid Mixer Granulator. *Der. Pharmacia Lettre,* 2**,** 23-38.

YANG, C. & MAO, Z.-S. 2014. Chapter 6 - Crystallizers: CFD–PBE modeling. *Numerical Simulation of Multiphase Reactors with Continuous Liquid Phase.* Oxford: Academic Press.

ZAJIC, L. & BUCKTON, G. 1990. The use of surface energy values to predict optimum binder selection for granulations. *International Journal of Pharmaceutics,* 59**,** 155-164.

Symbols

$\dot{A}$	Powder flux trough the spray zone
B_p	Big scrap (% w/w of dry granules with size greater than 2 mm)
BS	Big scrap (% w/w of wet granules with size between 10000 μm and 20000 μm)
d_d	Average drop size
d_g	Size of granule
d_i	Particles diameter in the class "i"
D-1	Fluid bed dryer
E	Percentage of HPMC eroded from granules
E_l	Young modulus
F	Compression force
GR-1	Granulator
G_1	Unloaded HPMC granules obtained using distilled water as binder
G_1-*B12*	Vitamin B12 loaded HPMC granules
G_2	Unloaded HPMC granules obtained using a solution of ethanol and water with a 75/25 v/v ratio as binder
G_2-*D2*	Vitamin D2 loaded HPMC granules
h	Height of the cone
k	Number of independent input variables (factors)
L	Levels of factors
m	Mass of the sample
m_i	Amount in grams of active molecule loaded into granules
m_t	Amount in grams of released active molecule
M_i	Amount in grams of HPMC introduced in the dissolution medium
M_t	Amount in grams of eroded HPMC

M-1	Magnetic stirrer
n	Number of data points
n_0	center point of work matrix (integer closest)
n_i	Particles number for class "i"
N_t	Number of experiments
p	Probability
p_{ii}	constants to be determined by fitting the experimental data
P-1	Peristaltic pump for binder phase
q	Distribution density
Q	Undersize cumulative distribution
Q_0	Undersize cumulative distribution by number
Q_3	Undersize cumulative distribution by volume/mass
$Q_{3_{size}}$	Volume-weighted undersize cumulative distribution at a fixed size
r	Radius of the cone
R	Percentage of active molecule released from granules
R^2	R-squared (guideline to measure the accuracy of the model equation to describe the experimental values)
R_{eff}	Effective pore size of the powder bed
s_{max}	maximum pore saturation
S_p	Small scrap (% w/w of dry granules with size lower than 0.45 mm)
SS	Small scrap (% w/w of wet granules with size between 60 μm and 2000 μm)
St_{def}	Stokes deformation number
S-1	Sieve
t_c	Circulation time
t_{dp}	Drop penetration time
T-1	Binder phase tank
U_c	Process agitation intensity
v	Speed of the powder after spray
$\dot{V}$	Volumetric flow rate of the droplets

V_b	Bulk volume
V_d	Sprayed droplets volume
V_t	Tapped volume
V-1	Valve
W	Powder size after wetting
w	Liquid to solid mass ratio
$wgt_{<0.45mm}$	Amount in grams of dry granules with size lower than 0.45 mm
$wgt_{0.45-2mm}$	Amount in grams of dry granules with size 0.45-2 mm
$wgt_{>2mm}$	Amount in grams of dry granules with size greater than 2 mm
W_a	Work of adhesion for an interface
W_{cl}	Work of cohesion for a liquid
W_{cs}	Work of cohesion for a solid
$x_{1,0}$	Arithmetic mean size
$x_{1,3}$	Volume-weighted mean size
y_g	Granulation yield (% w/w of wet granules with size between 2000 μm and 10000 μm)
Y_g	Granule dynamic yield stress
y_p	Product yield (% w/w of dry granules with size between 0.45 mm and 2 mm)
Z-1	Atomizer assisted by ultrasonic energy

α	Value depends on the factor number
γ_{lv}	Surface free energies between liquid and vapour phase
γ_{sl}	Surface free energies between solid and liquid phase
γ_{sv}	Surface free energies between solid and vapour phase
Δ	Total displacement of the moving platen
$\Delta\pi$	Difference between the number of parameters for the two compared models
ε_{eff}	Surface porosity
ε_{min}	Minimum porosity
θ	Solid-liquid angle of contact

λ	Spreading coefficients of the binder phase on the powder surface
λ_{ls}	Spreading coefficient: liquid may spread over the solid
λ_{sl}	Spreading coefficient: solid may spread or adhere to liquid
Λ	Degree of homogeneity
μ	Liquid viscosity
ν_l	Poisson ratio
ρ_b	Bulk density
ρ_g	Granule density
ρ_l	Liquid density
ρ_s	Solid particles density
ρ_t	Tapped density
σ	Granule mechanical strength
τ_p	Drop penetration time to circulation time ratio
ψ_a	Dimensionless spray flux

Abbreviations

AIC	Akaike Information Criterion
AR	Angle of Repose
ASTM	American Society for Testing and Material
CCD	Central Composite Design
CFD	Computational Fluid Dynamic
CI	Carr Index
DEM	Discrete Element Method
DIA	Dynamic Image Analysis
DoE	Design of Experiment
DPBE	Discretized Population Balance Equation
DSC	Differential Scanning Calorimetry
EKE	Equi Kinetic Energy
ER	Ellipse Ratio
ERM	Eccentric Rotating Mass
FDA	Food and Drug Administration
FFD	Full Factorial Design
HPMC	Hydroxypropil methylcellulose
HR	Hausner Ratio
MRN	Nucleation Regime Map
ODE	Ordinary Differential Equation
PBE	Population Balance Equation
PSD	Particle Size Distribution
rpm	Revolutions per minute
RSM	Responce Surface Methodology

SD	Standard Deviation
SEM	Scanning Electron Microscope
SSE	Sum of Square Errors
US	Ultrasonic source

Appendix

Publications

International journals

1. **De Simone V.**, Dalmoro A., Lamberti G., d'Amore M., Barba A.A, "Central composite design in HPMC granulation and correlations between product properties and process parameters", New Journal of Chemistry, 41 (2017) 6504-6513

NJC

PAPER

View Article Online
View Journal | View Issue

Check for updates

Cite this: *New J. Chem.*, 2017, 41, 6504

Central composite design in HPMC granulation and correlations between product properties and process parameters

Veronica De Simone,[ab] Annalisa Dalmoro,[b] Gaetano Lamberti,[a] Matteo d'Amore[b] and Anna Angela Barba*[b]

Particulate solids have received great interest in many industrial fields for both marketing reasons and technological aspects. In this study granular systems were achieved by using a wet granulation process using hydroxypropyl methylcellulose (*HPMC*) and distilled water as the binder phase. Particulates with a defined size (450–2000 mm) and good flowability together with a high granulation process yield, to reduce manufacturing scrap, were produced. To this aim a bench scale low-shear rate granulator apparatus was used; three process parameters were varied (impeller rotation speed, binder volume at constant mass, and binder flow rate) and, for each parameter, three intensities have been used. *HPMC* granule production was planned using the Central Composite Design (*CCD*) statistical protocol, which allowed us to minimize the number of runs to be performed for obtaining information about the relationship between granule properties and process parameters. The produced granules were stabilized by using a dedicated dynamic drying apparatus, then separated by sieving and then characterized in terms of size and flowability properties. The results of the experimental campaign have been used to develop semi-empirical correlations between granulated product properties and process parameters. A second-order polynomial law has shown the best comparison between experimental data and model predicted values. These correlations can constitute a reliable tool to help us to know more on the effect of operative parameter changes in *HMPC* or similar particulate solid production.

2. **De Simone V.**, Dalmoro A., Lamberti G., Caccavo D., d'Amore M., Barba A.A, "HPMC granules by wet granulation process: Effect of vitamin load on physicochemical, mechanical and release properties", Carbohydrate Polymers, 181 (2018) 939-947

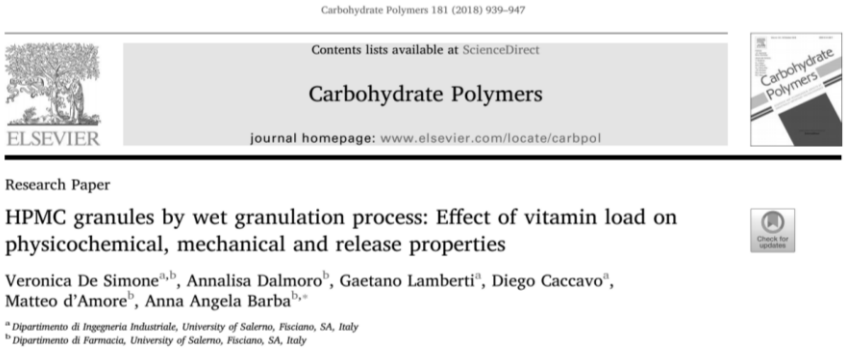
Carbohydrate Polymers 181 (2018) 939–947

Contents lists available at ScienceDirect

Carbohydrate Polymers

journal homepage: www.elsevier.com/locate/carbpol

Research Paper

HPMC granules by wet granulation process: Effect of vitamin load on physicochemical, mechanical and release properties

Veronica De Simone[a,b], Annalisa Dalmoro[b], Gaetano Lamberti[a], Diego Caccavo[a], Matteo d'Amore[b], Anna Angela Barba[b,*]

[a] Dipartimento di Ingegneria Industriale, University of Salerno, Fisciano, SA, Italy
[b] Dipartimento di Farmacia, University of Salerno, Fisciano, SA, Italy

Due to its versatile properties, hydroxypropyl methylcellulose (*HPMC*) is largely used in many applications and deeply studied in the various fields such as pharmaceuticals, biomaterials, agriculture, food, water purification. In this work, vitamin B12 loaded *HPMC* granules were produced to investigate their potential application as nutraceutical products. To this aim the impact of vitamin load on physico-chemical, mechanical and release properties of granules, achieved by wet granulation process, was investigated. In particular, three different loads of B12 (1 %, 2.3 % and 5 % w/w) were assayed. Unloaded granules (used as control) and loaded granules were dried, sieved, and then the suitable fraction for practical uses, 0.45–2 mm in size, was fully characterized. Results showed that the vitamin incorporation of 5 % reduced the granulation performance in the range size of 0.45–2 mm and led granules with higher porosity, more rigid and less elastic structures compared to unloaded granules and those loaded at 1 % and 2.3 % of B12. Vitamin release kinetics of fresh and aged granules were roughly found the same trends for all the prepared lots; however, the vitamin B12 was released more slowly when added with a load at 1 % w/w, suggesting a better incorporation.

3. **De Simone V.**, Caccavo D., Lamberti G., d'Amore M., Barba A.A., "Wet-granulation process: phenomenological analysis and process parameters optimization", Powder Technology, 340 (2018) 411-419

Powder Technology 340 (2018) 411–419

Contents lists available at ScienceDirect

Powder Technology

journal homepage: www.elsevier.com/locate/powtec

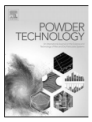

Wet-granulation process: phenomenological analysis and process parameters optimization

Veronica De Simone [a,b], Diego Caccavo [a,c,*], Gaetano Lamberti [a,c], Matteo d'Amore [b,c], Anna Angela Barba [b,c]

[a] Dipartimento di Ingegneria Industriale, Università di Salerno, Via Giovanni Paolo II, 132, Fisciano 84084, SA,Italy
[b] Dipartimento di Farmacia, Università di Salerno, Via Giovanni Paolo II, 132, Fisciano 84084, SA,Italy
[c] Eng4Life Srl, Spin-off Accademico, Via Fiorentino, 32, Avellino 83100, Italy

Wet granulation is a size-enlargement process applied in many industrial fields, such as pharmaceutical, nutraceutical, zootecnichal, to improve flowability and compressibility properties of powders. In this work analysis of the Particle Size Distribution (*PSD*) of granules was performed to understand the phenomena involved during the granulation process and to optimize the operating conditions. Hydroxypropyl methylcellulose (*HPMC*) granules were produced spraying distilled water as liquid binder on powders in a low-shear granulator. The experimental campaign was planned using the Full Factorial Design (*FFD*) statistical technique varying two factors (impeller rotation speed and binder flow rate), each at three intensities. *PSDs* of *HPMC* granules at different granulation times were obtained by an ad hoc dynamic image analysis device based on the free falling particle scheme. *PSD* measurements showed that wet granules size depends on the simultaneous presence of nucleation, agglomeration and breakage phenomena. The process parameters optimization was carried out using Response Surface Methodology (*RSM*) and using the granulation yield (% w/w of wet granules within the size range 2000–10000 μm) as the main variable of interest.

4. **De Simone V.**, Dalmoro A., Lamberti G., Caccavo D., d'Amore M., Barba A.A., "Effect of binder and load solubility properties on HPMC granules produced by wet granulation process", Journal of Drug Delivery Science and Technology, 49 (2019) 513-520


Journal of Drug Delivery Science and Technology 49 (2019) 513–520

Contents lists available at ScienceDirect

Journal of Drug Delivery Science and Technology

journal homepage: www.elsevier.com/locate/jddst

Effect of binder and load solubility properties on HPMC granules produced by wet granulation process

Veronica De Simone[a,b], Annalisa Dalmoro[b], Gaetano Lamberti[a], Diego Caccavo[a], Matteo d'Amore[b], Anna Angela Barba[b,*]

[a] Dipartimento di Ingegneria Industriale, University of Salerno, Fisciano, SA, Italy
[b] Dipartimento di Farmacia, University of Salerno, Fisciano, SA, Italy

Hydroxypropyl methylcellulose (HPMC) is one of the most important hydrophilic ingredients used in hydrogel matrices preparation (tablets or granules). In this work, HPMC was used to produce granules loaded with hydrophilic and hydrophobic active molecules to investigate their possible use as release dosage forms for pharmaceutical and nutraceutical applications. Unloaded and vitamins loaded HPMC granules were produced by wet granulation to investigate the effect of molecule solubility and granulation liquid type, on physical, mechanical and release properties. Water-soluble vitamin B12 and water-insoluble vitamin D2 were used as model molecules. Due to their different solubility, two granulation liquid phases were also used: distilled water for granules with B12, and ethanol-water for granules with D2. Results showed that use of ethanol in the liquid phase reduces the granulation yield and produces granules having a less defined shape, a smaller mean size, a less hard structure and a worse flowability. Moreover, ethanol slightly enhances the polymer erosion rate. Results also emphasized that the vitamins solubility does not affect either the physical and the mechanical properties of the produced granules. However, it plays a significant relevant role on the molecule release mechanism, being B12 and D2 were released by diffusion and erosion mechanism, respectively.

Book chapter

5. **De Simone V.,** Caccavo D., Dalmoro A., Lamberti G., d'Amore M.; Barba A.A., "Inside the phenomenological aspects of wet granulation: role of process parameters", chap. V in "Granularity in Materials Science", InTech Ed., 2018, ISBN *978-1-78984-308-8*

Chapter 5

Inside the Phenomenological Aspects of Wet Granulation: Role of Process Parameters

Veronica De Simone, Diego Caccavo,
Annalisa Dalmoro, Gaetano Lamberti,
Matteo d'Amore and Anna Angela Barba

Granulation is a size-enlargement process by which small particles are bonded, by means of various techniques, in coherent and stable masses (granules), in which the original particles are still identifiable. In wet granulation processes, the powder particles are aggregated through the use of a liquid phase called binder. The main purposes of sizeenlargement process of a powder or mixture of powders are to improve technological properties and/or to realize suitable forms of commercial products. A modern and rational approach in the production of granular structures with tailored features (in terms of size and size distribution, flowability, mechanical and release properties, etc.) requires a deep understanding of phenomena involved during granules formation. By this knowledge, suitable predictive tools can be developed with the aim to choose right process conditions to be used in developing new formulations by avoiding or reducing costs for new tests. In this chapter, after introductive notes on granulation process, the phenomenological aspects involved in the formation of the granules with respect to the main process parameters are presented by experimental demonstration. Possible mathematical approaches in the granulation process description are also presented and the one involving the population mass balances equations is detailed.

Acknowledgments

I would like to thank all people who helped and supported me during this great adventure, and without whom this PhD carrier would not have been possible.

I am extremely grateful to my supervisor Prof. Anna Angela Barba. Thank you for having given me the opportunity of a professional growth as PhD student. Thank you for all the precious comments and suggestions. You have been the most genuine, fairness, wise and humane supervisor I could hope!

I would like to thank Prof. Gaetano Lamberti for his availability, support and dedication to my work. You are one of the most specialist and kindness engineers I have known!

I would like to thank Prof. Matteo d'Amore for his great knowledge, experience and humanity. Thanks for the interesting narratives that have always left a teaching for the life.

Thanks to Annalisa and Sabrina for giving me your "time" and "advice", for having shared "joys" and "anxieties" with me unconditionally.

Thanks to all the colleagues with whom I shared ideas, concerns, PhD presentations and the wonderful GRICU experiences.

At the end, I would like to thank the most important people in my life. They have been, each in their own way, the architects of the person I am today. You have taught me so much.

I warmly thank Michele, my love mate. Thank you because your great patience has supported me during all the stages of my research activity. Thank you because your funny irony has made every obstacle a game to win. With love and respect you have shared my thoughts and projects reinforcing at the right time all my choices. You believed in me more than I did. You are a special guide for my life.

I am grateful to my family. Thank for your constant presence, for your encouragements, for having always motivated me to give my best but with humility.

Simply thanks to all people who have believed and still believe in me, which are next to me "always and anyway" and love me regardless.